Summer 8-16-2024

Screen for Candida albicans Virulence Factors that Modulate the Host Immune Response in the Larval Zebrafish

Bailey A. Blair
University of Maine, blair.ba93@gmail.com

SCREEN FOR *CANDIDA ALBICANS* VIRULENCE FACTORS THAT MODULATE THE HOST IMMUNE RESPONSE IN THE LARVAL ZEBRAFISH

By

Bailey A. Blair

B.S. Franklin Pierce University, 2016

A DISSERTATION

Submitted in Partial Fulfillment of the

Requirements for the Degree of

Doctor of Philosophy

(in Biomedical Sciences)

The Graduate School

The University of Maine

August 2024

Advisory Committee:

Robert T. Wheeler, Associate Professor of Microbiology, Advisor

Melody N. Neely, Associate Professor of Molecular and Biomedical Sciences

Melissa Maginnis, Associate Professor of Microbiology

Joshua Kelley, Associate Professor of Biochemistry

James A. Coffman, Associate Professor, MDI Biological Laboratory

SCREEN FOR *CANDIDA ALBICANS* VIRULENCE FACTORS THAT MODULATE THE HOST IMMUNE RESPONSE IN THE LARVAL ZEBRAFISH

By Bailey A. Blair

Dissertation Advisor: Dr. Robert Wheeler

An Abstract of the Dissertation Presented
in Partial Fulfillment of the Requirements for the
Degree of Doctor of Philosophy
(in Biomedical Sciences)
August 2024

Candida is one of the most frequent causes of bloodstream infections in the U.S. The first line of defense against these invasive infections is the innate immune system. Previous work suggests that early immune response is critical in controlling *C. albicans* infection, but *C. albicans* has several strategies to evade the host immune system. Evidence suggests that the ability to transition from yeast to hyphal growth may facilitate immune evasion by limiting early phagocyte recruitment and uptake of *Candida albicans*. Reduced containment of *C. albicans* can lead to uncontrolled hyphal growth, causing damage that can lead to death. However, the mechanism by which *C. albicans* limits recruitment or containment is unknown. To uncover factors important in innate immune evasion, we utilized the transparent larval zebrafish infection model to screen 131 *C. albicans* mutants for altered virulence and immune response. Several mutants with reduced virulence also induced an altered immune response. *NMD5* was found to play a role in limiting phagocytosis, while *BRG1* and *PEP8* were found to modulate the recruitment of macrophages and or neutrophils to the infection site.

Host cells interact with microbial cell wall proteins and secreted products. *RBT1* codes for a hyphal cell wall protein that also contains two secreted peptides, but little is known about its role in pathogenesis. Our preliminary studies suggest that Rbt1p-derived peptides may play a role in virulence. *C. albicans* also has a family of secreted lipases and little is known about how they contribute to virulence. We found that a lipase deficient mutant had reduced virulence. *LIP8* also appears to be important for virulence, but overexpression of this gene could not compensate for the loss of the other lipases.

These results begin to elucidate how lipases and other genes drive virulence. They also identify three new regulators of *Candida*-phagocyte interaction and distinguish recruitment from containment, suggesting that *Candida* modulates both events. This work highlights the ability of *C. albicans* to use multiple strategies that regulate different steps of the immune response such as recruitment and uptake.

ACKNOLEDGEMENTS

I would first like to thank Dr. Robert Wheeler for all of his patience, advice, support and guidance throughout this journey. I would like to thank Siham Hattab for being my partner in crime in the lab, listening to countless practice talks, and always providing valuable feedback. I would also like to thank my fellow graduate students past and present in the Wheeler Lab including Allison Scherer, Brittany Seman, Linda Archambault, Gursimran Dhillon, Nnamdi Baker, and Allie Conner. You all made lab a joy to come to everyday. Additionally, I would like to thank Emma Bragdon, Lena Stasiak, and Meg Caron, helped to contribute to the work in this thesis. I would like to thank Melissa Chisholm for her help in analyzing the *RBT1* whole genome sequencing data, and Caitlin Wiafe-Kwakye for always helping to attempt to figure out coding and bioinformatics. I would like thank Mark Nilan for his wonderful fish care, and the Hube lab for sharing the lipase strains with us. I would also like to thank the University of Maine Institute of Medicine for helping to support this work. Finally, I would like to thank all my friends and family who helped to support me along this journey. I would not have made it all this way without you guys.

TABLE OF CONTENTS

LIST OF TABLES

LIST OF FIGURES

CHAPTER 1

REVIEW OF THE LITERATURE

1.1 *C. albicans* pathogenesis and disease states

There are many *Candida* species that are capable of causing infection including *C. albicans, C. auirs*, *C. dubliensis*, *C. glabrata*, and *C. parapsilosis*. *C. albicans* is the most frequent cause of *Candida* infection, with *C. auris* being a rising concern. *Candida albicans* is a normal commensal of approximately 70% of the population. This fungus can colonize many niches within the host including the skin, mouth, gastrointestinal tract, and vaginal mucosa. While *C. albicans* doesn't typically cause serious infection in healthy individuals, serious life-threatening infections can occur in immunocompromised individuals. Candida is the fourth most common cause of infections in the U.S. (1). It is estimated that there are about 25,000 cases of candidemia annually with mortality rates up to 25% (2–4).

In addition to life threatening bloodstream infections, *C. albicans* can cause superficial infections like oral pharyngeal candidiasis (OPC) or vulvovaginal candidiasis (VVC). Oral infection by *C. albicans* typically occurs in babies or immunocompromised individuals including those with HIV/AIDS. Oral infection by *C. albicans* is characterized by white patches in the mouth, and soreness and redness of the mouth (5).

Most women will have at least one yeast infection in their lifetime, and 23% women will experience recurrent yeast infections (or VVC) (6). Symptoms of VVC include itching, soreness, and abnormal discharge (7). While the symptoms associated with systemic candidiasis and OPC are typically thought to be due to damage by the fungus, much of the pathogenesis associated with VVC is thought to be due to the overactivation of an inflammatory immune response (8). This highlights the importance of having a balanced

immune response to infection so as to defend against pathogens, while causing minimal harm to the host.

Treatment of *C. albicans* and other fungal infections is complicated by the fact that antifungals can be toxic, can have low efficacy, and the rise in antifungal resistance (9). In addition, there are only currently 3 classes of antifungal drugs available to treat fungal infections. New drugs are needed to treat fungal infections, but only one new drug has been introduced in the past ten years (9). Another promising avenue of treatment is drugs that enhance the activity of the immune system against the pathogen. However, in order to develop these types of drugs we must have a good understanding of how the host immune response effectively controls these infections, and any pathogen factors that affect host immune response.

1.2 *C. albicans* virulence

Candida albicans is able to colonize multiple locations within the human host that can vary widely in the local environment. These environments can vary in their pH, nutrient availability, and the cell types and molecules present. In order to survive and cause infection at these locations *C. albicans* has a number of virulence factors that allow it to adapt to the different stresses imposed by these different environments. The ability of *C. albicans* to adhere to and invade host surfaces is critical for causing infection and can also allow for biofilm formation. *C. albicans* biofilms are difficult to treat and are harder for immune cells to infiltrate. *C. albicans* biofilms are composed of both yeast and hyphal cells. The yeast-to-hyphal transition is one of the most well studied virulence traits of *C. albicans*, with filamentous growth allowing for penetration into tissues and causing damage during infection, and yeast cells allowing for dissemination to other tissues (10). *C. albicans* codes

for a number of secreted products including lipases, secreted aspartyl proteinases, and candidalysin. Secreted products can function in nutrient acquisition, and some have even been seen to have immunomodulatory effects. All of these virulence factors and more contribute to *C. albicans* ability to grow and cause infection at different sites within the host.

1.2.1 Yeast-hyphal transition

The ability of *C. albicans* to grow and transition between yeast, psuedohyphal, and hyphal forms is crucial for the virulence of this fungal pathogen. Strains locked in either the yeast or hyphal phase show highly attenuated virulence (11,12). There are many environmental conditions that can stimulate the transition from yeast to hyphal growth including: increased temperature to 37ºC, alkaline pH, 5% CO_2, serum, and N-acetyl glucosamine (13–18). There are many pathways that regulate yeast and hyphal growth, and the genes and pathways are important to induce filamentation is highly dependent on the environmental cues. While some genes/pathways may be important to induce hyphal growth in one environment, they may be dispensable in another. It is generally thought that yeast cells are more important for colonization and dissemination, while filamentous cells are the invasive form that causes damage during infection. However more recently, it has been seen that both yeast and hyphal forms are present during colonization, and that the ratio of yeast-to-hyphae may depend on the specific host niche (19). *C. albicans* hyphal cells can invade epithelial tissue by two mechanisms: induced endocytosis or active penetration.

Regulation of *C. albicans* hyphal growth is a highly complex process with multiple pathways that control hyphal growth and crosstalk between these pathways (Figure 1.1). Some pathways that induce hyphal growth include the MAPK pathway,

cAMP/PKA pathway, and the *RIM101* pathway (13). Transcription factors positively regulating the induction hyphal growth include: *EFG1*, *CPH1, TEC1, FLO8,* and *RIM101* (13,20–22). *EFG1* and *FLO8* work downstream of the cAMP/PKA pathway, while *CPH1* acts downstream of the MAPK pathway (13). Many environmental cues stimulate both MAPK pathway and the cAMP/PKA pathway as Ras1 can stimulate both pathways (13,20–24). The *RIM101* pathway controls hyphal growth in response to pH (25). Negative regulators of filamentation include: *TUP1*, *NRG1*, and *RFG1* (13,26–30). In addition to induction of hyphal growth, further signaling is required to maintain hyphal growth. The transcription factor Ume6, cyclin protein Hgc1, as well as the protein Eed1 are involved in this maintenance of hyphal growth as mutants with deletions of these genes are able to initiate hyphal growth but will only form short hyphae as they are not able to maintain hyphal growth (13,31,32).

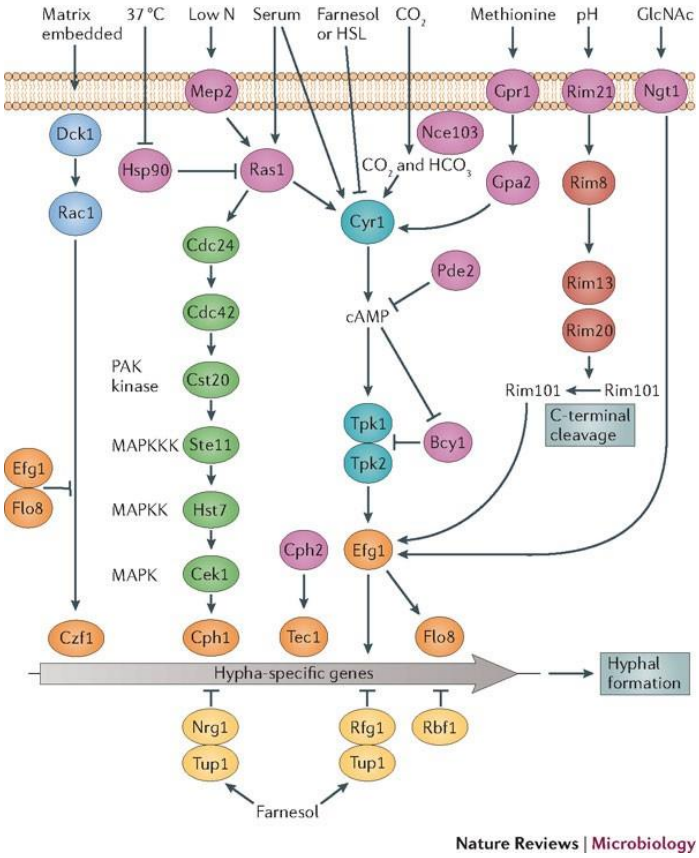

Figure 1.1 *C. albicans* hyphal signaling pathways. Signaling pathways that control hyphal growth in *C. albicans* with their environmental inputs. Different pathways are signified by different colors, with transcription factors in orange, and repressors of hyphal growth in yellow. Diagram from Sudbery (13).

Both yeast and hyphal cell walls are composed of an inner layer of chitin as the innermost layer, then β-1,3 glucan, and β-1,6 glucan, followed by a dense outer layer of O-linked and N-linked mannans and cell wall proteins (Figure 1.2) (33). Yeast cells tend to have more exposure of the β-glucan layer at bud scars (34). The yeast to hyphal transition causes changes in the cell wall proteins and secreted products. In addition, to the change in cell shape during the yeast-to-hyphal transition, there are also many

genes that are upregulated that are dispensable for hyphal growth itself. Many of the genes co-regulated with the yeast to hyphal transition have been found to be important for virulence including *HWP1*, *ECE1*, *ALS3,* and *RBT1* (12,35).

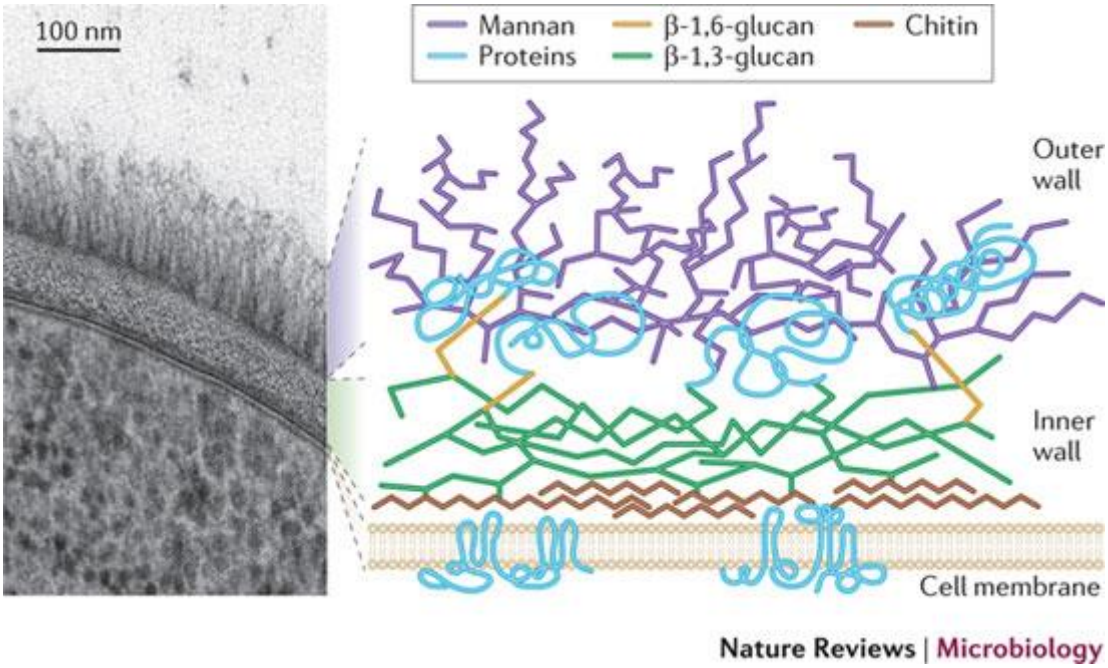

Figure 1.2 *C. albicans* cell wall structure. Structure and organization of the major components of the *C. albicans* cell wall. Diagram by Gow et al (36).

1.2.2 Adherence and invasion

The ability of *C. albicans* cells to adhere to each other and to host surfaces is critical for colonization, virulence, invasion, and biofilm formation. Hyphae are typically thought to be the more adhesive growth form however, it has been observed that yeast cells are better at adhering to endothelial cells under flow conditions (37). Adhesion is required for invasion into host tissues. *C. albicans* can invade host tissue in two ways: induced endocytosis or active penetration. Invasion of oral epithelial cells is mediated by both induced endocytosis and active penetration, while enterocytes are invaded solely by active penetration (38). Invasion via active penetration is mediated

by *C. albicans* while invasion via induced endocytosis is mediated by the host as non-viable *Candida* are also able to be endocytosed (38).

C. albicans has an agglutinin-like sequence (Als) gene family consisting of 8 genes (*AlS1-7* and *ALS9*) (39). These genes code for cell surface proteins that have been seen to play roles in adhesion and invasion into host tissue. Als1-4 are found on the surface of hyphae, while Als5-7 and 9 are on the surface of yeast cells (40). When expressed in *S. cerevisiae ALS1*, *ALS3*, and *ALS5* were able to mediate adhesion to gelatin, fibronectin, laminin, epithelial and endothelial cells (41). Als3 is hyphal expressed and can bind host E-cadherin and N-cadherin to promote endocytosis by epithelial and endothelial cells (42). Another gene that is important in adhesion and biofilm formation that is not a part of the Als family is the hyphal cell wall protein. Hwp1 is seen to bind host transglutaminases to allow attachment to epithelial cells (43).

C. albicans can also bind functionally active plasminogen (via Pra1 & Gpm1 and fibrinogen (via Gpm1) at its cell surface. Pra1 is seen on the yeast and hyphal cell surface, particularly at the tip of hyphae. It is therefore hypothesized that binding of plasminogen and fibrinogen may contribute to tissue invasion by *C. albicans* (44–46).

1.2.3 Biofilms

C. albicans biofilms can form on both biotic surfaces such as epithelial cells and abiotic surfaces such as implanted medical devices like catheters. Biofilms on implanted medical devices can lead to systemic infections (47). Biofilms are difficult to treat because they are more resistant to antimicrobial treatments, and it is harder for immune cells to penetrate the biofilm. Treatment of biofilms from implanted medical

devices typically requires removal of the device along with antifungal treatment (48,49). Biofilms are difficult to treat with antifungals because of the extracellular matrix, upregulation of efflux pumps, and presence of metabolically inactive persister cells within the biofilm (48,50–54).

C. albicans biofilm formation begins with yeast cells adhering to a surface, followed by proliferation of yeast cells. Maturation of the biofilm continues with proliferation of hyphal growth, psuedohyphal growth, yeast cells, and extracellular matrix production. Following maturation yeast cells can then disperse. These dispersed cells can then go on to form new biofilms in a different location (47,55,56). The extracellular matrix of biofilms is comprised of both *C. albicans* and host proteins *in vivo* and can help to provide structural stability to the biofilm (57). The majority of *C. albicans* matrix material is comprised of α-1,6 linked mannan and α-1,2 linked side chains linked to β-1,6-glucan. In addition, the matrix also contains a lot of polysaccharides including glucose, mannose, rhamnose, and *N*-acetylglucosamine (58). Fourteen host proteins have been observed in *in vivo C. albicans* biofilms. These proteins include inflammatory, leukocyte, and heme-related proteins (57). In addition, in the host biofilms are typically multispecies, and *C. albicans* can form biofilms with many different bacterial species.

Many genes are differentially regulated in biofilms compared to planktonic cells. There are six transcription factors that are considered master regulators of biofilm formation. These are Efg1, Tec1, Bcr1, Ndt80, Brg1, and Rob1 (59). These transcription factors regulate 44 additional transcription factors that have been seen to have some role in biofilm formation (60,61). Different transcription factors and their

targets may be required for different stages of biofilm formation. *BRG1* deleted strains are seen to form smaller and morphologically distinct biofilms (59). Bcr1 and downstream targets Als1, Als3, and Hwp1 are necessary for the adherence step of biofilm formation (62–65). Efg1, Tec1, Ndt80, and Rob1 are required for proper hyphal growth during biofilm formation, and Bcr1 is required for hyphae-hyphae adherence in the biofilm (59,65,66). Rlm1 and Zap1 are seen to be important regulators of extracellular matrix formation (67,68). Nrg1 and Pes1 are positive regulators of dispersal, while Ume6 is a negative regulator (69,70). Importantly, yeast cells that are dispersed from biofilms are seen to have increased adherence, biofilm formation capacity, and virulence compared to normal planktonic yeast cells (70).

1.2.4 Secreted products

C. albicans secretes a number of products that can serve a variety of different functions from nutrient acquisition to immune evasion. For example, farnesol is a secreted product that represses hyphal growth in high concentrations. Pra1 is a cell surface and secreted protein that contributes to complement evasion. *C. albicans* also has three types of hydrolytic enzymes that are thought to contribute to virulence including secreted aspartic proteases, lipases, and phospholipases. Lipases and secreted aspartic proteases are discussed further below. Phospholipases are thought to contribute to virulence by disrupting host cell membranes.

1.2.4.1 Lipases

Lipases are proteins that break down triglycerides. *C. albicans* has a family of 10 lipase genes (71). Expression of these genes can differ depending on the environment they are in, and during the different stages of colonization and infection

(71–73). *C. albicans* lipases have not been well studied as of yet and their role in virulence remains largely unknown. However, their expression even in the absence of lipids suggests that they may have roles beyond that of just nutrient acquisition (71). Studies in mice as well as patient samples suggest that there are differences in the lipases expressed during OPC compared to colonization (72,73). In addition, both *LIP2* and *LIP8* have been shown to be important for virulence in models of murine systemic candidiasis (74,75). While these two individual lipases have been implicated in virulence it may be difficult to tease out the roles of all of the individual lipases as expression of one lipase may be able to compensate for the loss of another. Lipases are further discussed in chapter 4.

1.2.4.2 Secreted aspartyl proteinases

C. albicans has a family of 10 secreted aspartyl proteinases (saps). Saps 1-8 are secreted while Saps 9 & 10 GPI-linked cell surface proteins (76). The *SAP* genes are found to be differentially regulated during infection. *SAP9* is seen to be constitutively expressed at high levels with *SAP10* constitutively expressed at lower levels. *SAP5* expression is induced during infection of oral and vaginal reconstituted human epithelium (RHE) cells (77). Saps are thought to contribute to *C. albicans* virulence in multiple ways. Like the family of lipase genes it may be difficult to tease out the individual roles of the *SAP* genes as deletion of one may be compensated by upregulation of another. Indeed, in a model oral RHE infection with a *sap1-3* mutant *SAP5* showed increased expression compared to WT SC5314, and the *sap4-6* mutant showed increased expression of *SAP2* compared to SC5314 (77).

Initial experiments with sap mutant strains implicated saps1-3 in OPC and saps 4-6 in systemic candidiasis, however, these results are complicated due to the use of *URA3* as a selection marker in these strains (78). Saps 1, 2, and 3 have been shown to be able to cleave complement factors C3b, C4b, and C5 *in vitro*. In addition, they limited C3b surface deposition and generation of C5a (79). Evidence suggests that *SAP2* and *SAP6* can induce activation of the NLRP3 inflammasome (80). In addition, *SAP2* and *SAP6* were seen to increase IL-8 and MIP-2 to increase neutrophil recruitment in vaginal epithelial cells as well as the mouse vaginal epithelium, possibly due to increased IL-1β production (81). *SAP5* expression in a *rim101*Δ/Δ restored the ability to degrade E-cadherin and invasion of *C. albicans* between oral mucosal cells (82). It also appears that Sap6 plays a role in oral infection as strain overexpressing Sap6 formed thicker tongue plaques and increased adherence to oral epithelial cells, while *SAP6* mutants showed thinner plaques and reduced adherence (83). This suggests that Sap2 and Sap6 may contribute to the pathology associated with VVC. Sap9 was seen to be able to cleave histatin-5 which has potent anti-candidal activity and is important in defense against OPC. Cleavage of histatin-5 by Sap9 rendered it unable to kill *C. albicans* (84). In addition, *sap9*Δ/Δ and *sap10*Δ/Δ showed a reduced ability to invade and damage oral RHE. For *sap10*Δ/Δ this may be due to reduced adherence, but *sap9*Δ/Δ had increased adherence suggesting *SAP9* has another role in inducing damage to oral epithelial cells (85). These studies suggest Saps play a role in *C. albicans* virulence by promoting adhesion, invasion, and modulation of the host immune response.

1.2.4.3 Candidalysin

Candidalysin is a fungal toxin coded for by the *ECE1* gene in *C. albicans* that is upregulated during hyphal growth. The polypeptide produced by the *ECE1* gene is processed into 8 different peptides, the third of which being the candidalysin peptide (86). Candidalysin has been seen to cause damage to epithelial cells, endothelial cells, and macrophages, leading to damage response signaling patterns (86). During infection *C. albicans* hyphae can form an invasion pocket in host cells into which candidalysin is secreted generating higher concentrations of this toxin within this pocket. In aqueous solutions candidalysin is able to self-assemble into a ring formation that can insert into host membranes leading to calcium influx into these cells and ATP leakage (87,88). This can lead to EGFR activation and MAPK signaling leading to the production of proinflammatory cytokines such as G-CSF, GM-CSF, IL-1α, IL-1β, and IL-6 (86,89). In addition, candidalysin has been observed to activate the NLRP3-inflammasome in macrophages (90,91).

Multiple studies have demonstrated candidalysin to be an important virulence factor during infection. Clinical isolates from patients with vulvovaginal candidiasis (VVC) showed higher expression of *ECE1* than isolates colonizing asymptomatic carriers (88,92). In addition, in a murine model of VVC candidalysin deficient mutants induced less proinflammatory cytokine production and neutrophil recruitment resulting in less tissue damage (88,93). Mucosal infection with candidalysin deficient *C. albicans* showed reduced pathogenesis in murine OPC, and swimbladder infection with candidalysin deficient *C. albicans* showed reduced neutrophil recruitment to the infection site. (86). Candidalysin was also demonstrated to be important for virulence in both murine and

zebrafish disseminated infection (94). While at 1 day post infection mice infected with candidalysin deficient strains had increased fungal burden compared to WT infected, mice still had reduced survival. Candidalysin deficient infected mice had reduced proinflammatory cytokines and neutrophil infiltration in the kidneys. By 4 days post infection fungal burdens were similar, but WT *C. albicans* was more invasive. This data may suggest that the excess inflammation and immune infiltration early on during infection caused more damage and worsened infection outcomes for WT infected mice (94). In addition to playing a role in promoting the recruitment of neutrophils to the infection site, candidalysin also appears to contribute to the stimulation of neutrophil extracellular trap (NET) formation. Candidalysin deficient *C. albicans* induced less NET formation and incubation of neutrophils with the peptide alone induce formation of more condensed NET like structures (95).

1.3 Immune response to *C. albicans*

Host cells detect *C. albicans* through their pattern recognition receptors (PRRs). The two main classes of PRRs that recognize *C. albicans* are toll-like receptors (TLRs), and C-type lectin receptors (CLRs). TLRs signal through the adaptor protein MyD88, while CLRs signal through Card9, but both stimulate activation of NF-κB (40,96–99). NF-κB then translocates to the nucleus to drive transcription of proinflammatory cytokines. Host PRRs recognize pathogen associated molecular patterns on *C. albicans.* TLR2, TLR4, dectin-2, and mincle are able to bind different mannans of *C. albicans* cell wall, while dectin-1 can recognize and bind β-glucan (9,40,100–103).

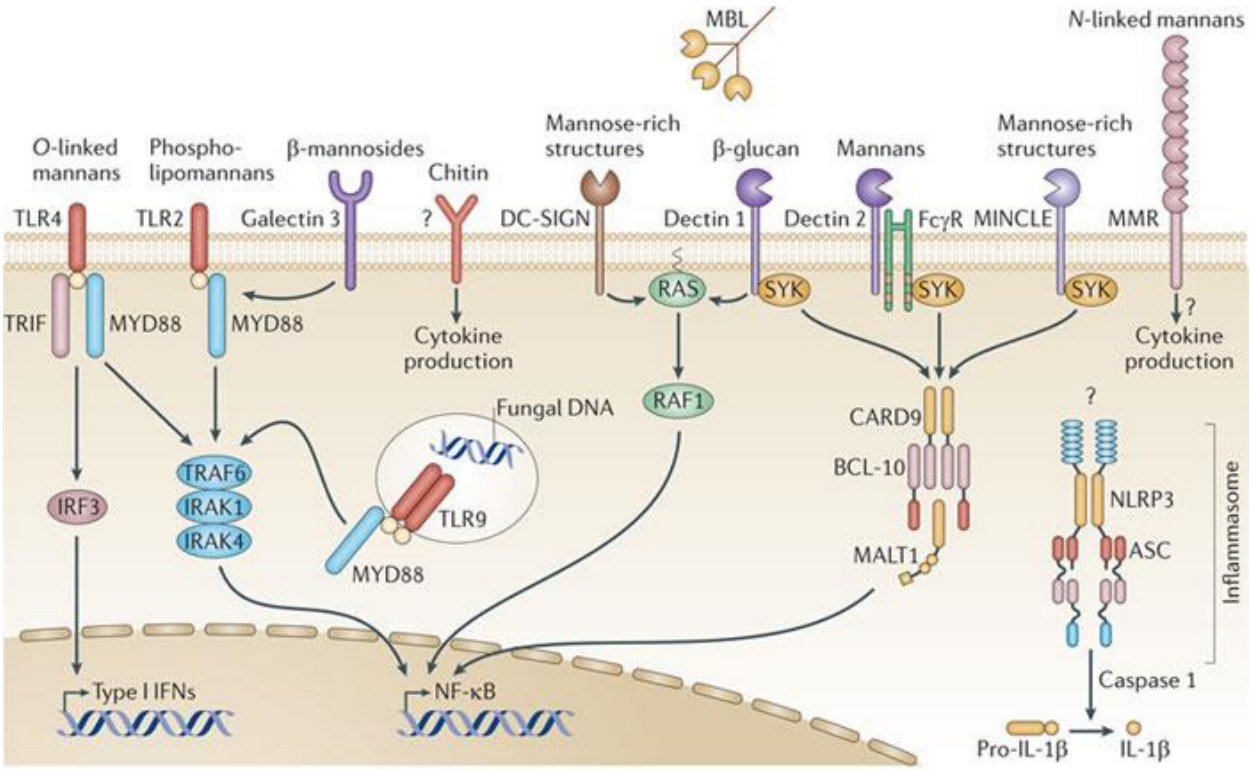

Figure 1.3 Cell wall recognition by host cell receptors. Host cell receptors that recognize and the respective *C. albicans* PAMPs that they recognize. Downstream signaling pathways leading to cytokine/chemokine production are also shown. Diagram by Gow et al (36).

Epithelial cells are typically the first cells to come into contact with *C. albicans*. Epithelial cells can differentiate between colonizing yeast and infection (104). Upon detection of *C. albicans* infection epithelial cells secrete antimicrobial peptides such as β-defensins to directly fight off infection. Many antimicrobial peptides against *C. albicans* work by disrupting the cell membrane, and many also act as chemoattractants (105). In addition, epithelial cells can produce proinflammatory cytokines and reactive oxygen species (ROS) to recruit immune cells such as phagocytes to the infection site. Both dual oxidase and phagocyte oxidase were seen to be important for the control of infection and recruitment of phagocytes to a *C. albicans* zebrafish hindbrain infection model (106,107). Epithelial cells

can secrete granulocyte colony-stimulating factor (G-CSF), granulocyte-macrophage colony-stimulating factor (GM-CSF), IL-1α, IL-1β, IL-6, IL-8, and RANTES to promote the recruitment of phagocytes (105,108).

Macrophages and neutrophils detect PAMPs of *C. albicans* cell wall through the use of pattern recognition receptors PRRs. Binding of *C. albicans* via PRRs, complement receptor 3 (CR3), or the Fc receptor triggers phagocytosis (9,109). Fusion of the phagosome and lysosome forms the phagolysosome in which many stresses are imposed to kill the fungus. The phagolysosome is acidified, and ROS and reactive nitrogen species (RNS) are produced in a concerted effort to kill *C. albicans* (9,110). However, *C. albicans* hyphal cells are often too large to be effectively phagocytosed. In these cases, phagocytes have been seen to undergo 'frustrated phagocytosis' where they wrap themselves around the hyphae (111). Macrophages are able to fold *C. albicans* hyphae at septal junctions damaging the cells wall, exposing β-glucan and chitin, and inhibiting growth (112). Macrophages can secrete TNF-α, IL-1α, IL-1β, and IL-6, and this can promote recruitment of neutrophils (40).

Neutrophils are known to be important for protection against *C. albicans* and can be recruited and activated by IL-6, IL-8, TNF-α, G-CSF, and GM-CSF (113). In addition to phagocytosis neutrophils also have methods to kill *C. albicans* extracellularly. Neutrophils contain granules with a number of fungicidal molecules including myeloperoxidase, cathepsins, defensins, and lactoferrin (40,114). Degranulation and extracellular production of ROS assist with killing *C. albicans* extracellularly (115). In addition, neutrophils can produce neutrophil extracellular traps (NETs). NETs are decondensed chromatin expelled from the neutrophil extracellularly and contain antimicrobial molecules such as calprotectin (116). NETs may also stimulate neutrophil swarming (117). Neutrophil swarming is the coordinated

migration of a group of neutrophils to clusters of microbes. Swarming can help to enhance the activities of the neutrophils within the swarm and helps to contain the infected area and restrict C. albicans growth (118–120).

Complement has been shown to be crucial to the immune response against *C. albicans*, as mice that are complement deficient are more susceptible to infection (121,122). *C. albicans* activates all three complement pathways, however, the thick cell wall of *C. albicans* seems to protect it from the membrane attack complex. C3b can be deposited on the cell surface of *C. albicans* as well as an anti-*Candida* antibody (123). These can be recognized by the CR3 and Fc receptor respectively on phagocytes. Interaction with these receptors triggers phagocytosis of *C. albicans*. In addition, C5a can induce production of proinflammatory cytokines IL-6 and IL-1β (124).

Platelets are beginning to be recognized as having an important role in the immune response to microbial pathogens. Platelets have been observed to directly bind to and be activated by both *C. albicans* yeast and hyphal cells (125,126). Platelets can secrete antimicrobial peptides, cytokines, chemokines, and complement proteins (127). Recently, thrombin stimulated platelets were seen to kill *C. albicans* (128) . In addition, platelets can guide neutrophils and monocytes to help them reach the site of infection and extravagate (129). They are also often associated with NETs (130,131). Studies suggest that platelets play an important role in promoting the recruitment of neutrophils to the site of infection. Indeed, *il17ra*$^{-/-}$ mice with reduced platelet numbers showed increased susceptibility to OPC, with a reduction in neutrophils to the tongue tissue (132).

C. albicans also triggers the activation of the NLRP3, NLRC4, and NLRP10 inflammasomes (133). The inflammasome is important for protection against *C. albicans* as

mice deficient in NLRP3 are more susceptible to systemic and oral candidiasis (134,135). Inflammasome activation leads to the production of IL-1 β and IL-18 (133). *C. albicans* has been seen to activate the NLRP3 inflammasome in macrophages which can lead to pyroptosis. Both a priming and an activating signal must occur in order to trigger pyroptosis. A *C. albicans* cell surface protein Pga52 was seen to be important for activating pyroptosis in macrophages. Importantly, in infections with mutants that did not trigger pyroptosis, there was reduced neutrophil recruitment (136,137).

Dendritic cells are the bridge between the innate and adaptive immune response to *C. albicans* as the main antigen presenting cell (APC). Dendritic cells are recruited to *C. albicans* infection via CCL20 and β-defensins (138,139). Dendritic cells phagocytose *C. albicans*, degrade them, then display the antigen peptides on the surface to stimulate T-cell differentiation (133). Dendritic cells can stimulate the differentiation of both CD4+ T-helper cells, and CD8+ cytotoxic T-cells (133). While cytotoxic T-cells have been seen to inhibit hyphae *in vitro*, T-helper cells seem to be the main adaptive immune cell type for protection against *C. albicans* (140). This is highlighted by the fact that HIV/AIDS patients with reduced CD4+ T-cells are more susceptible to OPC. Yeast cells push T-cell differentiation towards a Th1 response, whereas hyphae push towards a Th2 response (141,142). While Th1 and Th17 cells are seen to be protective against *C. albicans* infection, a Th2 phenotype is associated with increased *C. albicans* growth and dissemination (133). Th1 differentiation is driven by IL-12 and Th2 differentiation is driven by IL-4 (143). IL-1 β, IL-23, and IL-6 promote polarization to the Th17 phenotype (133,144,145). Th17 cells secrete IL-17 and IL-22. IL-17 can recruit and activate neutrophils, while IL-22 enhances barrier function of epithelial cells (146,147). While antibodies against Als3, SAPs, or Hsp90 (heat shock protein

90) have been seen to be experimentally protective against *C. albicans* mice deficient in B-cells are not any more susceptible to *C. albicans* infection suggesting they don't play a large role in the defense against *C. albicans* (148–152).

A coordinated and controlled immune response against *C. albicans* is critical to effectively control infection. Overstimulation of the inflammatory response can be harmful to the host and cause damage. This can be seen during sepsis, and much of the pathology associated with VVC is thought to be due to an overactive inflammatory response. Therefore, there must be balance in the inflammatory response to promote fungal killing and prevent excessive host damage.

1.4 *C. albicans* immune evasion mechanisms

C. albicans has several mechanisms to help it avoid destruction by the host immune response. However, the molecular mechanisms behind many of the different strategies of immune evasion is not entirely understood. The first strategy to evade the host immune response is to avoid detection by host cells. *C. albicans* is recognized by host cells via pathogen associated molecular patterns (PAMPs) in its cell wall such as β-glucan. β-glucan of the cell wall is usually shielded with the outer layer of mannans and is exposed more at areas like bud scars. To avoid detection *C. albicans* can shield or mask the PAMPs in its cell wall. *C. albicans* can mask its cell wall epitopes due to different environmental cues such as changes in oxygen availability, carbon source, or hormone levels (153).

It is also thought that *C. albicans* can limit the recruitment of macrophages and neutrophils to the infection site, but few details into this mechanism are known other than that it is associated with the ability to transition to hyphal growth (106). Once immune cells are recruited to the infection site *C. albicans* may be able to limit the ability of these cells to

engulf *C. albicans*. One which way that *C. albicans* can limit phagocytosis is through filamentous growth as hyphal cells can become too large to be able to be fully engulfed by host cells.

If engulfed by host cells *C. albicans* has methods to survive the stresses imposed on it. *C. albicans* has been seen to be able to inhibit the fusion of the phagosome with the lysosome (154). *C. albicans* can detoxify the phagolysosome by producing Super oxide dismutase's and catalase to counteract ROS (155,156). In addition, *C. albicans* can also detoxify RNS converting nitric oxide to ammonia via Yhb1 (157). This ammonia can also help to alkanize the phagolysosome (158). *C. albicans* also protects itself from multiple host antimicrobial peptides by shedding Msb2 from its surface to bind and inactivate these peptides (159,160).

If *C. albicans* survives within the host cells it may be able to then escape from these cells, and this may be at sites away from the original site of infection causing a disseminated infection. *In vitro*, *C. albicans* can switch to hyphal growth inside of host macrophages eventually piercing and killing these cells, allowing their escape (161,162). However, this has not been observed *in vivo*. While this mechanism for escape is not certain, *C. albicans* has been observed to escape from immune cells via non-lytic expulsion (163,164). In addition, *C. albicans* has been seen to activate the NLRP3 inflammasome which can lead to pyroptosis and possible escape this way (136,161).

1.4.1 Complement evasion by *C. albicans*

C. albicans also has the ability to limit the complement pathway via Saps, Gpm1, and Pra1. Gpm1 is a cell surface protein that is seen to bind Factor H, Factor H like protein (FHL-1), and plasminogen (44). Pra1 is a yeast and hyphal cell surface and secreted protein that has been shown to bind Factor H, FHL-1, C3, C3b, C4BP,

plasminogen, and fibrinogen (45,46,165,166). While Pra1 is seen on the surface of both yeast and hyphal cells expression of *PRA1* is induced with hyphal growth and significantly more Pra1 is seen on the surface of hyphae than yeast cells (45). Factor H, FHL-1, or C4BP are complement inhibitors, and when bound to the cell surface of *Candida* retain their activity and therefore can continue to further inhibit complement activation. Secreted Pra1 can bind C3 blocking its cleavage and preventing the C3a and C5a generation. In addition, this can inhibit C3b/iC3b surface deposition leading to reduced phagocytosis by human macrophages (165).

1.5 Zebrafish as a model of infection

The larval zebrafish is a unique and powerful model to study host pathogen interactions. This model helps to bridge the gap between the more simplistic *in vitro* systems, and the less visible mammalian models. Larval zebrafish provide the complexity of the host environment with multiple cells types able to respond to infection, while also being transparent to allow visualization of host pathogen dynamics in real time. This model has been used to gain insight into many different pathogens including several bacterial, viral, and fungal pathogens (167,168). Not only has this allowed us to learn about the virulence factors of these pathogens, but also the dynamics of the host response to these infections.

Zebrafish have a largely conserved immune system to humans. All of the major human immune cells have been identified in zebrafish, as well as the complement system. In addition, zebrafish have all of the major classes of pattern recognition receptors and pro- and anti- inflammatory signaling molecules (168). As early as 1 day post fertilization (dpf) zebrafish have a functional innate immune system that is able to respond to infection. Functional zebrafish macrophages are present as early as 26 hours post fertilization (hpf) and

neutrophils at 34 hpf (168). While the innate immune system is active from 1 dpf the adaptive immune system isn't fully functional until approximately 3-4 weeks post fertilization. This allows the focused study on the role of the innate immune system in the zebrafish without influence of the adaptive immune response.

There are many mutant and transgenic zebrafish lines available that enable the study of the immune response to infection. Fish with fluorescently marked macrophages or neutrophils allow us to visualize recruitment and phagocytosis dynamics during infection. In addition, there are fish with fluorescent reporters for immune signaling molecules such as *tnfa*, or *nfkb*. These transgenic zebrafish lines allow for the visualization of the immune response to infection in real time. An advantage of the larval zebrafish is that infections in this model can be followed over the course of multiple days. Time course and time lapse imaging can lead to important insights into the temporal dynamics of the immune response to pathogens such as *C. albicans*.

In addition to allowing for the visualization of the immune response via fluorescently labeled immune cells there are several mutant fish lines, morpholinos, or chemical treatments that allow perturbation of the immune response (167). Both chemical inhibition by DPI (diphenyleneiodonium) and morpholino knockdown have been used to inhibit reactive oxygen species production in zebrafish (106,107). *Tg(mpx:mCherry-2A-Rac2)* and *Tg(mpx:CXCR4-WHIM-GFP)*fish are both transgenic fish lines with non-functional neutrophils (169,170). Macrophages can be depleted in larval zebrafish through injection of clodronate liposomes or addition of metronidazole to the water of *Tg(mpeg1:Gal4/UAS:NfsB-mCherry)* (171–173). All of these methods and more have provided valuable insight into the importance of different immune components to infection.

There are several sites of injection available for use in the larval zebrafish. Disseminated infection models include injection into the caudal vein or duct of Cuvier. Localized infections include the hindbrain ventricle, yolk sack, otic vesicle, muscle, and swimbladder. The use of different infection sites is advantageous for the study of many pathogens such as *C. albicans* that can colonize and infect multiple sites in humans. The zebrafish swimbladder is an air-filled organ with similarities to the human lung. This provides a mucosal surface in which we can study infection. Use of localized infections can allow for insight into immune recruitment dynamics, as well as dissemination of the pathogen to other host tissues. At 36 hpf the zebrafish hindbrain is a fluid filled cavity with very few immune cells present. This makes the hindbrain infection model a good model to study immune recruitment to infection allowing us to gain insight into both host and pathogen factors influencing recruitment.

1.5.1 Insights gained into *C. albicans* infection using larval zebrafish

While the standard temperature for raising zebrafish is 28ºC, another advantage of this model is their ability to live at a temperature range from 21ºC to 33ºC. This is advantageous in the study of *C. albicans* to allow for the manipulation of *Candida* morphology using temperature. Growth at lower temperatures promotes more yeast growth in the zebrafish, while raising the temperature promotes more hyphal growth. This has allowed valuable insight into the roles of yeast and hyphae in dissemination and damage associated with infection. Use of the yolk infection model was used to demonstrate the roles for yeast in dissemination and filamentous growth in causing damage during infection (10). Scherer et al (164) observed that host macrophages were able to carry *C. albicans* away from the initial infection site of the yolk sac and into the bloodstream where these yeast cells were then able to exit from the macrophages. While dissemination via macrophages was observed, host

phagocytes were not necessary for dissemination, as there was still dissemination in fish without functional macrophages and neutrophils. This work demonstrated that there are multiple routes in which *C. albicans* dissemination can occur.

The swimbladder infection model has been used to demonstrate the synergistic relationship between *C. albicans* and *P. aeruginosa* during mucosal infection, with co-infected fish showed decreased survival compared to those infected with *C. albicans* or *P. aeruginosa* alone (174). Archambault et al. (175) demonstrated differences in the ability of *C. albicans* and *C. parapsilosis* to stimulate an inflammatory response during swimbladder infection. *C. albicans* was able to induce greater production of inflammatory cytokines and had increased numbers of neutrophils and macrophages recruited compared to *C. parapsilosis*.

Using the hindbrain zebrafish infection model Brothers et al. (106) demonstrated the importance of reactive oxygen species in the recruitment of immune cells early on during *C. albicans* infection. This early recruitment was crucial for the containment of infection and survival of zebrafish larvae. In addition, work in this model suggested that *C. albicans* can limit phagocyte recruitment to the hindbrain ventricle, and that this may be linked to the ability to transition and grow in the hyphal form.

1.6 Summary

Candida albicans can cause infections ranging from superficial mucosal infections to deadly systemic blood stream infections. The ability to cause infection at these different sites within the body is aided by an arsenal of virulence factors that *C. albicans* possesses, including the ability to switch between yeast and hyphal forms, secreted proteins, and immune evasion. The larval zebrafish is a powerful model that

allows for visualization of host pathogen interactions. We leveraged this model to screen for *C. albicans* virulence factors, and the impact that they have on the host immune response.

CHAPTER 2

SCREEN FOR *C. ALIBICANS* VIRULENCE FACTORS THAT MODULATE THE HOST IMMUNE RESPONSE

2.1 Introduction

Candida albicans is the one of most common bloodstream infections in the U.S. causing approximately 25,000 cases annually (2). *C. albicans* can normally be found as a commensal in the gastrointestinal tract, mouth, skin, or vagina in up to 70% of the population (3,8,176). While *C. albicans* is found in healthy individuals it can also cause infections ranging from superficial mucosal infections such as vulvovaginal candidiasis and oropharyngeal candidiasis, to lethal systemic infections with attributable mortality rates of approximately 25% (177,178). The host immune response is tasked with protecting individuals from these infections with the innate immune system being of special importance in fighting systemic *Candida* infections. In turn, *C. albicans* employs many mechanisms to subvert the actions of the host immune attack (153,179–186). While we understand some of how *C. albicans* can evade host immune responses *in vitro*, we still know little about this during vertebrate infection.

The innate immune response is the first line of defense against *C. albicans* and is critical in controlling and preventing systemic candidiasis (187–191). This is highlighted by the fact that patients with neutropenia are more susceptible to invasive *Candida* infections, and mice with macrophage defects survive experimental systemic infection poorly. Phagocytes get to the infection site by following cytokine and chemokine gradients and presumably identify fungal cells for ingestion using fungal-derived chemoattractants (189,190,192). While phagocytes play crucial roles, other innate immune cells such as epithelial cells, microglia,

natural killer cells and innate lymphocytes also play important roles (190,193). Cytokines and chemokines, which bring phagocytes to the infection site, simultaneously activate them and induce their differentiation. Once there, they must locate fungal cells by soluble cues, recognize them based on surface patterns and opsonins, and initiate phagocytosis.

Immune cells such as phagocytes recognize pathogen associated molecular patters (PAMPs) in *C. albicans* cell wall, but *C. albicans* is able to shield them from immune cells behind a layer of mannosylated proteins of the outer cell wall (153). Macrophages and neutrophils are the main effector cells against *C. albicans* and employ many strategies to kill *C. albicans.* These cells are able to phagocytose *C. albicans* yeast as well as short hyphae, produce antimicrobial peptides, reactive oxygen species, and extracellular traps to combat *C. albicans* (181,185,186,194). Not only can *C. albicans* shield its cell wall PAMPs from these cells, but once taken up by a phagocyte *C. albicans* can survive by preventing the fusion of the phagosome with the lysosome, alkanizing the acidic environment of the phagolysosome, producing catalase and superoxide dismutase to counteract ROS, and upregulating DNA repair systems and heat shock proteins to counteract damage caused to DNA and proteins (195,196). In addition, *C. albicans* has also been seen to escape from host cells such as macrophages by inducing pyroptosis; or also, although rare, vomocytosis (195,197). The interactions between host phagocytes and *C. albicans* are complex and we do not fully understand the mechanisms at play, especially from the side of *C. albicans*. If we are able to better understand how *C. albicans* is able to subvert the host immune system, we may be able to come up with new targets for treatment.

The larval zebrafish provides a great model to investigate the interactions between *C. albicans* and the host innate immune response (9,167,198). The transparency and availability

of many transgenic lines allow us to watch the immune response to *C. albicans* infection in the context of a live host. Previous results suggest that the early phagocyte response is critical to zebrafish's ability to survive a *C. albicans* hindbrain ventricle infection (106,199). Evidence from the larval zebrafish also suggest that *C. albicans* has the ability to limit this response be reducing the recruitment of phagocytes to the infection site (106). This ability to limit phagocyte recruitment was observed for a WT *C. albicans* strain, but not a yeast locked strain, suggesting this response (mechanism) may be regulated with the yeast to hyphal transition.

We sought to identify new *C. albicans* factors playing a role in limiting early phagocyte responses by leveraging the transparent zebrafish infection model. Since virulence is linked to early phagocytic containment, we screened 131 engineered *C. albicans* mutants for virulence defects in the larval zebrafish hindbrain infection model. Since there may be links between evasion of phagocyte recruitment and the yeast-to-hyphal transition, we chose mutants that had been characterized to have either an infectivity defect only or a morphogenesis defect only (200). Since little is known about soluble chemoattractants secreted by *Candida*, we also included single mutants from groups of genes that code for secreted proteins. Mutations that were associated with hypovirulence and could be faithfully complemented were then screened for multiple phagocyte recruitment and containment phenotypes during early infection. We identified three genes that regulate early phagocyte-*Candida* immune interactions, and this revealed some surprising relationships among immune recruitment, fungal containment, and overall immunity.

2.2 Materials and methods

2.2.1 *C. albicans* strains and growth conditions

C. albicans mutant strains for screening were obtained from the Noble library (200). For infection, strains were grown on yeast-peptone-dextrose (YPD) agar at 30ºC (20 g/L glucose, 20 g/L peptone, 10 g/L yeast extract, 20 g/L agar, Difco, Livonia, MI). Single colonies were picked from plates and inoculated into 5mL liquid YPD and grown overnight on a wheel at 30°C. Overnight cultures were resuspended in PBS (phosphate buffered saline, 5 mM sodium chloride, 0.174 mM potassium chloride, 0.33 mM calcium chloride, 0.332 mM magnesium sulfate, 2 mM HEPES in Nanopure water, pH = 7) and stained with Calcofluor white (750 µg/ml) when necessary. Cultures were washed twice with PBS and the concentration was adjusted to $1x10^7$ CFU/ml in PBS for injection. For imaging, strains were transformed with pENO1-iRFP-NAT^r according to (174). Strains were screened by fluorescence microscopy and flow-cytometry to pick the brightest isolates. Full deletion of *RBT1* from SN250 was achieved using the SAT-flipper method as described previously (201) using LiAC transformation. The deletion cassette was generated by integrating 514 bp up and 485 bp downstream of *RBT1* into a pSFS2 derivative (201) and was excised by restriction digest with KpnI and SacI.

2.2.2 Complementation of mutant strains

Complementation constructs were ordered from Genscript (Piscataway, NJ) in the pUC57 backbone and contain the ORF with 200 bp upstream and 50 bp downstream, followed by *C. dubliensis ARG4* (Figure A.1A). Restriction sites were eliminated from the ORF during gene synthesis. A restriction site was designed within the 200 bp

upstream region, an NdeI cutsite at the start of the ORF, a BamHi restriction site in *ARG4* upstream region, and a BglII site in the downstream *ARG4* region. An *NMD5* complementation construct was ordered from Twist Bioscience (South San Francisco, CA) without *ARG4.* This construct included an upstream XbaI restriction site, a 200 bp *NMD5* upstream region containing an XhoI restriction site, the *NMD5* ORF, the mNeon ORF (202) flanked by NcoI restriction sites and a PacI restriction site, then 50 bp of the *NMD5* downstream region, and a BamHi site in an *ARG4* upstream region. This region was then cloned into the Genscript pUC57 backbone by cutting with the with XbaI and BamHi to remove the *PEP8* region and replace it with the *NDM5* region to get an *NMD5* construct containing *ARG4* (Figure A.1B). For complementation, constructs were cut with the appropriate restriction enzymes, and a LiAC transformation was performed using rescue of the *ARG4* autotrophy as a selection marker. PCR was performed to ensure correct integration. *NMD5* complementation colonies were screened by flow cytometry for mNeon-positive cells. Sequences of the complementation constructs are provided in Table A.3.

Table 2.1: *Candida albicans* strains

Strain	Parental Strain	Genotype	Reference
*yfg*Δ/Δ (Your Favorite Gene) See Table A.1 for complete list of mutant strains	SN152	*ura3*Δ-*iro1*Δ::*imm*^{434}/*URA3-IRO1*, *his1*Δ/*his1*Δ, *arg4*Δ/ *arg4*Δ, *leu2*Δ/*leu2*Δ, *yfg*Δ::*C.mLEU2*/ *yfg*Δ::*C.dHIS1*	(200)
SN250-iRFP	SN152	*ura3*Δ-*iro1*Δ::*imm*^{434}/*URA3-IRO1*, *his1*Δ/*his1*Δ, *arg4*Δ/ *arg4*Δ, *leu2*Δ::*C.m.LEU2/leu2*Δ::*C.d.HIS1*, *pENO1-iRFP-NATR*	(200), This Study
*rbt1*Δ/Δ$^{968\text{-}2166}$- iRFP	SN152	*ura3*Δ-*iro1*Δ::*imm*^{434}/*URA3-IRO1*, *his1*Δ/*his1*Δ, *arg4*Δ/ *arg4*Δ, *leu2*Δ/*leu2*Δ, *rbt1*Δ$^{967\text{-}}$	(200), This Study

Table 2.1 continued

		*^{2166}::C.mLEU2/rbt1*Δ*$^{967-3166}$::C.dHIS1*, *pENO1-iRFP-NATR*	
*cht2*Δ/Δ- iRFP	SN152	*ura3*Δ-*iro1*Δ::*imm^{434}/URA3-IRO1*, *his1*Δ/*his1*Δ, *arg4*Δ/ *arg4*Δ, *leu2*Δ/*leu2*Δ, *cht2::C.mLEU2/cht2::C.dHIS1*, *pENO1-iRFP-NATR*	(200), This Study
*rim101*Δ/Δ- iRFP	SN152	*ura3*Δ-*iro1*Δ::*imm^{434}/URA3-IRO1*, *his1*Δ/*his1*Δ, *arg4*Δ/ *arg4*Δ, *leu2*Δ/*leu2*Δ, *rim101::C.mLEU2/rim101::C.dHIS1*, *pENO1-iRFP-NATR*	(200), This Study
*brg1*Δ/Δ- iRFP	SN152	*ura3*Δ-*iro1*Δ::*imm^{434}/URA3-IRO1*, *his1*Δ/*his1*Δ, *arg4*Δ/ *arg4*Δ, *leu2*Δ/*leu2*Δ, *brg1::C.mLEU2/brg1::C.dHIS1*, *pENO1-iRFP-NATR*	(200), This Study
*cek1*Δ/Δ- iRFP	SN152	*ura3*Δ-*iro1*Δ::*imm^{434}/URA3-IRO1*, *his1*Δ/*his1*Δ, *arg4*Δ/ *arg4*Δ, *leu2*Δ/*leu2*Δ, *cek1::C.mLEU2/cek1::C.dHIS1*, *pENO1-iRFP-NATR*	(200), This Study
*pep8*Δ/Δ- iRFP	SN152	*ura3*Δ-*iro1*Δ::*imm^{434}/URA3-IRO1*, *his1*Δ/*his1*Δ, *arg4*Δ/ *arg4*Δ, *leu2*Δ/*leu2*Δ, *pep8::C.mLEU2/pep8::C.dHIS1*, *pENO1-iRFP-NATR*	(200), This Study
*nmd5*Δ/Δ- iRFP	SN152	*ura3*Δ-*iro1*Δ::*imm^{434}/URA3-IRO1*, *his1*Δ/*his1*Δ, *arg4*Δ/ *arg4*Δ, *leu2*Δ/*leu2*Δ, *nmd5::C.mLEU2/nmd5::C.dHIS1*, *pENO1-iRFP-NATR*	(200), This Study
*apm1*Δ/Δ- iRFP	SN152	*ura3*Δ-*iro1*Δ::*imm^{434}/URA3-IRO1*, *his1*Δ/*his1*Δ, *arg4*Δ/ *arg4*Δ, *leu2*Δ/*leu2*Δ, *apm1::C.mLEU2/apm1::C.dHIS1*, *pENO1-iRFP-NATR*	(200), This Study
*mad2*Δ/Δ- iRFP	SN152	*ura3*Δ-*iro1*Δ::*imm^{434}/URA3-IRO1*, *his1*Δ/*his1*Δ, *arg4*Δ/ *arg4*Δ, *leu2*Δ/*leu2*Δ,, *mad2::C.mLEU2/mad2::C.dHIS1*, *pENO1-iRFP-NATR*	(200), This Study
*ece1*Δ/Δ - dtom	BWP17	*ura3::imm434/ura3::imm434*, *iro1::imm434/iron1::imm434*, *his1::hisG/his1::hisG*, *arg4::hisG/arg4::hisG*,	(203)

Table 2.1 continued

		ece1::HIS2/ece1::ARG4, RPS1/rps1::URA3, ENO1/eno1::dTom-NATR	
*ece1*Δ/Δ+*ECE1* - dtom	BWP17	*ura3::imm434/ura3::imm434, iro1::imm434/iron1::imm434, his1::hisG/his1::hisG, arg4::hisG/arg4::hisG, ece1::HIS2/ece1::ARG4, RPS1/rps1::URA3-ECE1, ENO1/eno1::dTom-NATR*	(203)
NRG1^{OEX}-iRFP	THE21	*ade2::hisG::/ade2::hisG ura3::imm434/ura3::imm434::URA2-tetO ENO1/eno1::ENO1 tetR – ScHAP4AD-3XHA-ADE2 pENO1-iRFP-NATR*	(10,204)
*rbt1*Δ/Δ$^{968\text{-}2166}$ +*RBT1*	*rbt1*Δ/Δ$^{968\text{-}2166}$	*ura3*Δ*-iro1*Δ*::imm*^{434}*/URA3-IRO1, his1*Δ*/his1*Δ, *arg4*Δ*/ arg4*Δ, *leu2*Δ*/leu2*Δ, *rbt1*Δ$^{967\text{-}2166}$*::C.mLEU2/rbt1*Δ$^{967\text{-}2166}$*::C.dHIS1 RBT1::C.d.ARG4*	This Study
*rim101*Δ/Δ+*RIM101*	*rim101*Δ/Δ	*ura3*Δ*-iro1*Δ*::imm*^{434}*/URA3-IRO1, his1*Δ*/his1*Δ, *arg4*Δ*/ arg4*Δ, *leu2*Δ*/leu2*Δ, *rim101*Δ*::C.mLEU2/ rim101*Δ*::C.dHIS1 RIM101::C.d.ARG4*	This Study
*brg1*Δ/Δ+*BRG1*	*brg1*Δ/Δ	*ura3*Δ*-iro1*Δ*::imm*^{434}*/URA3-IRO1, his1*Δ*/his1*Δ, *arg4*Δ*/ arg4*Δ, *leu2*Δ*/leu2*Δ, *brg1*Δ*::C.mLEU2/ brg11*Δ*::C.dHIS1 BRG11::C.d.ARG4*	This Study
*cek1*Δ/Δ+*CEK1*	*cek1*Δ/Δ	*ura3*Δ*-iro1*Δ*::imm*^{434}*/URA3-IRO1, his1*Δ*/his1*Δ, *arg4*Δ*/ arg4*Δ, *leu2*Δ*/leu2*Δ*, cek1*Δ*::C.mLEU2/ cek1*Δ*::C.dHIS1 CEK1::C.d.ARG4*	This Study
*pep8*Δ/Δ+*PEP8*	*pep8*Δ/Δ	*ura3*Δ*-iro1*Δ*::imm*^{434}*/URA3-IRO1, his1*Δ*/his1*Δ, *arg4*Δ*/ arg4*Δ, *leu2*Δ*/leu2*Δ, *pep8*Δ*::C.mLEU2/ pep8*Δ*::C.dHIS1 PEP8::C.d.ARG4*	This Study
*nmd5*Δ/Δ+*NMD5-mNeon -iRFP*	*nmd5*Δ/Δ*-iRFP*	*ura3*Δ*-iro1*Δ*::imm*^{434}*/URA3-IRO1, his1*Δ*/his1*Δ, *arg4*Δ*/ arg4*Δ, *leu2*Δ*/leu2*Δ, *ndm5*Δ*::C.mLEU2/ nmd5::C.dHIS1 NMD5-mNeon::C.d.ARG4, pENO1-iRFP-NATR*	This Study
*amp1*Δ/Δ+*APM1*	*apm1*Δ/Δ	*ura3*Δ*-iro1*Δ*::imm*^{434}*/URA3-IRO1, his1*Δ*/his1*Δ, *arg4*Δ*/ arg4*Δ, *leu2*Δ*/leu2*Δ, *apm21*Δ*::C.mLEU2/ apm1*Δ*::C.dHIS1 APM1::C.d.ARG4*	This Study

Table 2.1 continued

*mad2*Δ/Δ+*MAD2*	*mad2*Δ/Δ	*ura3*Δ-*iro1*Δ::*imm*^{434}/*URA3-IRO1*, *his1*Δ/*his1*Δ, *arg4*Δ/ *arg4*Δ, *leu2*Δ/*leu2*Δ, *mad2*Δ*::C.mLEU2/ mad2*Δ*::C.dHIS1 MAD2::C.d.ARG4*	This Study
*rbt1*Δ/Δ	SN250	*ura3*Δ-*iro1*Δ::*imm*^{434}/*URA3-IRO1*, *his1*Δ/*his1*Δ, *arg4*Δ/ *arg4*Δ, *leu2*Δ::*C.m.LEU2/leu2*Δ::*C.d.HIS1*, *rbt1*Δ$^{1\text{-}2166}$/Δ$^{1\text{-}2166}$	This Study

2.2.3 Zebrafish care and maintenance

Adult zebrafish were held in the University of Maine Zebrafish facility at 28°C in a recirculating system (Aquatic Habitats, Apopka Fl) under a 14 hr/10 hr light/dark cycle and fed Hikari micropellets (catalogue number HK40; Pentair Aquatic Ecosystems). All zebrafish studies were carried out in accordance with the recommendations in the Guide for the Care and Use of Laboratory Animals of the National Research Council (205). All animals were treated in a humane manner and euthanized with Tricaine overdose according to guidelines of the University of Maine Institutional Animal Care and Use Committee (IACUC) as detailed in protocols A2015-11-03, A2018-10-01 and A2021-09-01.

Table 2.2: Zebrafish lines

Zebrafish Line	Allele	Source/Reference
AB (Wild Type)	n/a	Zebrafish International Resource Center
Tg(mpeg1:EGFP)/ Tg(lysC:dsRed)	gl22Tg nz50Tg	(206,207)

2.2.4 Hindbrain Infections

Zebrafish were raised at 33°C for the first 24 hours, in E3 plus 0.3 mg/L methylene blue for the first 6 hours then E3 plus PTU (0.02 mg/ml, Sigma-Aldrich, St. Louis, Missouri) thereafter. At 24 hpf, embryos were dechorionated. Injection solutions were made up at 1x10^7 cells/ml in PBS and stained with Calcofluor white

(750 μg/mL) as necessary to visualize non-fluorescent or far-red candida by eye. Embryos were anesthetized in tricaine (160 μg/ml; Tricaine; Western Chemicals, Inc., Ferndale, WA) for injection into the hindbrain ventricle through the otic vesicle at the prim-25 stage (208). Embryos that were injured during the injection process were removed. After infection fish were placed at 30°C (28°C for SC5314 background strains) for the remainder of the experiment and monitored for survival out to 72 hpi. For pilot experiments, fish were screened after injection on a Zeiss Axio Observer Z1 microscope (Carl Zeiss Microimaging, Thornwood, NJ) to ensure that they received between 10-25 *C. albicans* cells. In these experiments, 2 mutant *C. albicans* strains were tested per experiment along with the SN250 WT control and PBS mock infected fish. 3 biological replicates were performed in this manner to total approximately 50 fish per strain. For large scale virulence screening, 5 *C. albicans* mutants were tested along with SN250 WT control and PBS mock infected fish in one experiment with approximately 50 fish per strain. Due to the large number of injected fish, fish were not screened after injection and *C. albicans* was not stained with Calcofluor white. As another check, if survival of SN250 infected fish fell outside of 5.3-72.18% survival (by 72 hpi) the experiment was eliminated from consideration, and all mutant strains were retested.

2.2.5 Quantitative real-time PCR

Fish were infected as described above, screened for correct inoculum, and euthanized at 4 hpi or 24 hpi for qPCR. Pools of 5-10 larvae were homogenized in TRIzol (Invitrogen, Carlsbad, CA) and stored at -80ºC. RNA isolation was performed using the Direct-zol RNA MinipPrep kit (Zymo Research, Irvine, CA) following their

protocol. cDNA was synthesized from 500 ng of RNA using iSCRIPT reverse transcription (RT) supermix for RT-qPCR (Bio-Rad, Hercules, CA). qPCR was performed using SsoAdvanced Universal SYBR Green Supermix (Bio-Rad) with 1 µl of cDNA in 10 µl reactions with primers listed in the table below. qPCR was run on a CFX96 Real time system, C1000 touch thermal cycler (Bio-Rad).

Table 2.3: qPCR primers

Gene	Sequence	Reference
cxcl8b	Fw: GCTGGATCACACTGCAGAAA Rv: TGCTGCAAA CTTTTCCTTGA	(209)
tnfa	Fw: TTCACGCTCCATAAGACCCA Rv: CCGTAGGATTCAGAAAAGCG	(210)
il1b	Fw: GTCACACTGAGAGCCGGAAG Rv: TGGAGATTCCCAAACACACA	(211)
gapdh	Fw: TGGGCCCATGAAAGGAAT Rv: ACCAGCGTCAAAGATGGATG	(212)

2.2.6 Fluorescence microscopy

For analysis of the phagocyte response at 4-6 hpi, embryos were placed in 0.4% low melting point agarose in E3 with 160 µg/ml tricaine in a glass bottom 24-well plate (MatTek Corporation, Ashland, MA) and the hindbrain ventricle imaged. Images were taken on an Olympus IX-81 inverted microscope with an FV-1000 laser scanning confocal system (Olympus, Waltham, MA) with a 20x (0.75 NA) objective with 5 µm increments for approximately 25-35 slices.

2.2.7 Image analysis

Images were imported into Fiji (ImageJ) and made into composite 4-channel z-stacks for quantification. Number of *mpeg1*:GFP+ or *lysC*:dsRed+ cells were counted manually for the hindbrain region throughout the z-stack. In addition, *C. albicans* cells were manually counted for whether they were intracellular (inside *mpeg1*:GFP+,

lysC:dsRed+, or other), or extracellular to determine the percent of *C. albicans* cells that were taken up by the host. The total number of cells recruited to the infection included *mpeg1*:GFP+ cells, *lysC*:dsRed+ cells, as well as non-fluorescent cells phagocytosing *Candida*. Fish were excluded from the total cells recruited count if they did not contain both GFP+ and dsRed+ cells.

2.2.8 Statistical Analysis

Statistical analysis was performed using GraphPad Prism software. For analysis of survival, Kaplan-Meier curves were generated from at least 3 pooled experiments with the same mutant *C. albicans* strains, and Mantel-Cox log rank tests were performed with Bonferroni correction. For analysis of differences in phagocyte recruitment and containment, a normality test was performed, followed by a t-test if normal or Mann-Whitney test if not normal. All mutants were compared with wildtype SN250 in each experiment for significance testing. For simplicity to present all data in one graph, data was normalized to WT, SN250 values. For normalization the average SN250 value for a set of experiments was divided by the average SN250 value for all experiments, to get an adjustment value. The value for each individual fish was then divided by this adjustment value, to get a normalized value for each fish. Normalized values were used to generate the violin plots presented. Violin plots show the median and interquartile range, while normalization was done using the average, so not all of the SN250 medians are at the same y-value.

2.3 Results

2.3.1 Forward genetic screen for altered fungal immune evasion based on loss of virulence

C. albicans is known to limit immune recruitment and phagocytosis during infection, although morphological switching can regulate phagocyte recruitment, few molecular details are known about how this occurs (106,213,214). The zebrafish hindbrain infection model provides a useful *in vivo* system to intravitally image early fungal and host dynamics, and has identified a close correlation between early phagocyte-mediated fungal containment and overall survival (106,199,214). We leveraged these advantages to screen individual *C. albicans* mutants for virulence and phagocytosis defects. A set of 131 genes were selected, based either on their selective role in either morphogenesis or virulence, or on their predicted role encoding a secreted product (Table A.1, (200)).

We used a small number of mutants to define infection parameters and enable high-throughput screening. In initial virulence tests, two mutant strains were tested at a time along with controls and at least 3 biologically independent experiments were performed with approximately 50 fish infected per mutant (Figure 2.1A). Inoculums were counted by fluorescence microscopy to ensure they received the correct amount of *Candida.* Three of the nine initial strains tested had significantly reduced (*ssu81*Δ/Δ & *mad2*Δ/Δ) or abolished virulence *rbt1*Δ/Δ$^{968\text{-}2166}$ (Figure 2.1B-C). We then used the average and standard deviation of 72 hours post infection (hpi) survival for wildtype-infected fish to determine z-score cutoffs for subsequent experiments to exclude data in which wildtype-infected survival was out of range (average +/- 2.5 SD [20 - 80%

survival]). In addition, we quantified host-pathogen interactions by confocal microscopy at 4-6 hpi (Figure 2.1D). One strain, *mad2*Δ/Δ, did show a trend for increased fungal containment compared to the control SN250 (Figure 2.1E, p=0.0508), although this method was limited because only the initial inoculum was fluorescently stained. Interestingly, *mad2*Δ/Δ was also one of the three strains with reduced virulence (Figure 2.1B). There were no qualitative differences in the amount of filamentous growth between SN250 and any of the mutant strains.

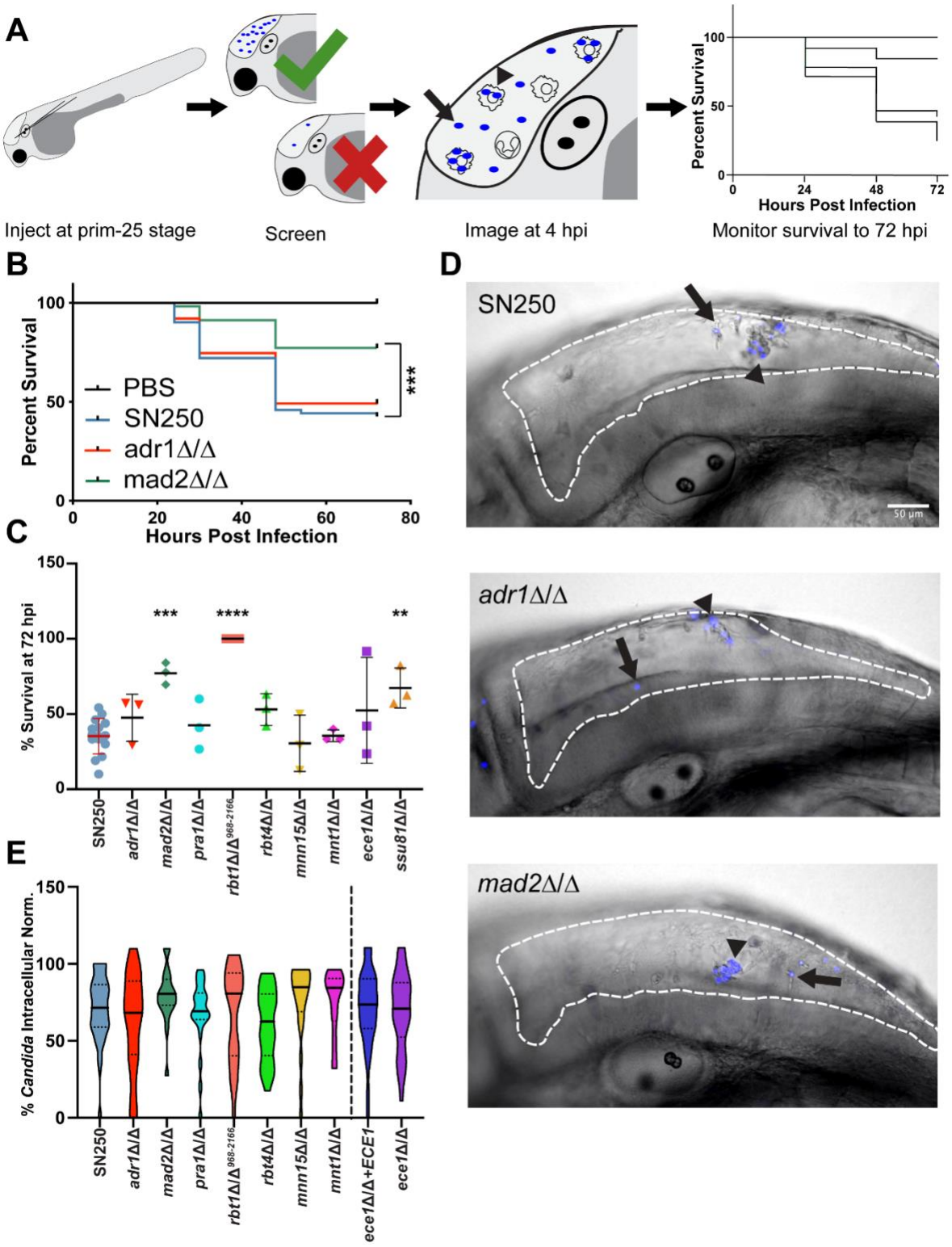

Figure 2.1 Defining infection parameters. **A)** Flow chart showing workflow of pilot experiments. Hindbrain infections were performed at the prim-25 stage, and fish were then screened to ensure they received the correct inoculum (10-25 cells). At 4-6 hours post-infection, fish were imaged by confocal microscopy to score fungal containment; survival was monitored

Figure 2.1 continued
out to 72 hpi. **B)** Example Kaplan-Meier survival curves pooled from 3 experiments showing fish injected with PBS (Control, n=83), SN250 (WT, n=61), *adr1*Δ/Δ (n=63), or *mad2*Δ/Δ (n=57). Fish injected with *mad2*Δ/Δ showed increased survival compared to SN250 (p=0.0001). **C)** Survival of fish injected with each strain at 72 hpi in three independent experiments. Individual points represent biologically independent experiments on different days. Bars show means and standard deviations with SN250 in red to depict WT cutoff range for inclusion of experiments. Significant differences in survival curves were determined by Mantel-Cox log rank tests comparing the mutant strain to SN250 from data pooled from three biological replicates of the same experiments. Two mutants were tested per experiment, and Bonferroni corrections were performed. **D)** Representative images of hindbrain ventricle infection to score fungal containment at 4 hpi. *C. albicans* initial inoculum was stained with Calcofluor white, shown in blue. The hindbrain ventricle is outlined by a white dashed line. Scalebar is 50μm. Arrows point to extracellular *Candida*, while arrowheads point to intracellular *Candida*. **E)** Quantification of the percent of intracellular *Candida* was counted by eye from slices of z-stack images of individual fish taken at 4 hpi for each strain. Significance was determined by Mann-Whitney test with Bonferroni correction from three independent experiments comparing fish of the mutant strain to SN250 infected fish from the same experiments.

A total of 131 mutant *C. albicans* strains with expected deficiencies in predicted secreted factors, hyphal growth, or virulence were selected for screening, based on their phenotypes observed in previous screens (200). Strains were chosen for inclusion in the screen based on previously observed phenotypes observed from Noble et al (200). Strains were included if they were seen to have a defect in hyphal growth on Spider medium, as we hypothesized that immune evasion mechanisms may be coregulated with the yeast-to-hyphal transition (182). While these strains have a morphogenesis defect on Spider plates, defects in filamentous growth are often very dependent on the environmental context and strain, and therefore may or may not have a filamentous growth defect in the zebrafish hindbrain (215–217). We also chose to include strains that had a competitive defect in pooled mouse infection, as we reasoned these strains may be cleared more effectively by the host immune response. This included 69 mutants that had a morphogenesis defect on Spider agar but no pooled

virulence defect, 41 that had an infectivity defect in pooled infection but no Spider morphogenesis defect, one had both defects, and 20 genes encoding secreted peptides, but no spider morphogenesis or pooled virulence defect (200) (Table A.1).

To facilitate high-throughput screening for cell-autonomous virulence defects, inoculums were not counted and no replicates were performed. Virulence testing revealed several mutants with greatly reduced virulence. Seventeen of the mutants had a fish survival z-score > 3, while 27 mutants had a z-score between 2 and 3 (Figure 2.2). Of the 41 strains that previously showed an infectivity defect, 6 of these had a z-score >3, with another 6 between z-scores of 2 and 3. Out of the 70 morphogenesis defective mutants, 11 had z-score > 3, with another 16 between 2 and 3. In addition, 4 genes from the SAP family of genes had z-scores between 2 and 3. As these fish were not screened to ensure the correct number of *C. albicans* injected, we first retested hypovirulent strains with z-scores > 3 with an added step of screening for inoculum per fish. On retest, both independent isolates from the Noble library were tested and in addition, strains were genotyped to confirm the correct gene deletion. After retesting, this led to a total of 10 mutants with reproducible hypovirulence: *rbt1*Δ/Δ$^{968\text{-}2166}$, *orf19.5547*Δ/Δ, *pep8*Δ/Δ, *cht2*Δ/Δ, *apm1*Δ/Δ, *rim101*Δ/Δ, *brg1*Δ/Δ, *nmd5*Δ/Δ, *mad2*Δ/Δ, and *cek1*Δ/Δ. Hypovirulent strains were then complemented to assess if complementation restored virulence. When available, *in vitro* phenotypes (e.g. morphogenesis defect on Spider media) were used to assess functional complementation of strains prior to assessing virulence in hindbrain infection. Complementation successfully restored some virulence of *brg1*Δ/Δ, *pep8*Δ/Δ, *nmd5*Δ/Δ, *rim101*Δ/Δ, *cek1*Δ/Δ, *apm1*Δ/Δ, and *mad2*Δ/Δ (Figure 2.3). We were not

able to generate complemented strains that restored even partial virulence to *cht2*Δ/Δ, *orf19.5547*Δ/Δ, or *rbt1*Δ/Δ$^{968\text{-}2166}$ (Figure 2.4). Consistent with the failure to complement this partial ORF deletion, an independently created full deletion of *RBT1* in the SN250 background did not cause a virulence defect (Figure 2.4). Strains were then transformed with the pENO1-iRFP (174) for cytosolic expression of a near-

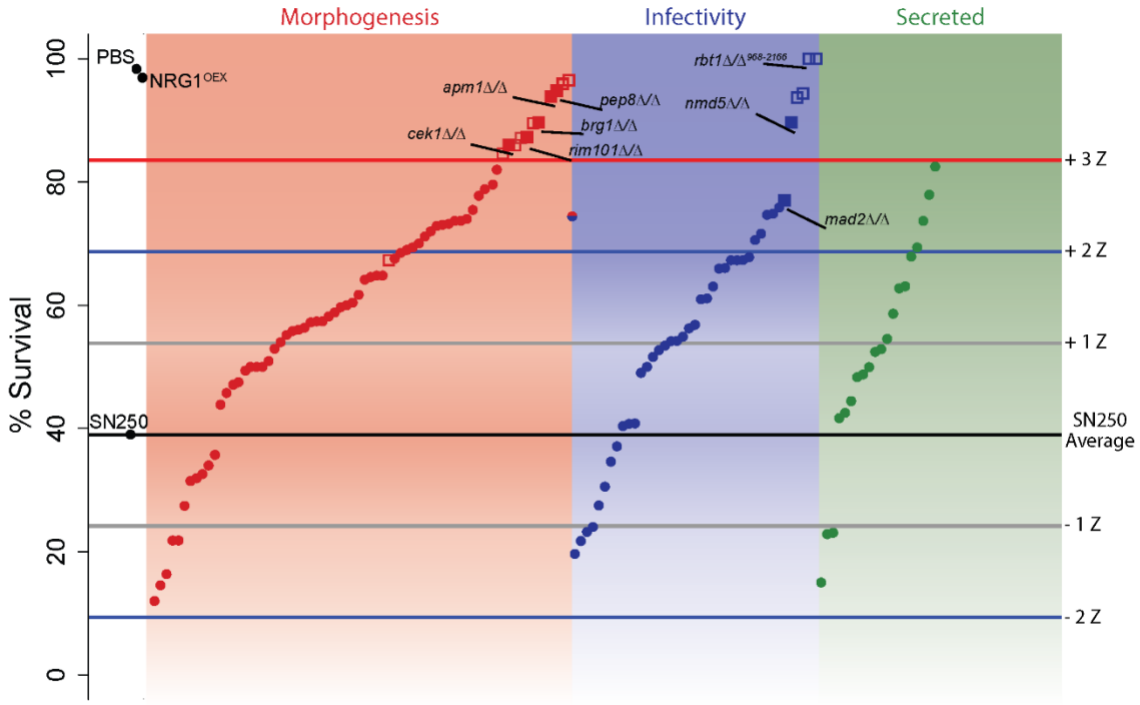

infrared fluorescent protein for intravital imaging of infections.

Figure 2.2 High-throughput virulence screening. Average survival of fish infected with individual mutant *C. albicans* strains (n ≈ 50 fish per mutant strain). Mock infected (PBS) and NRG1^{OEX} infected fish were included as controls. The average survival of the WT SN250 strain is shown by the black line, while gray lines show 1-Z away, blue lines show 2-Z's away, and red 3-Z's away. Strains in the red panel were previously seen to have a morphogenesis defect on spider agar, while those in the blue panel showed a defect in pooled virulence tests, and those in the green panel code for secreted proteins. Mutant strains that had a z-score of over 3 were passed to the next phase of screening showed as squares. Those where both independent mutants showed hypovirulence genotyped correctly, and complementation restored virulence, are shown as filled in squares and were passed to the imaging phase of screening. Those that did not pass secondary screening are shown as empty squares. Complete data is found in Supplementary Table S1.

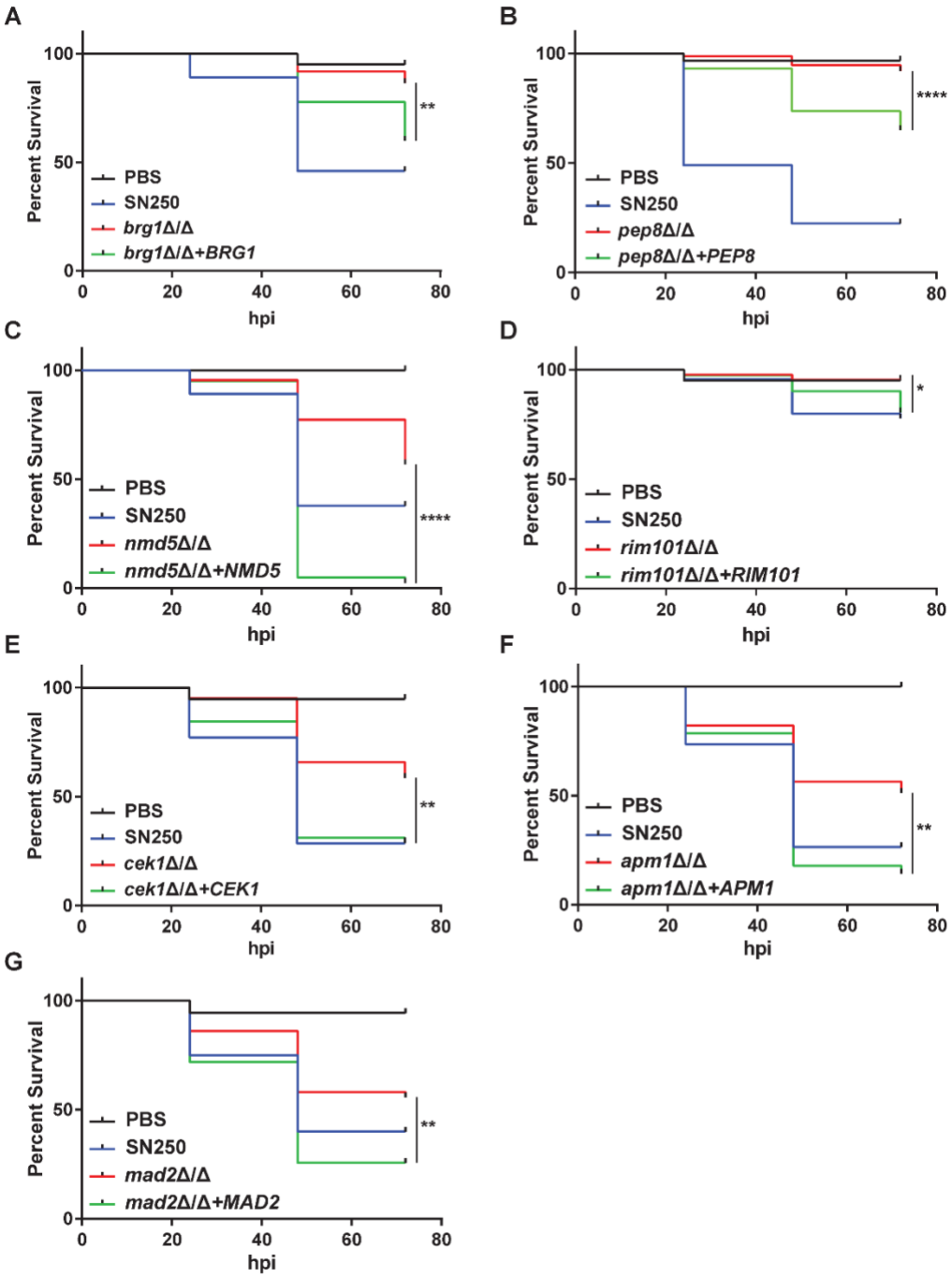

Figure 2.3 Complementation restores virulence to hypovirulent *C. albicans* mutants. Kaplan-Meier survival curves show restoration of virulence of with complementation. All data in survival curves are pooled from 2 experiments unless otherwise noted. **A)** Fish injected with SN250 (WT, n=37), *brg1*Δ/Δ (n=37), *brg1*Δ/Δ+*BRG1* (n=45), PBS (mock, n= 20). Complementation of *brg1*Δ/Δ restores some virulence (*brg1*Δ/Δ vs. *brg1*Δ/Δ+*BRG1* Mantel-Cox log rank test p=0.0083). **B)** Fish injected with SN250 (WT, n=49), *pep8*Δ/Δ (n=75), *pep8*Δ/Δ-+*PEP8* (n=57), or PBS (mock, n= 30). Complementation of *pep8*Δ/Δ restores some virulence

Figure 2.3 continued
(*pep8*Δ/Δ vs. *pep8*Δ/Δ+*PEP8* Mantel-Cox log rank test p<0.0001, data pooled from 3 experiments). **C)** Fish injected with PBS (mock, n=20), SN250 (WT, n=37), *nmd5*Δ/Δ (n=44), *nmd5*Δ/Δ+NMD5 (n=41). Complementation significantly increases virulence of *nmd5*Δ/Δ (*nmd5*Δ/Δ vs. *nmd5*Δ/Δ+NMD5 Mantel-Cox log rank test p<0.0001). **D)** Fish injected with SN250 (WT, n= 45), *rim101*Δ/Δ (n=43), *rim101*Δ/Δ+*RIM101* (n=41), or mock infected fish (PBS, n=20). Complementation of *rim101*Δ/Δ restores virulence (*rim101*Δ/Δ vs. *rim101*Δ/Δ+*RIM101* Mantel-Cox log rank test p=0.0410). **E)** Fish injected with SN250 (WT, n=35), *cek1*Δ/Δ (n=41), *cek1*Δ/Δ+*CEK1* (n=45), or mock infected fish (PBS, n= 19). Complementation of *cek1*Δ/Δ restores virulence (*cek1*Δ/Δ vs. *cek1*Δ/Δ+*CEK1* Mantel-Cox log rank test p=0.0033). **F)** Fish injected with PBS (mock, n=21), SN250 (WT, n=34), *apm1*Δ/Δ (n=39), or *apm1*Δ/Δ+*APM1* (n=28). Complementation significantly increases virulence of *apm1*Δ/Δ (*apm1*Δ/Δ vs. *apm1*Δ/Δ+*APM1* Mantel-Cox log rank test p=0.0053). **G)** Fish injected with PBS (mock, n=18), SN250 (WT, n=40), *mad2*Δ/Δ (n=43), or *mad2*Δ/Δ+*MAD2* (n=39). Complementation significantly increases virulence of *mad2*Δ/Δ (*mad2*Δ/Δ vs. *mad2*Δ/Δ+*MAD2* Mantel-Cox log rank test p=0.0053).

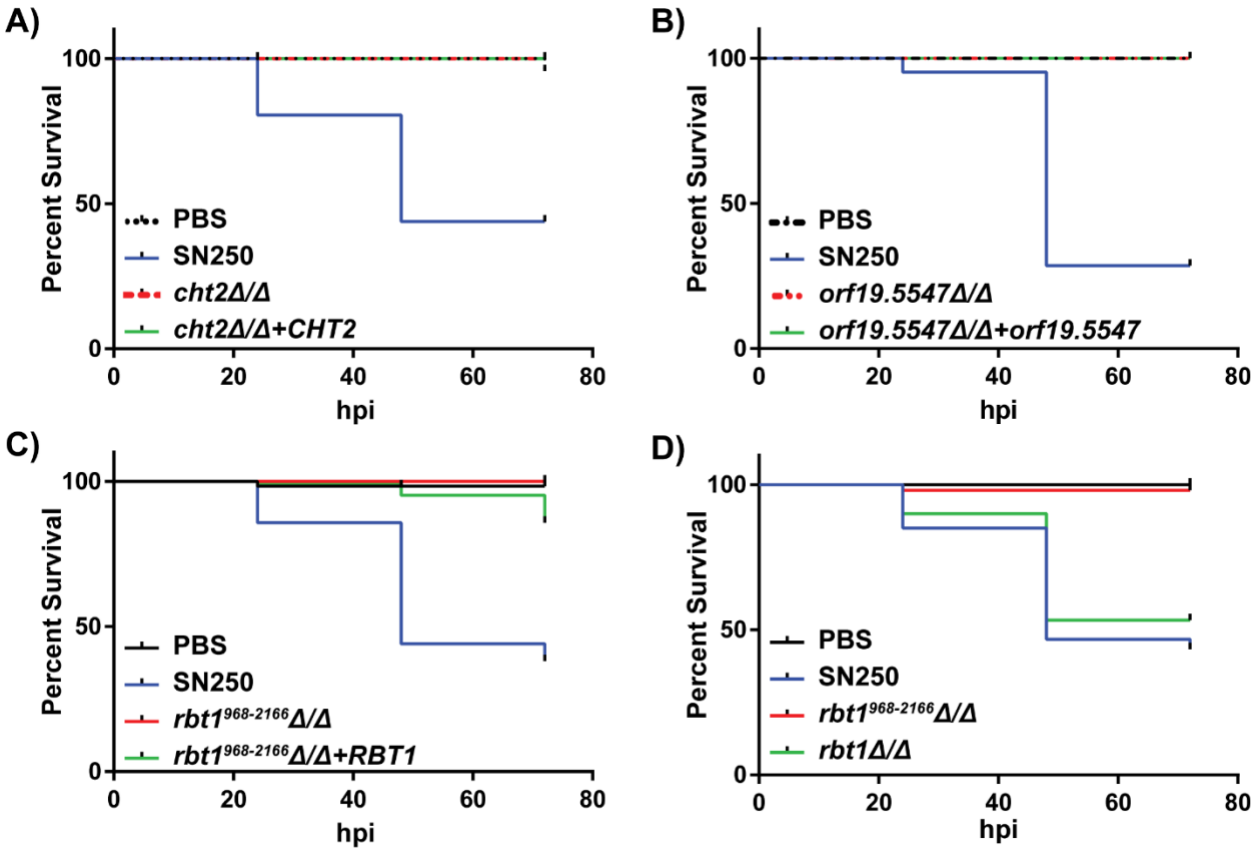

Figure 2.4 Complementation did not restore virulence of *cht2*Δ/Δ, *orf19.5547*Δ/Δ, or *rbt1*$^{968-2166}$Δ/Δ. A) Kaplan-Meier survival curve of fish injected with PBS (mock, n=23), SN250 (WT, n=41), *cht2*Δ/Δ (n=31), or *cht2*Δ/Δ+*CHT2* (n=44). Data pooled from 2 experiments. **B)** Kaplan-Meier survival curve of fish injected with PBS (mock, n=10), SN250 (WT, n=21), *orf19.5547*Δ/Δ

Figure 2.4 continued
(n=16), or *orf19.5547*Δ/Δ+*ORF19.5547* (n=19). Data from 1 experiment. **C)** Kaplan-Meier survival curve of fish injected with PBS (mock, n=58), SN250 (WT, n=84), *rbt1*$^{968\text{-}2166}$Δ/Δ (n=90), or *rbt1*$^{968\text{-}2166}$Δ/Δ+*RBT1* (n=105). Data pooled from 5 experiments. **D)** Kaplan-Meier survival curve of fish injected with PBS (mock n=35), SN250 (WT, n=60), *rbt1*$^{968\text{-}2166}$Δ/Δ (n=52), or *rbt1*Δ/Δ (n=60). Data pooled from 3 experiments.

2.3.2 Altered phagocyte responses to hypovirulent *Candida* mutants

Previous work has linked early immune containment of fungi to enhanced survival (106,199). To determine if the virulence defects for these mutants were due to a more effective early immune response, we imaged *Tg(mpeg1:GFP)/(lysC:dsRed)* larvae (green macrophages and red neutrophils) infected with iRFP-expressing *Candida* at 4-6 hpi. From these images, we assessed the number of macrophages and neutrophils responding to infection as well as containment of *Candida* (Figure 2.5A). Surprisingly, we saw a significantly decreased number of macrophages in *brg1*Δ/Δ infections (Figure 2.5A & 2.5B, p= 0.0454) and a significantly decreased number of neutrophils in *pep8*Δ/Δ infections (Figure 2.5C, p=0.0383). While not significant, we saw a trend for increased macrophage recruitment to *cek1*Δ/Δ (p=0.1274) (Figure 2.5B). This resulted in an overall trend of and decreased phagocyte recruitment to *brg1*Δ/Δ (p=0.0734; Figure 2.5D).

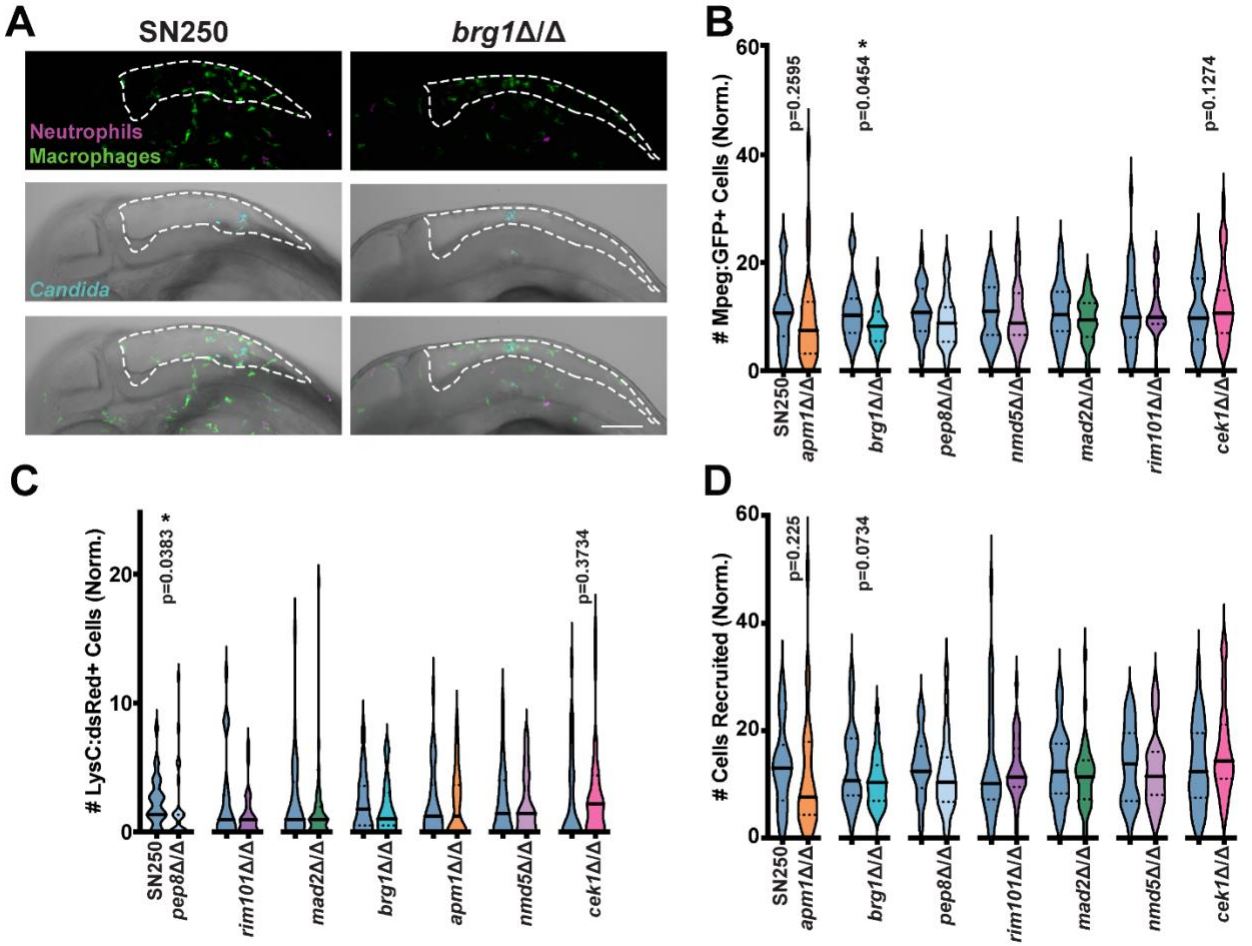

Figure 2.5 Phagocyte recruitment to hypovirulent *C. albicans* mutants. A) Example representative images from SN250- and *brg1*Δ/Δ-infected fish at 4-6 hours post-infection. Images were scored by eye for the number of macrophages (*mpeg1*:GFP+ cells) shown in green and number of neutrophils (*lysC*:dsRed+ cells) in magenta recruited to the infection, as well as if the *Candida* was intracellular or extracellular. Scalebar is 100 μm. **B)** Violin plots showing the number of *mpeg*:GFP+ macrophages recruited to the infection site normalized to the average amount of *mpeg*:GFP+ macrophages recruited to SN250. **C)** Violin plots showing the number of *lysC*:dsRed+ neutrophils recruited to the infection site normalized to the average amount of *lysC*:dsRed+ neutrophils recruited to SN250 for each mutant. **D)** Violin plots showing the number of cells recruited to the infection site normalized to the average recruited to SN250. Cells include *mpeg1*:GFP+ and *lysC*:dsRed+ recruited to the hindbrain, as well as non-fluorescent cells containing *Candida*. Bars on violin plots represent median and interquartile range. Statistics were performed from data pooled from at least 3 independent experiments for each mutant, for approximately 30 fish per strain were imaged. A test for normality was performed and significance was then determined by performing a T-test if normal, or Mann-Whitney test if not normal.

However, zebrafish infected with *nmd5*Δ/Δ were more effective at fungal containment (Figure 2.6A-B, p = 0.00153), while fish infected with *rim101*Δ/Δ trended towards increased containment (Figure 2.6B, p=0.0567). In addition to increased containment, infections with *nmd5*Δ/Δ and *rim101*Δ/Δ along with *cek1*Δ/Δ also trended towards having fewer extracellular *Candida*, which is associated with longer-term survival (106,199) (Figure 2.6C, p=0.0616, p=0.0775, and p=0.0762 respectively). There were no significant differences in containment of *Candida* in infections with *mad2*Δ/Δ, *apm1*Δ/Δ, *brg1*Δ/Δ or *pep8*Δ/Δ mutants, despite differences in phagocyte recruitment to *brg1*Δ/Δ and *pep8*Δ/Δ infections. On the other hand, for *mad2*Δ/Δ and *apm1*Δ/Δ mutants there were neither differences in phagocyte recruitment to nor containment of fungi (Figures 2.5B-D & 2.6B-D). Despite some of these mutants having differences in recruitment or containment, none had a significant difference in the average number of *Candida* taken up per cell recruited (Fig. 2.6D).

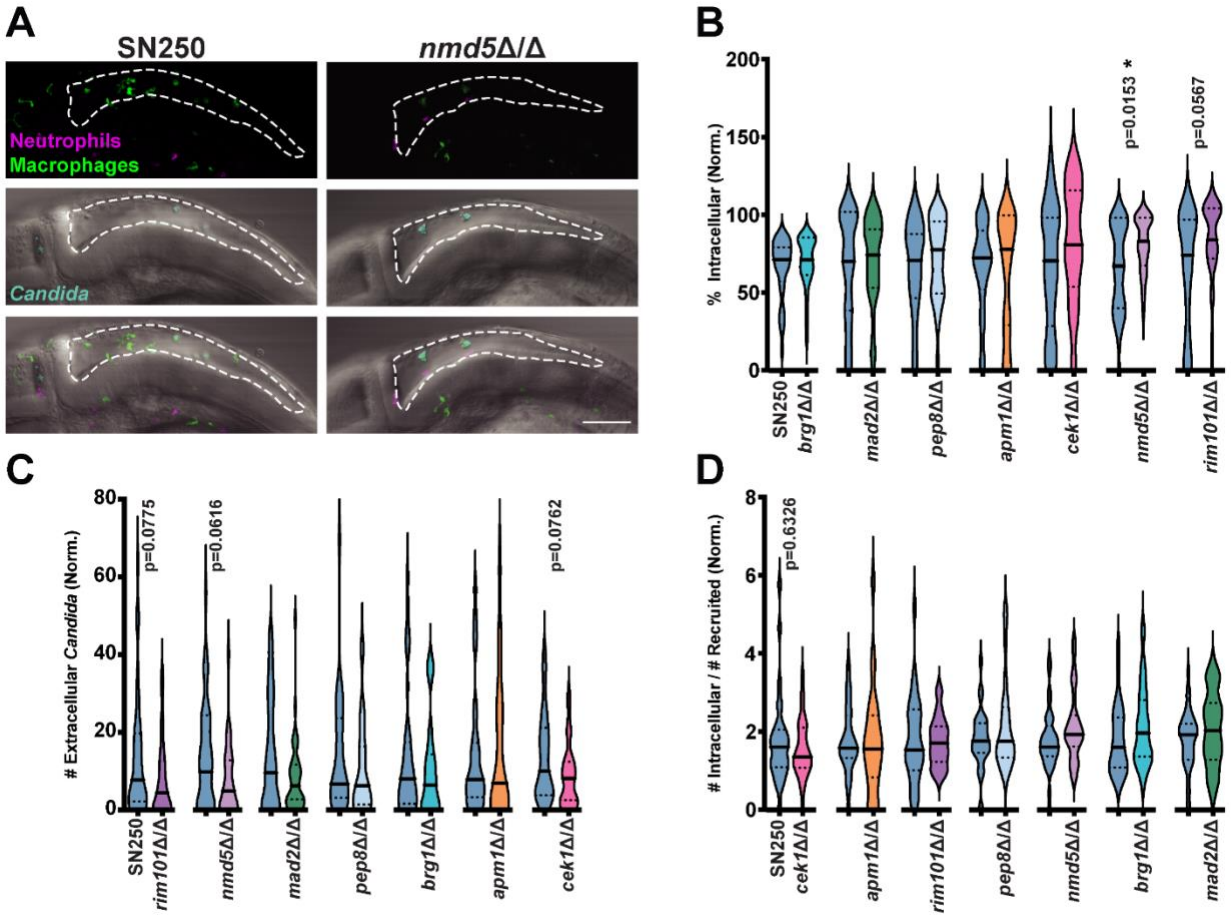

Figure 2.6 Containment of hypovirulent *C. albicans* mutants. A) Example representative images from SN250 and *nmd5*Δ/Δ infected fish at 4 hours post infection. Images were scored by eye for the number of macrophages (Mpeg1-GFP+ cells) shown in green and number of neutrophils (LysC-dsRed+ cells) in magenta recruited to the infection, as well as if the *Candida* was intracellular or extracellular. Scalebar is 100 μm. **B)** Violin plot of the percent intracellular *Candida* normalized to the average percent intracellular *Candida* for SN250. **C)** Violin plot showing the number extracellular *Candida* normalized to the average amount for SN250. **D)** Violin plot showing the number of intracellular *Candida*, divided by the number of cells recruited, normalized to the average for SN250 for that experimental set. Bars on violin plots represent medians and interquartile ranges. Statistics were performed from pooled data from at least 3 independent experiments for each mutant, for approximately 30 fish per strain imaged. A test for normality was performed and significance was then determined by performing a T-test if normal, or Mann-Whitney test if not normal.

As noted above, several of the mutants identified in our screen were later eliminated from analysis due to an inability to complement the virulence phenotype and/or an inability to reproduce the virulence phenotype in the original SN250

background. Although we were not able to restore virulence of *cht2*Δ/Δ or *rbt1*Δ/Δ$^{968\text{-}2166}$ (Figure 2.4A & C), we did observe a trend for increased macrophage recruitment to *cht2*Δ/Δ, and a trend for increased neutrophil recruitment to *rbt1*Δ/Δ$^{968\text{-}2166}$ and *cht2*Δ/Δ (Table A.2). It is likely that these mutants sustained additional genomic changes during their original construction, and analysis of whole-genome sequence may reveal the identities of other novel regulators of immune evasion.

Both *brg1*Δ/Δ and *pep8*Δ/Δ have been implicated in having a role in hyphal growth *in vitro* (218–220). Since both showed a decrease in recruitment of macrophages or neutrophils, we analyzed the amount of ovoid vs elongated cells at 4-6 hours post infection (Figure 2.7A & B). Both *brg1*Δ/Δ and *pep8*Δ/Δ had about 20% fewer elongated cells compared to SN250 (Figure 2.7C & D, $p<0.0001$ & $p=0.0023$ respectively). Given that the percentage of fungal cells in the extracellular space is the same for both mutants (Figure 2.6B), and nearly all filamentous growth is extracellular, this suggests that both have partial deficiencies and/or delays in extracellular germination during infection.

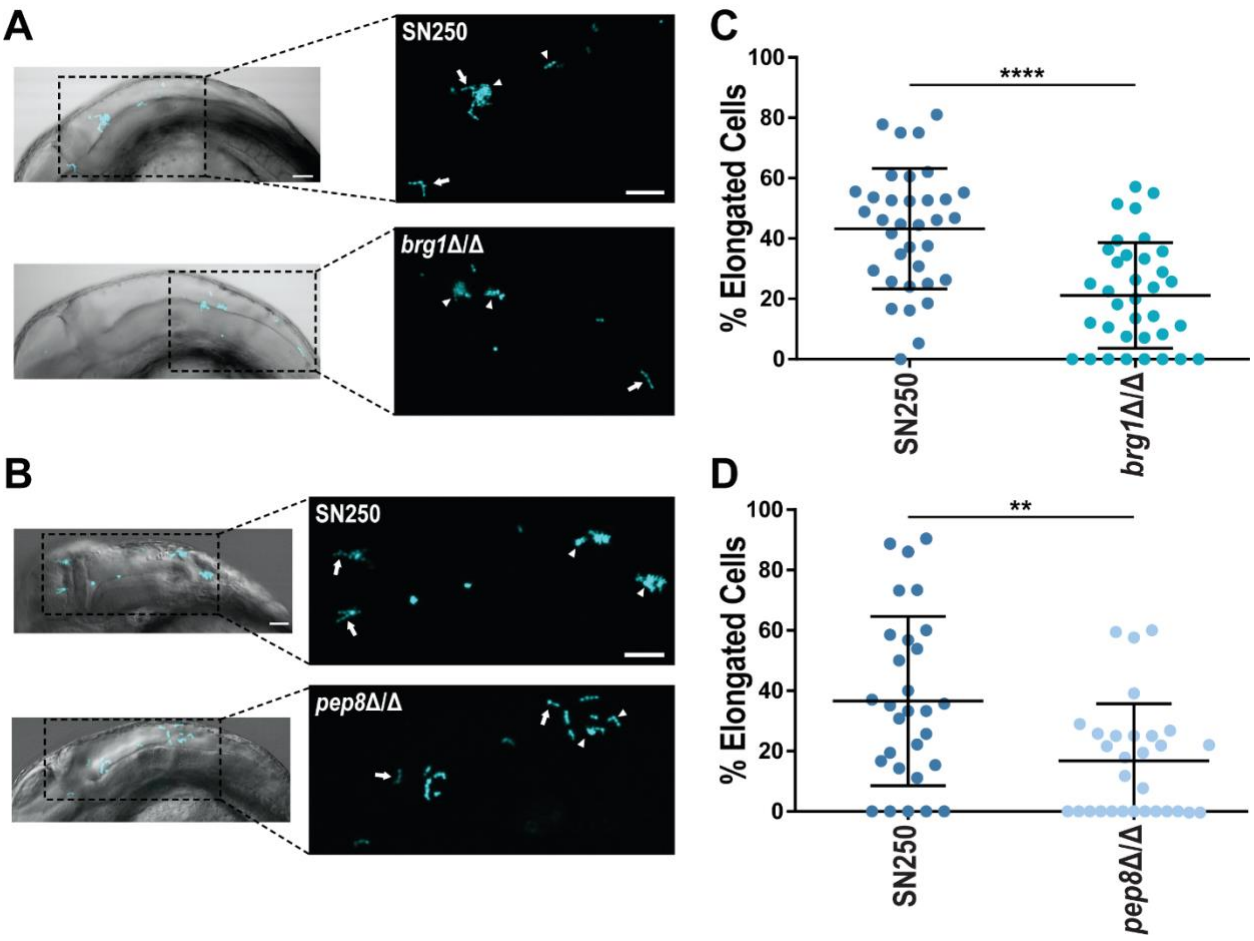

Figure 2.7 *brg1*Δ/Δ and *pep8*Δ/Δ show fewer elongated cells in the zebrafish hindbrain at 4-6 hours post infection. A) Images of SN250 and *brg1*Δ/Δ infected fish showing yeast (arrow heads) and elongated cells (arrows) in the zebrafish hindbrain at 4-6 hours post infection. Scalebars are 50µm. **B)** Images of SN250 and *pep8*Δ/Δ infected fish showing yeast (arrow heads) and elongated cells (arrows) in the zebrafish hindbrain at 4-6 hours post infection. Scalebars are 50µm. **C)** Percent elongated cells in fish infected with SN250 (WT, n=35 fish) or *brg1*Δ/Δ (n=35 fish). Each dot represents a different fish. The percent of elongated cells was significantly less for *brg1*Δ/Δ infections (Students t-test $p<0.0001$, data pooled from 4 experiments). **D)** Percent elongated cells in fish infected with SN250 (WT, n=29 fish) or *pep8*Δ/Δ (n=30 fish). Each dot represents a different fish. The percent of elongated cells was significantly less for *pep8*Δ/Δ infections (Students t-test $p=0.0023$, data pooled from 3 experiments).

2.3.3 Altered cytokine responses to hypovirulent *Candida* mutants

Because immune recruitment and phagocytosis were altered, we reasoned that there would be altered expression of proinflammatory cytokines and chemokines in

our mutants that showed an altered immune response. We measured the expression of key proinflammatory cytokines *tnfa* and *il1b* and the zebrafish IL-8 homolog. Interestingly, at 4 hours post infection, there was not a significant induction of pro-inflammatory gene expression (data not shown). However, at 24 hpi fish infected with *brg1*Δ/Δ or *pep8*Δ/Δ showed a significant reduction in *cxcl8b*, *tnfa*, and *il1b* production, while fish infected with *nmd5*Δ/Δ showed a significant reduction in *cxcl8b* and *il1b* production, but not *tnfa* (Figure 2.8A-C). Fish infected with *nmd5*Δ/Δ+*NMD5* showed a trend for increased proinflammatory chemokine/cytokine production, even compared to SN250, which reached significance for *il1b*. This matches well with the decreased survival of fish infected with this complemented strain and the complete complementation phenotype (Figure 2.3C). On the other hand, *cxcl8b*, *tnfa*, and *il1b* expression for *brg1*Δ/Δ+*BRG1* and *pep8*Δ/Δ+*PEP8* tended to be between SN250 and the mutant strain, which matches the partial complementation of virulence exhibited by these strains (Figure 2.3A & B). These decreased proinflammatory gene expression signatures are consistent with the effective containment of the mutants and their overall reduced virulence.

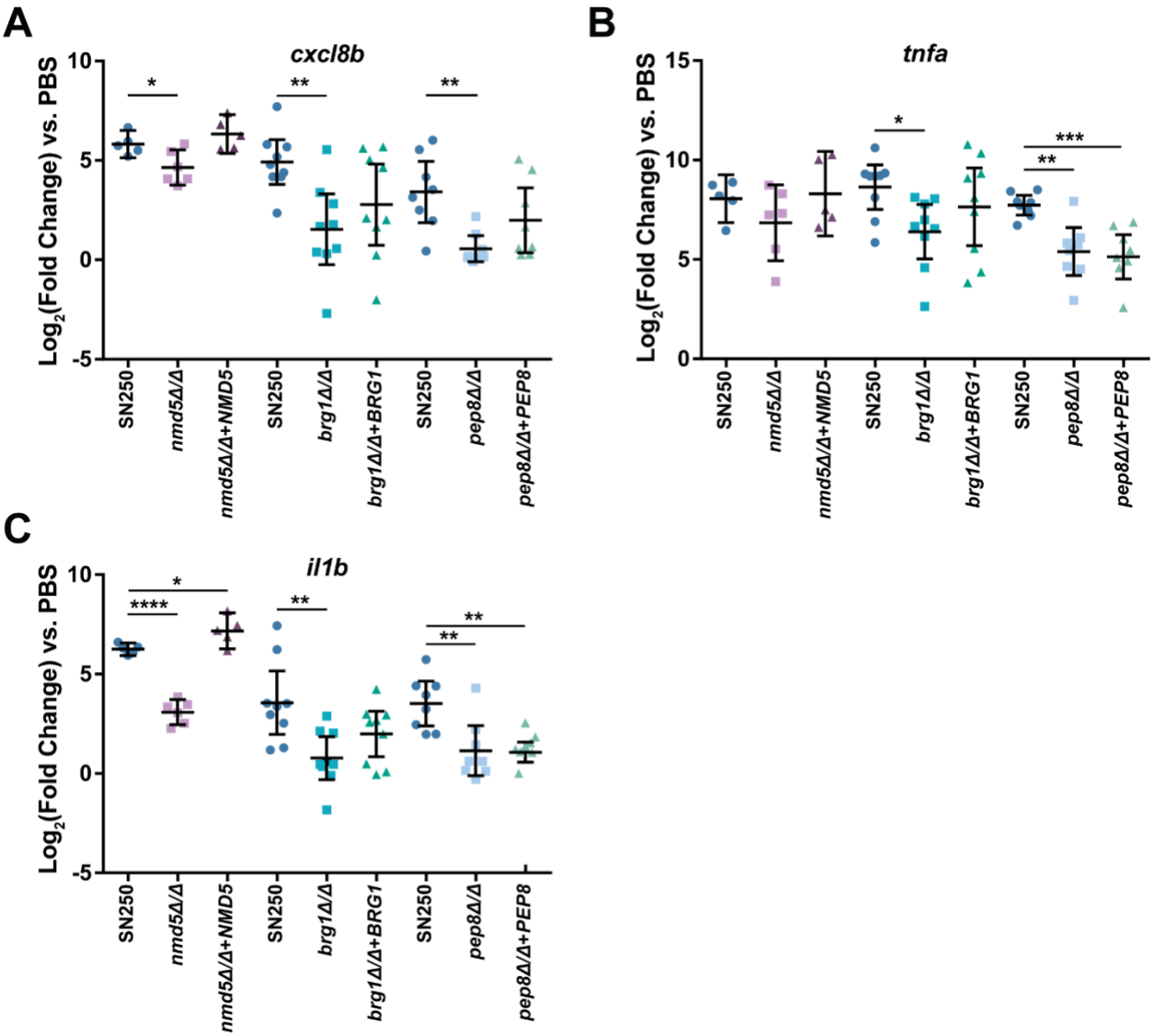

Figure 2.8 Hypovirulent *C. albicans* mutants elicit a reduced proinflammatory expression at 24 hours post infection. Expression of *cxcl8b* (**A**), *tnfa* (**B**), or *il1b* (**C**) by qPCR analysis of fish infected with WT (SN250), mutant (*nmd5*Δ/Δ, *brg1*Δ/Δ, or *pep8*Δ/Δ), or complemented (*nmd5*Δ/Δ+NMD5, *brg1*Δ/Δ+BRG1, or *pep8*Δ/Δ+PEP8) *C. albicans* at 24 hpi. Each point represents a pool of at least 5 larvae, and data was pooled from 3 (*NMD5*) or 4 (*BRG1* & *PEP8*) independent experiments. Gene expression was normalized to *gapdh* and induction was determined relative to PBS mock infected larvae. Significance was determined by one-way ANOVA with Dunnett's multiple comparisons tests.

2.4 Discussion

Candida albicans has evolved over many generations with vertebrate hosts and has developed the ability to avoid immune clearance through activities such as filamentous

growth, masking of cell wall epitopes, production of a toxin and avoidance of antibody opsonization (153,179–186). However, we still know little about how each of these abilities effects immune evasion during vertebrate infection and we know even less about which fungal genes and pathways regulate immune evasion. The transparency of the larval zebrafish model is a powerful tool that can be utilized to elucidate the different mechanisms of immune evasion in *C. albicans*. Previous work in this infection model has shown that differential immune recruitment and fungal containment represent important predictors for the fate of individual hosts (106,199). These conditions led us to undertake the first medium-scale screen of 131 *C. albicans* mutants for virulence, with subsequent analysis for early immune-mediated fungal containment. We identified several fungal genes with previously unappreciated roles in regulating early immune response, finding evidence for differential regulation of phagocyte recruitment and pathogen containment.

This is the first single-mutant infection screen of more than 100 individual *C. albicans* mutants in any vertebrate infection model, made possible by the use of a zebrafish model. Very few virulence screens of more than 100 mutants have been conducted, all using pooled/barcode screening methodology (19,200,221). We chose a zebrafish larval hindbrain infection model because it has been shown to reproduce many aspects of murine disseminated infection and provides a useful infection route for quantifying phagocyte recruitment and response (106,167,208). While conditions are different from the mouse kidney, the zebrafish has the unique advantage of allowing intravital observation of the early innate immune response.

Interestingly, ten mutants had reproducible hypovirulence defects and seven of the ten could be complemented to restore virulence. Of these, four mutants—in *RIM101*, *BRG1*,

MAD2, *CEK1*—have published virulence defects in murine tail vein infection, while *PEP8*, *APM1* and *NMD5* don't have any published phenotypes in individual murine systemic infection (219,222–224). Previous large-scale virulence screens used pools of normal and defective mutants, which allows for cross-complementation and therefore tests for similar but distinct phenotypes from individual screens. Nonetheless, strong virulence phenotypes are seen for both pooled disseminated murine candidiasis and our individual screens of mutants for both *MAD2* and *NMD5* (200). Borderline virulence defects were also previously seen for mutants of *PEP8*, but this was stronger in single-mutant screening. On the other hand, pooled screens identified significant defects in GI colonization for all but the *brg1*Δ/Δ mutant (19). Interestingly, *brg1*Δ/Δ has a defect in disseminated murine infection but outcompetes wildtype in the GI, drawing a clear connection between zebrafish hindbrain infection and the well-characterized murine tail vein infection (19,219). The strong conservation of virulence defects between the zebrafish and murine disseminated models suggests that the zebrafish is useful for understanding *Candida* pathogenesis in vertebrate hosts—virulence factors required in both hosts might identify pathways that are important in human disseminated infection.

The most pronounced effect on early immune response was with *nmd5*Δ/Δ infections, raising the question of what this little-studied protein does in immune evasion. Somewhat paradoxically, *nmd5*Δ/Δ cells were contained more effectively by immune cells, even though the same number of phagocytes were present at the infection site. This disconnect might be due to a separation between two key immune functions: recruitment of phagocytes to an infection site and environment versus effective phagocytosis of pathogens at the infection site. The former is mediated by pathogen-derived chemoattractants, host-derived short-range

ROS, long-range chemokines, and cues for extravasation. The latter is mediated by short-range pathogen-derived chemoattractants and the interaction between opsonic and non-opsonic receptors with opsonins and pathogen-associated molecular patterns (225–228).

NMD5 has not previously been implicated in virulence and codes for a putative karyopherin with a potential role in nuclear protein import. In *S. cerevisiae*, Nmd5p is required for the transport of the Hog1p and Crz1p transcription factors into the nucleus, under induction of different cell stressors (229,230). In *C. albicans*, the *nmd5*Δ/Δ mutant has defects in white-opaque switching and *NMD5* gene expression is altered in biofilms and under oxidative, osmotic, and heavy metal stress conditions (59,231,232). Given the likely role of Nmd5p in nuclear import of transcription factors, it will be interesting to identify differential transcription patterns in this mutant that may account for the loss in immune evasion.

Since strong early phagocyte recruitment correlates well with survival from infection with wildtype *Candida*, our initial expectation had been that lower virulence would be associated with higher phagocyte recruitment and containment. Surprisingly, despite higher host survival in *brg1*Δ/Δ and *pep8*Δ/Δ infections, there were actually significantly fewer macrophages recruited early to a *brg1*Δ/Δ infection, and fewer neutrophils recruited to a *pep8*Δ/Δ infection. Despite having fewer macrophages or neutrophils recruited to the infection site, containment of *Candida* was not compromised—suggesting that our current models may need to be revised and there might be alternative strategies for effective fungal containment. Since phagocytosis prevents further direct interaction of fungi with new phagocytes and epithelial cells, this limits the further pattern recognition receptor activation and production of chemotactic cues that would further promote the recruitment of

phagocytes. Thus, the lower number of phagocytes at these infection sites at 4-6 hours could indicate that there is earlier containment of these two strains, thereby limiting further inflammation and additional recruitment. Consistent with this idea, phagocytic containment has previously been found to correlate with reduced epithelial NF-kB activation during mucosal *Candida* infection (211).

BRG1 and *PEP8* have not previously been identified as regulating immune responses, although both are linked to *Candida* virulence. *BRG1* (previously known as *GAT2*) is a transcription factor that regulates adhesion, is important for systemic virulence in mouse, and is redundant with *EFG1* in murine oropharyngeal candidiasis (217,219). *BRG1* can also play an important role in biofilm formation and filamentous growth *in vitro* (59). *PEP8* is predicted to play a role in endosome-to-Golgi retrograde transport (233). It appears to play a role in hyphal growth, as *pep8*Δ/Δ cells grow in smooth colonies on Spider media and have shorter, stunted, hyphae with less ability to survive in and lyse macrophages *in vitro* (220,234). The mechanisms underlying the roles of these two genes in regulating early immune responses are unknown, although it is possible that *BRG1* might regulate adhesion proteins that limit phagocytosis. Similarly, *PEP8* may regulate the export of surface adhesion proteins. While both mutants made filamentous cells in zebrafish infection, both had approximately 20% reductions in the number of filamentous cells present at 4-6 hpi (Figure 2.7). Thus, altered phagocyte interactions could also be related to filamentous growth defects, earlier fungal containment and/or to other fungal activities.

In each of the hypovirulent mutant infections with altered early phagocyte responses we found lower proinflammatory cytokine induction after one day of infection. This is consistent with the idea that earlier and/or more efficient fungal containment of the *pep8*Δ/Δ, *nmd5*Δ/Δ

and *brg1*Δ/Δ mutants reduces subsequent immune responses. Since these genes were not induced significantly at 4-6 hpi, this suggests that early immune containment may be driven by alternate signals such as reactive oxygen species or bioactive lipids (235–237). Given the potential for immune pathology-related host death (238–240), it is likely that these reduced levels of proinflammatory cytokines in mutant infections is protective for the host. It is also possible that lower cytokine gene expression is due to lower overall burden, reduced tissue damage or altered stimulation of host pattern recognition receptors, especially given the cell wall-related functions of *pep8*Δ/Δ, *nmd5*Δ/Δ and *brg1*Δ/Δ (59,174,220,229,230,241). Overall, the gene expression results suggest that lower, not higher, cytokine production is associated with immunity and host survival.

For four of the mutants with lower virulence, there were no significant changes to the early phagocyte response to infection. Fish infected with *mad2*Δ/Δ, *apm1*Δ/Δ, *rim101*Δ/Δ and *cek1*Δ/Δ mutants did not show differences in recruitment of macrophages or neutrophils, nor did they show differences in containment of *Candida*. This suggests that the reduced virulence of these mutants is not primarily due to a stronger early innate immune response. Previous work showed that *MAD2* mutants have increased sensitivity to hydrogen peroxide and suggests that they may have reduced survival in mouse macrophages (222). *RIM101* and *CEK1* are known to play a role in regulating filamentous growth. *RIM101* codes for a pH-responsive transcription factor which induces hyphal growth and represses acid-response genes; it is implicated in virulence and *Candida*-epithelial interactions (82,224). Therefore, reduced virulence of these mutants could be due to a loss of other virulence-associated attributes such as intraphagocyte survival, filamentous growth or ability to cause tissue damage at later times during infection.

Our identification of three *Candida* genes that regulate early innate immune recruitment in unexpected ways challenges our simple ideas of how phagocytes function early during fungal infection. In this targeted forward genetics screen, we sought to identify new genes and pathways that regulate early innate immune responses to *Candida* infection. Despite enriching for potential immune evasion factors, we did not see any mutants that showed a significant increase in recruitment of macrophages or neutrophils to the site of infection. Instead, our finding that some infections were highly contained with lower levels of immune recruitment raises two important questions about regulation of innate immune responses in the vertebrate host. First, is the level of recruitment in the first six hours a highly-regulated phenomenon that depends on the level of extracellular fungi? Second, can *Candida* regulate the signals that drive phagocytosis once macrophages and neutrophils get to the infection site? Leveraging the ability to intravitally image early immune dynamics in the zebrafish will allow us to understand if the temporal dynamics of immune response is regulated by the activity of these fungal genes.

CHAPTER 3

THE ROLE OF *RBT1* IN *C. ALBICANS* VIRULENCE

3.1 Introduction

Microorganisms interact with host cells, including immune cells, through their cell wall and secreted peptides. These interactions can promote adhesion, survival, and virulence of microbes such as *Candida albicans*. *RBT1* codes for a GPI linked cell wall protein that is found on the surface of *C. albicans* hyphae (242,243). In addition, two peptides coded for by *RBT1* can be found secreted in the supernatants of *C. albicans* cultures (86). This makes Rbt1p a good candidate for an immunomodulatory virulence factor of *C. albicans*.

RBT1 was first discovered in a screen for genes that are regulated by Tup1p, a transcriptional repressor of filamentous growth. Deletion of *TUP1* results in constitutively filamentous growth and leads to increased expression of several genes most of which, including *RBT1*, are also induced in WT cells undergoing filamentous growth (243). In the common lab reference strain SC5314, *RBT1* has alleles of different lengths resulting in peptides of 750 amino acids and 611 amino acids. Immunofluorescence experiments with epitope-tagged proteins revealed that both the long and short versions of Rbt1 were seen on the surface of hyphae but not on the surface of yeast cells. Analysis of clinical isolates revealed that many have *RBT1* alleles of differing lengths, and although the insertions or deletions tended to be in the same locations, they were not the same as the reference strain (242). Rbt1p shares 43% identity with another hyphal cell wall protein, Hwp1p. Hwp1p (Hyphal wall protein 1) is a hyphal-expressed protein that plays a role in biofilm formation and adhesion to host epithelial cells (244). While Rbt1p is similar to Hwp1p, the portion of

the protein that is displayed on the outside of the cell wall is the least similar, with only 16% identity, suggesting that these proteins have different functions (243).

RBT1 is upregulated very early in the yeast-to-hyphal transition, as early as 30 minutes after induction of hyphal growth (243,245). There are many pathways in *C. albicans* that control the expression of hyphal expressed genes. The cAMP/PKA pathway is one of these major pathways. *EFG1* codes for a transcription factor of the cAMP/PKA pathway, that has been shown to induce expression of *RBT1* (246–248). In addition, the transcription factor *CPH2* was seen to positively regulate *RBT1* expression in response to Lee's medium (247), and the transcription factor *RIM101* induces expression in response to alkaline pH (248–250). However, *CPH1* a transcription factor of the MAPK pathway regulating hyphal growth, does not seem to regulate *RBT1* expression (246,247). *NRG1*, like *TUP1*, is a repressor of filamentous growth and represses a number of hyphal expressed genes including *ECE1* and *HWP1*. However, it seems that it only minimally represses *RBT1*, if at all (251). While *RBT1* is upregulated in hyphal cells and this protein is incorporated into the hyphal cell wall, *RBT1* does not appear to be required for hyphal growth as no defects in hyphal growth have been observed *in vitro* for *RBT1* mutants (243).

Evidence suggests Rbt1p plays a role in biofilm formation in both *C. albicans* and *C. parapsilosis*. *RBT1* was shown to be upregulated in *C. parapsilosis* biofilms, and its deletion reduced biofilm depth and mass on Thermanox slides (252). Deletion of *HWP1, HWP2,* or *RBT1* in *C. albicans* decreased biofilm mass with *hwp1*Δ/Δ showing the greatest reduction (only statistically significant one). Deletion of all 3 genes resulted in an even further decrease in biofilm formation (253). Furthermore, overexpression of the long or short alleles of *RBT1* resulted in increased biofilm formation as well as increased aggregation under hyphal

inducing conditions (242). Overexpression of the full-length allele showed consistently bigger aggregates and biofilms than the short-length allele. While overexpression increased cell to cell adhesion, overexpression of the full-length allele reduced *C. albicans* attachment to human epithelial cells and there was no significant difference in epithelial cell adhesion with the short-length allele (242).

Braun et al (243) found that *RBT1* was important for virulence in both mouse systemic infection and rabbit corneal infection. Intravenous infection of mice with *C. albicans* over a period of up to 20 days showed a significant decrease in virulence for *rbt1*Δ/Δ, with no *C. albicans* cells detectable in the kidneys of these mice. In addition, strains that had either allele of *RBT1* deleted also showed a significant decrease in virulence, but this virulence defect was not as severe as the homozygous *RBT1* mutant. While this loss of virulence was observed for 6 independent *rbt1*Δ/Δ strains, reintegration of the WT allele was not able to restore virulence to the *rbt1*Δ/Δ or *rbt1/RBT1* strains. Thin rabbit cornea sections taken after 6 days of infection with WT *C. albicans* show hyphal invasion into the cornea, but the *RBT1* mutant showed little to no invasion. While a severe defect for *rbt1*Δ/Δ was seen in rabbit corneal infection, a much more mild phenotype was observed in a mouse corneal infection model. In this model, a difference was only observed after 4 days of infection with an initial inoculum of 10^6 CFU. Keratitis scores for *rbt1*Δ/Δ (the same mutant as used in rabbit corneal infection) decreased from severe at 4 days post infection to mild by 8 days post infection, while the WT Caf2-1 infections remained severe over this period. However, no difference was seen between a *rbt1*Δ/Δ transposon mutant and its WT control SC5314, or for either mutant at an inoculum of 10^5. Both yeast and hyphal growth and neutrophilic infiltration was observed in corneal sections at 1 day post infection for both WT and *RBT1* mutant strains

(254). While these studies implicate the importance of *RBT1* in (255)virulence, the lack of data for complemented mutants leaves calls into question the overall relevance of the mutant infection data, and almost nothing is known about the mechanisms underlying how this gene might contribute to virulence.

3.2 Materials and methods

3.2.1 *C. albicans* strains and growth conditions

C. albicans strains were maintained and grown for infection as described in section 2.2.1.

3.2.2 Sequencing of *RBT1*

DNA was isolated from *C. albicans* following using a phenol chloroform extraction with ethanol precipitation following the smash and grab protocol (255). *RBT1* was amplified using RBT1-Fw1-tcaactatgagatttgcaactgc with RBT1-w1-acaaatatctcaattatctgaaacg or RBT1-Rv2-cgaaaatgaaaagcagaataagaagaaaatacg for WT SN250. Amplification of the mutant *rbt1*Δ/Δ$^{968\text{-}2166}$ was carried out using primer pairs: HIS-FwS–gtgtaaaatgctgcgtagcc & RBT1-Rv2, HIS-RvS–ttgcgtaaacttggatttgg & *RBT1*-Fw1, LEU-FwS–ggttctgctcctgatttacc & RBT1-Rv2, and LEU-RvS–ggaaacattcacacaacctgg & RBT1-Fw1. DNA was purified by gel extraction, and both long and short alleles were cloned into *E. coli* DH5α cells. Four individual colonies were picked for each and propagated. Plasmids were then isolated using Qiagen mini prep kit (Qiagen, Hilden, Germany) and sent for sequencing. Two samples for each allele/primer combo were sent for sequencing. Sequencing was performed using the same primers as above for *rbt1*Δ/Δ$^{968\text{-}2166}$. For WT sequencing was performed using primers: RBT1-Fw1, RBT1-Rv2, RBT1-w6- agaaagttactggtggatgtgatac, RBT1-IF2-

caccccatctccatcaactacc, and RBT1-IF3-aagtcaaagccttccctgcc. Sequences were trimmed and imported into Geneious Prime for alignment.

For whole-genome sequencing DNA was isolated following the smash and grab protocol, concentrations were checked via nano-drop and DNA was sent to Seqcenter (Pittsburgh, PA) for Illumina whole genome sequencing.

3.2.3 Full deletion of *RBT1*

Full deletion of *RBT1* from SN250 or SC5314 was achieved using the SAT-flipper method as described previously (201) using LiAC transformation. The deletion cassette was generated by integrating 514 bp up and 485 bp downstream of *RBT1* into a pSFS2 derivative (201) and was excised by restriction digest with KpnI and SacI.

3.2.4 Complementation of *rbt1*Δ/Δ$^{968\text{-}2166}$

Complementation constructs were ordered from Genscript (Piscataway, NJ) in the pUC57 backbone and contain the ORF with 185 bp upstream and 50 bp downstream, followed by *C. dubliensis ARG4* (Figure A.1A). Restriction sites were eliminated from the ORF during gene synthesis. An EcoRV restriction site was designed within the 185 bp upstream region, an NdeI cutsite at the start of the ORF, a BamHi restriction site in *ARG4* upstream region, and a BglII site in the downstream *ARG4* region. EcoRV and BamHi were used to excise fragment for complementation.

Table 3.1 *Candida albicans* strains

Strain	Parental Strain	Genotype	Reference
SN250	SN152	*ura3*Δ*-iro1*Δ*::imm*^{434}*/URA3-IRO1, his1*Δ*/his1*Δ*, arg4*Δ*/arg4*Δ*., leu2*Δ*::C.m.LEU2/leu2*Δ*::C.d.HIS1*	(256)
*rbt1*Δ/Δ$^{968\text{-}2166}$	SN152	*ura3*Δ*-iro1*Δ*::imm*^{434}*/URA3-IRO1, his1*Δ*/his1*Δ*, arg4*Δ*/arg4*Δ*., leu2*Δ*/leu2*Δ *, rbt1*Δ$^{967\text{-}2166}$*::C.mLEU2/rbt1*Δ$^{967\text{-}3166}$*::C.dHIS1*	(256)

Table 3.1 continued

SN250-iRFP	SN152	*ura3Δ-iro1Δ::imm^{434}/URA3-IRO1, his1Δ/his1Δ, arg4Δ/arg4Δ., leu2Δ::C.m.LEU2/leu2Δ::C.d.HIS1 pENO1-iRFP-NATR*	(256), This Study
*rbt1*Δ/Δ$^{968\text{-}2166}$- iRFP	SN152	*ura3Δ-iro1Δ::imm^{434}/URA3-IRO1, his1Δ/his1Δ, arg4Δ/arg4Δ., leu2Δ/leu2Δ , rbt1Δ$^{967\text{-}2166}$::C.mLEU2/rbt1Δ$^{967\text{-}3166}$::C.dHIS1, pENO1-iRFP-NATR*	(256), This Study
*rbt1*Δ/Δ$^{968\text{-}2166}$ +*RBT1*	*rbt1*Δ/Δ$^{968\text{-}2166}$	*ura3Δ-iro1Δ::imm^{434}/URA3-IRO1, his1Δ/his1Δ, arg4Δ/arg4Δ., leu2Δ/leu2Δ , rbt1Δ$^{967\text{-}2166}$::C.mLEU2/rbt1Δ$^{967\text{-}3166}$::C.dHIS1, RBT1::C.d.ARG4*	This Study
*rbt1*Δ/Δ	SN250	*ura3Δ-iro1Δ::imm^{434}/URA3-IRO1, his1Δ/his1Δ, arg4Δ/arg4Δ., leu2Δ::C.m.LEU2/leu2Δ::C.d.HIS1, rbt1Δ$^{1\text{-}2166}$/rbt1Δ$^{1\text{-}2166}$*	This Study
SC5314			
*rbt1*Δ/Δ-5	SC5314	*rbt1*Δ/Δ	This Study
*rbt1*Δ/Δ-9	SC5314	*rbt1*Δ/Δ	This Study

3.2.5 Zebrafish care and maintenance

Zebrafish were maintained and cared for as described in section 2.2.3.

3.2.6 Zebrafish infections

Hindbrain infections were performed as described in section 2.2.4 with infection with SN250 background strains being carried out at 30ºC and infections with SC5314 background strains being carried out a 28ºC. Yolk infections were performed at the same stage as hindbrain infections using the same dose and were carried out at 30ºC.

Infections with peptides were performed as described in section 2.2.4 except after screening fish were split groups with approximately the same *Candida* burden. Half of the fish for each group received ~6-8ng of both the long (ELDEFEELSNDGVTHS) and short (EAEIANKDGTIEK) *RBT1* peptides, and the other half received ~3-4nl PBS (vehicle control).

3.2.7 Quantitative real-time PCR

Quantitative real-time PCR was performed as described in section 2.2.5.

3.2.8 Fluorescence microscopy

Microscopy was carried out as described in section 2.2.6.

3.2.9 Image analysis for *rbt1*Δ/Δ$^{968\text{-}2166}$ infections

Images were analyzed as described in section 2.2.7.

3.2.10 Image analysis for *RBT1* peptide infections

To analyze the immune response to *RBT1* peptide infections, images from 6 hpi and 24 hpi were imported in Fiji (ImageJ). The hindbrain ventricle/infection area was outlined on each z-slice, and masks were made from this defining the hindbrain ventricle/infection area. For the *Candida*, macrophage (mpeg:GFP+), and neutrophil (lysC:dsRed+) channels 5 background measurements were taken and a threshold set 1 above the max background fluorescent intensity measurement. This threshold was then used to create a mask. All masks were then imported into Matlab. In matlab pixel area was converted into in μM, and the area of *Candida*, macrophages, and neutrophils summed. A distance map was created for *Candida*, macrophages, and neutrophils using the bwdistc function (257). The distance of each *Candida* pixel from the closest macrophage pixel and neutrophil pixel was found, and vice versa. The closest distance to a macrophage or neutrophil pixel for each *Candida* pixel was then determined (tie going to the neutrophil). The amount of *Candida* total intracellular or inside a macrophage or neutrophil was then determined. *Candida* was considered intracellular if it was within 3 pixels of a macrophage or neutrophil pixel. The sum of intracellular *Candida* was then taken (total, inside macrophage, inside neutrophil), and this was

divided by the total sum of *Candida* to get a percentage of *Candida* that was intracellular. Note that this does not take into account *Candida* taken up by a non-fluorescent cell.

3.2.11 Statistical analysis

Statistical analysis was performed using GraphPad Prism software. For analysis of survival, Kaplan-meier curves were generated from pooled experiments and Mantel-Cox log rank tests were performed with Bonferroni correction. For analysis of differences in phagocyte recruitment and containment, T-tests were performed if normally distributed, or Mann-Whitney tests were performed if not normally distributed. For analysis of qPCR results unpaired T-tests were performed.

3.3 Results

*rbt1*Δ/Δ$^{968\text{-}2166}$ was avirulent in the zebrafish hindbrain infection model (Figure 2.1D & Figure 2.2). To determine if this virulence defect was due to an enhanced immune response we transformed this strain and the SN250 with pENO1-iRFP, and performed infections in *Tg(mpeg1:GFP)/(lysC:dsRed)* larval zebrafish (Green macrophages and red neutrophils) and imaged infection at 4 hpi (Figure 3.1A). While similar numbers of macrophages were recruited to SN250 and *rbt1*Δ/Δ$^{968\text{-}2166}$ infections, there was a trend for increased neutrophil recruitment to *rbt1*Δ/Δ$^{968\text{-}2166}$ infections (Figure 3.1B-C, Table A.2). Despite the trend for increased neutrophil recruitment there were similar levels of containment of *Candida* between the SN250 and the mutant strain (Figure 3.1D-E, Table A.1). Interestingly despite the immune recruitment at 4-6 hpi, we saw little induction of the inflammatory response at 4hpi as assessed by qPCR of *cxcl8b*, *tnfa*, and *il1b* (Figure 3.2A). However, at 24 hpi we see a significant reduction of *cxcl8b* and *il1b* in our *rbt1*Δ/Δ$^{968\text{-}2166}$ infected larvae compared to

SN250 infected larvae (Figure 3.2B). This may be due to enhanced containment and clearance of *rbt1*Δ/Δ$^{968\text{-}2166}$ infected larvae by 24 hpi requiring less of an immune response as in the SN250 which still needs to control the infection.

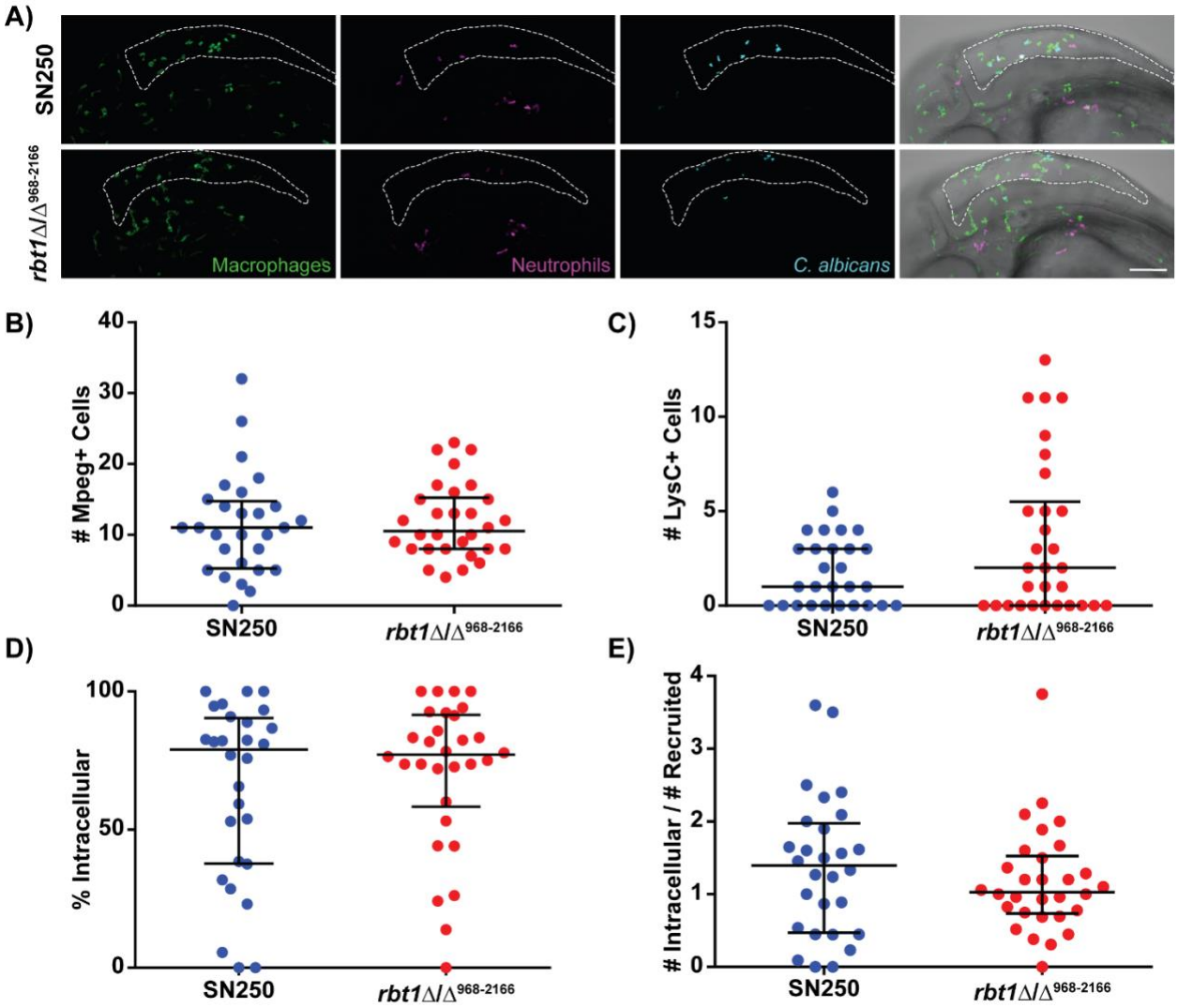

Figure 3.1. A trend for increased neutrophil recruitment to *rbt1*Δ/Δ$^{968\text{-}2166}$. A) Representative images of SN250 and *rbt1*Δ/Δ$^{968\text{-}2166}$ infected fish at 4-6 hours post infection. Images were scored by eye for the number of macrophages (*mpeg1*:GFP+ cells) shown in green and number of neutrophils (*lysC*:dsRed+ cells) in magenta recruited to the infection, as well as if the *Candida* was intracellular or extracellular. Scalebar is 100 μm. **B)** Plot showing the number of *mpeg1*:GFP+ cells recruited to hindbrain. **C)** Plot showing the number of *lysC*:dsRed+ cells recruited to hindbrain shows a trend for increased neutrophil recruitment to *rbt1*Δ/Δ$^{968\text{-}2166}$ (Students t-test, p=0.0567). **D)** Plot showing the % of *Candida* that was intracellular inside an

Figure 3.1 contiuned
mpeg1:GFP+ cell, *lysC*:dsRed+ cell, or non-fluorescent cell. **E)** Plot showing the number of *Candia* taken up per phagocyte. Data pooled from 3 independent experiments (SN250 n=28, *rbt1*Δ/Δ$^{968\text{-}2166}$ n =30).

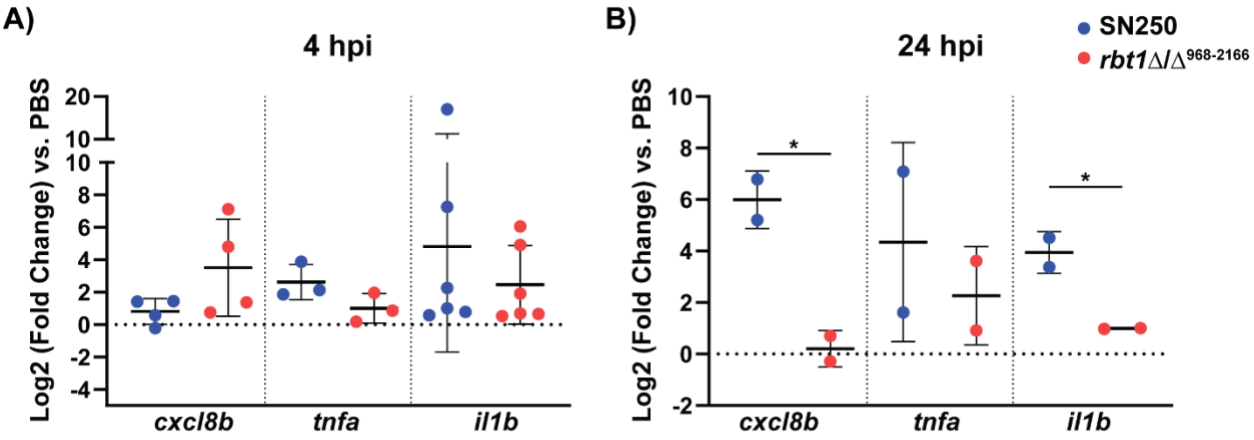

Figure 3.2. Inflammatory response to *rbt1*Δ/Δ$^{968\text{-}2166}$. A) Expression of *cxcl8b*, *tnfa*, and *il1b* in SN250 and *rbt1*Δ/Δ$^{968\text{-}2166}$ infected fish at 4 hours post infection by qPCR analysis shows little induction of inflammatory response. **B)** Expression of *cxcl8b*, *tnfa*, and *il1b* in SN250 and *rbt1*Δ/Δ$^{968\text{-}2166}$ infected fish at 24 hours post infection by qPCR analysis shows increased expression of *cxcl8b* (Students t-test, p=0.0251) and *il1b* (Students t-test, p=0.0354).

In WT infected larvae the cause of death is typically due to invasive hyphal growth typically observed by 24 hpi. However, in *rbt1*Δ/Δ$^{968\text{-}2166}$ infected larvae we never observed invasive hyphal growth. In fact, only 1 fish was observed to have filamentous growth at 24 hpi, and this was gone by 48 hpi. To assess if there was a filamentation defect of *rbt1*Δ/Δ$^{968\text{-}2166}$ in our larvae we next performed yolk infections. Here larvae are infected at the same stage as hindbrain injection, but there tends to be a delayed immune response in this infection model and more filamentous growth. During yolk infection *rbt1*Δ/Δ$^{968\text{-}2166}$ did form invasive hyphae that caused mortality in the larvae, though still significantly less than SN250 (Figure 3.3, p<0.0001).

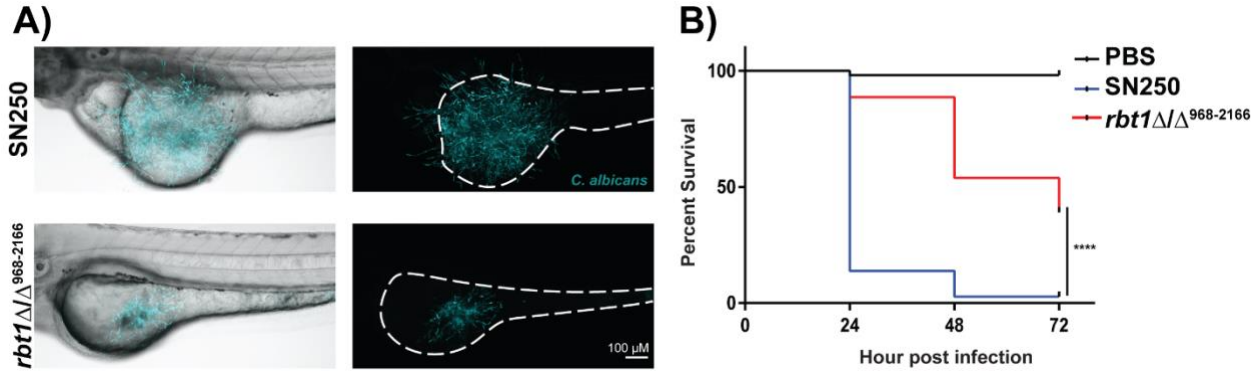

Figure 3.3. *rbt1*Δ/Δ$^{968\text{-}2166}$ shows reduced invasion and damage in yolk infection. A) Images of SN250 and *rbt1*Δ/Δ$^{968\text{-}2166}$ infected fish at 24 hours post infection. Scalebar is 100 µm. Images show that *rbt1*Δ/Δ$^{968\text{-}2166}$ is still able to form invasive hyphae. **B)** Kaplan-Meier survival curve of fish injected with PBS (n=108), SN250 (n=108), or *rbt1*Δ/Δ$^{968\text{-}2166}$ (n=115). Curves show a significant reduction in virulence of *rbt1*Δ/Δ$^{968\text{-}2166}$ ($p<0.0001$).

To confirm the virulence defect of *rbt1*Δ/Δ$^{968\text{-}2166}$, two independent isolates were tested, and both were avirluent in the hindbrain infection model. In the process of confirming the deletion region we discovered that the presence of a long and short allele in the WT SN250 strain as previously described, but in contrast to the current annotation in the Candida Genome Database (Figure A.2 & A.3) (242). In addition, the mutant *orf19.3384*Δ/Δ (*rbt1*Δ/Δ$^{968\text{-}2166}$) from Assembly 19 has since been deleted and merged with *RBT1* (*orf19.1327*), and the corrected annotation revealed that the deletion only eliminates the C-terminus of the *RBT1* gene. Sequencing of this mutant revealed that the deletion leaves intact the first 967 base pairs of *RBT1*, which are common between both alleles, so we have renamed this mutant *rbt1*Δ/Δ$^{968\text{-}2166}$. The remaining portion of *RBT1* in the *rbt1*Δ/Δ$^{968\text{-}2166}$ mutant encodes at least two secreted peptides that are detectable in fungal supernatants by LC-MS (Figure 3.4A) (86). The function of these peptides is unknown, and it is unknown whether they are still produced in this mutant. In order to test if the avirulence phenotype was associated with the partial deletion of *RBT1*, a full deletion mutant

was made in both SN250 and SC5314 backgrounds. Surprisingly, these *rbt1*Δ/Δ full-deletion mutants showed only a mild virulence defect in SC5314, with no significant effect on virulence in the SN250 background (Figure 2.4, Figure3.4B).

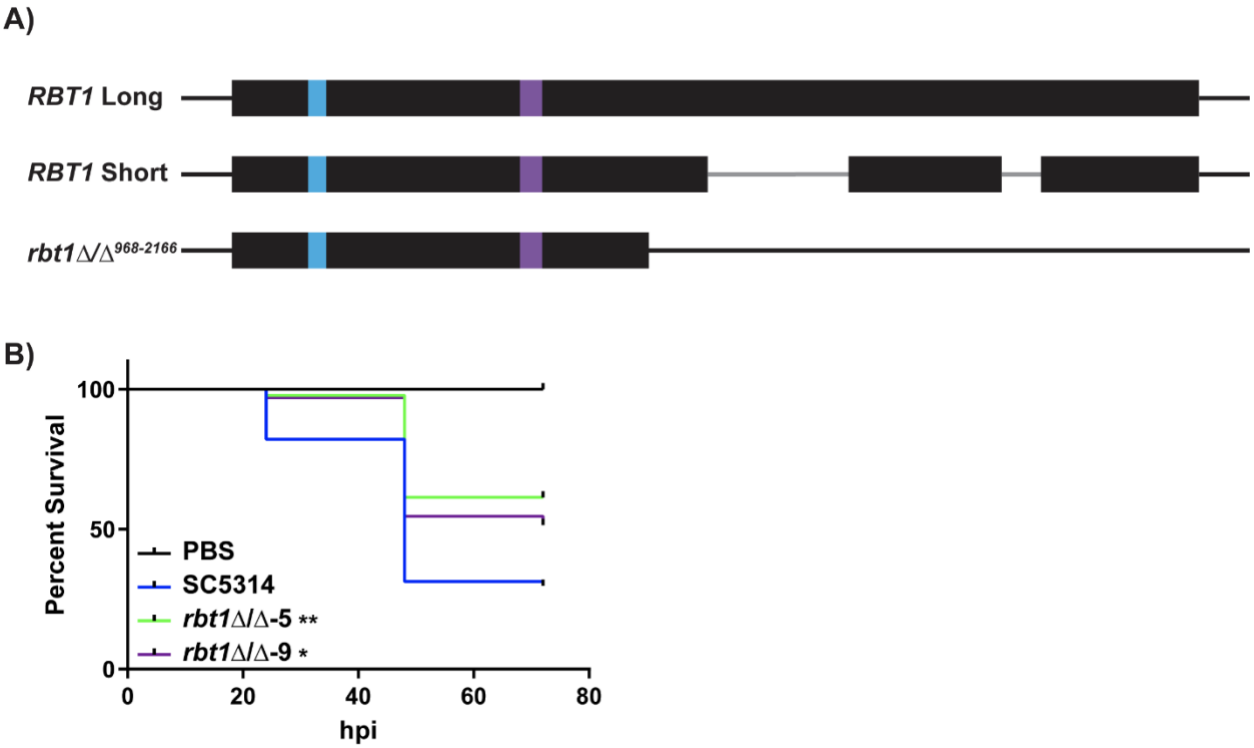

Figure 3.4. Variation of *RBT1* alleles and mutants. A) Schematic showing the different *RBT1* alleles. Areas missing in the short allele are shown in grey. The region coding for the short peptide is shown in light blue, and the long peptide in purple. The *rbt1*Δ/Δ$^{968\text{-}2166}$ mutant deletion starts at base pair 968, shown by the end of the black box. **B)** Kaplan-Meier survival curve of fish injected with PBS (n=37), SC5314 (n=67), *rbt1*Δ/Δ-5 (n=44), or *rbt1*Δ/Δ-9 (n=33). Curves show a significant reduction in virulence of *rbt1*Δ/Δ-5 (Mantel-Cox log rank test, p=0.0012), and *rbt1*Δ/Δ-9 (Mantel-Cox log rank test, p=0.0468).

Because of the differing phenotypes between the full deletion mutants and *rbt1*Δ/Δ$^{968\text{-}2166}$ we decided to investigate the role of the peptides encoded within the first 967 bp of *RBT1*. Here hindbrain infections were performed with SC5314 or *rbt1*Δ/Δ. Fish were screened and split so that both groups received larvae with approximately the same fungal burden. Half of the fish were then injected with the two *RBT1* peptides (~6-8ng each peptide, Genscript) and the other half PBS (vehicle control). Interestingly, larvae injected with the peptides showed a

trend toward increased survival for both SC5314 and *rbt1*Δ/Δ, with survival of 37.5% & 31.373% compared to 24.242% & 20.0% for those only receiving PBS respectively (Figure 3.5A). Imaging of these infections in *Tg(mpeg1:GFP)/(lysC:dsRed)* larvae and quantifying the recruitment by area of pixels showed a trend for increased macrophage recruitment to *rbt1*Δ/Δ infections compared to SC5314 both with and without peptides at 6-8 hpi (Figure 3.5B). Furthermore, addition of the peptides to the *rbt1*Δ/Δ infected fish significantly increased neutrophil recruitment (Figure 3.5C, Mann-Whitney, p=0.0179). In addition, in the presence of the peptides *rbt1*Δ/Δ showed a trend for increased containment compared to SC5314 (Figure 3.5D, p=0.0657). At 24 hpi, there does not appear to be a difference in the recruitment of macrophages or neutrophils to the infection site (Figer 3.6A-B). The addition of peptides shortly after infection resulted in a trend for reduced *Candida* amount (measured by area in 24 hpi images) by 24 hpi (Figure 3.6C, p=0.1732). In addition, it appears that fewer fish have invasion of hyphae out of the hindbrain in the SC5314 + peptides group compared to the SC5314 group alone (Figure 3.6D).

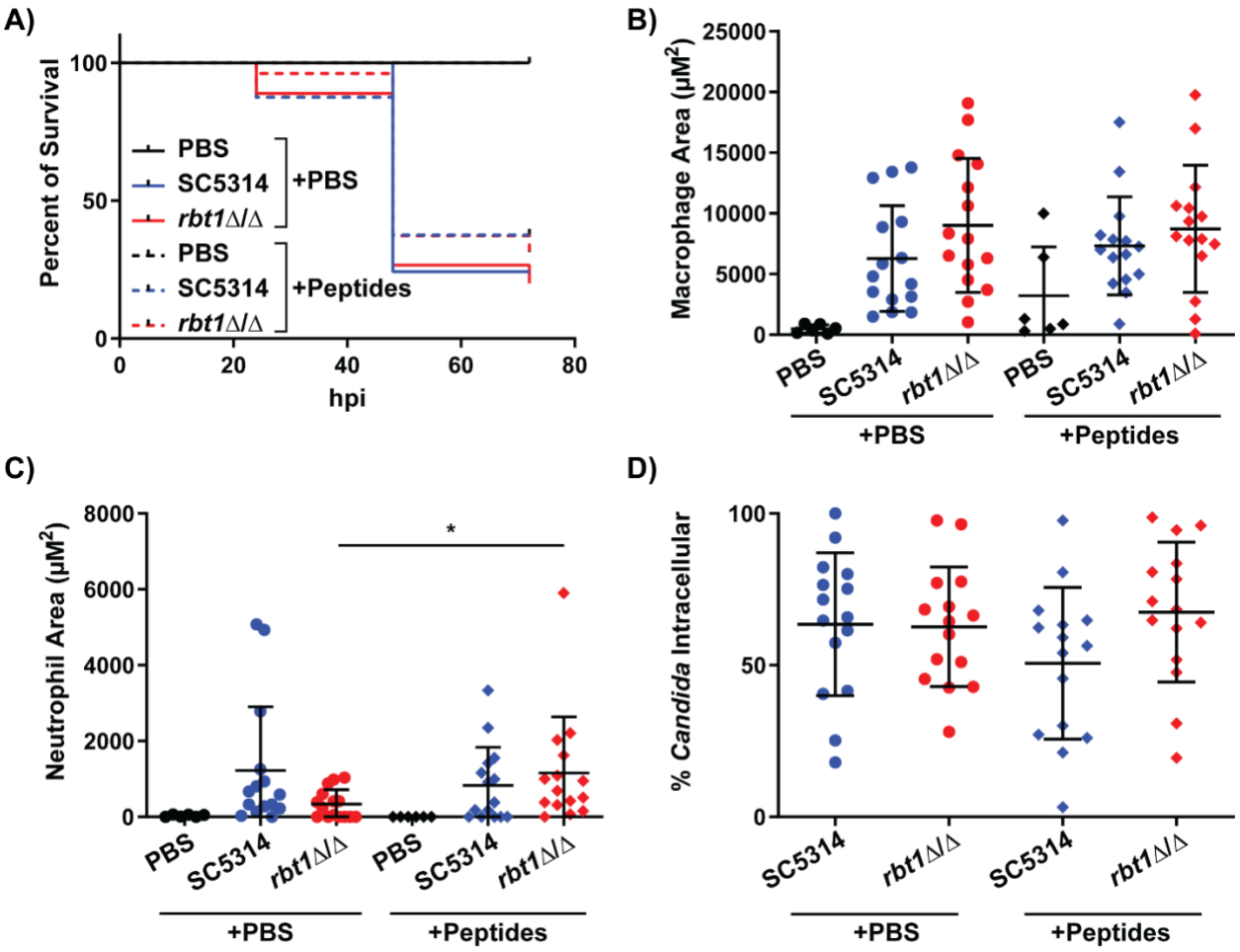

Figure 3.5 Addition of *RBT1* peptides show a trend for improving host response at 6 hours post infection. A) Kaplan-Meier survival curve of fish injected with PBS, SC5314, or *rbt1*Δ/Δ, and receiving peptides or PBS vehicle control. Fish receiving injection of peptides show a trend for increased survival (SC5314 PBS vs peptides p=0.7501, *rbt1*Δ/Δ PBS vs. peptides p=1229). PBS + PBS n=34, SC5314 + PBS n=33, *rbt1*Δ/Δ + PBS n=45, PBS + peptides n=34, SC5314 + peptides n=32, *rbt1*Δ/Δ + peptides n=51. **B)** Area of recruited macrophages as quantified by area of pixels at 6 hpi. **C)** Area of recruited neutrophils as quantified by area of pixels at 6 hpi. Addition of peptides to *rbt1*Δ/Δ infection significantly increased neutrophil recruitment (Mann-Whitney, p=0.0179). **D)** Percent of *Candida* intracellular within an *mpeg1*:GFP+ cell or *lysC*:dsRed+ cell. *Candida* was considered intracellular if a *Candida* pixel was within 3 pixels of a macrophage or neutrophil pixel.

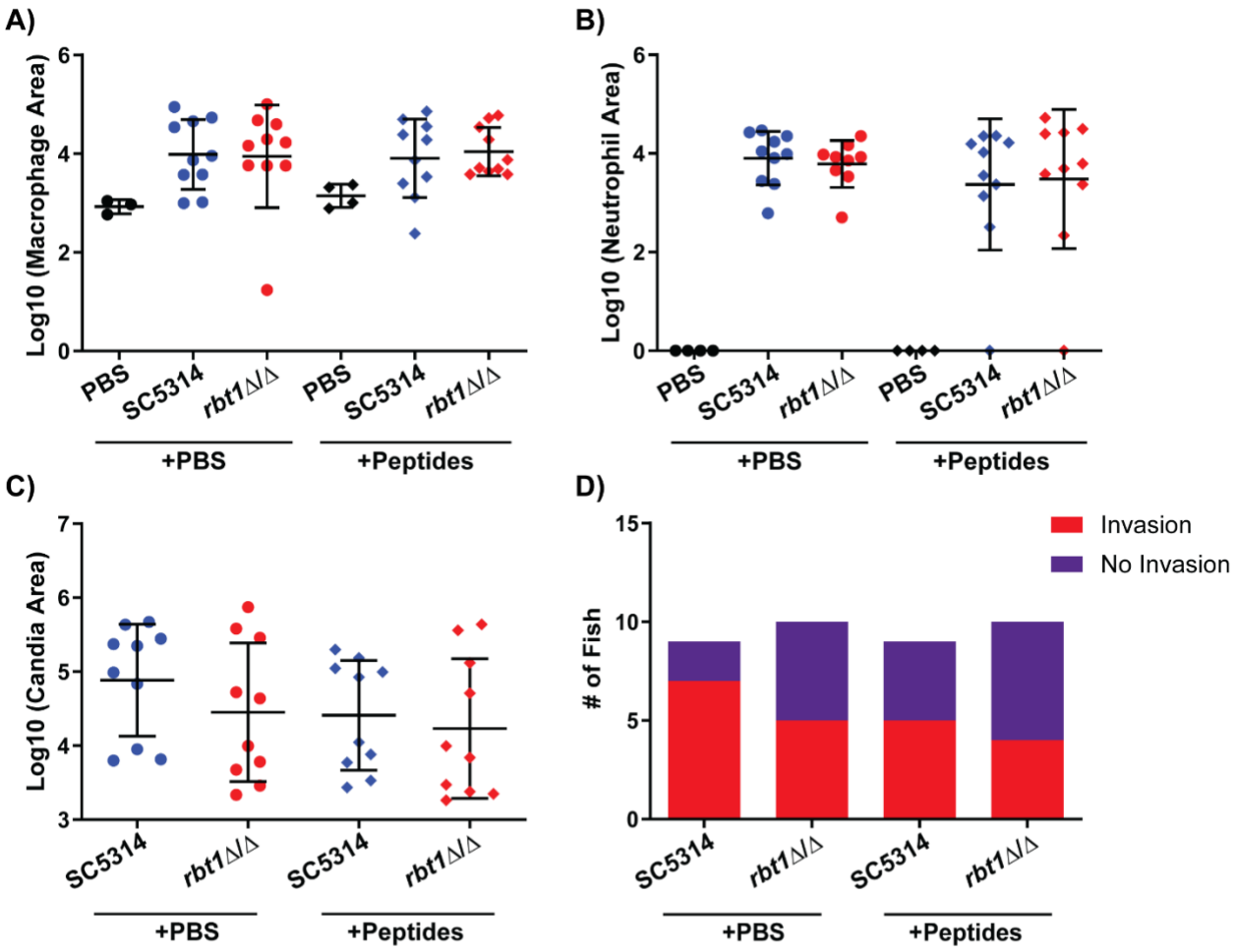

Figure 3.6 Addition *RBT1* peptides show a trend for reduced *Candida* growth and invasion at 24 hours post infection. A) Area of recruited macrophages as quantified by area of pixels at 24 hpi. **B)** Area of recruited neutrophils as quantified by area of pixels at 24 hpi. **C)** Area of *Candida* growth as quantified by area of pixels at 24 hpi. The addition of peptides shows a trend of reducing *Candida* growth. **D)** Number of fish with or without invasion out of the hindbrain at 24 hpi. Addition of peptides to SC5314 infection shows a trend of reducing invasion.

Because of the difference in the phenotypes of the partial deletion mutant and the full deletion mutant, along with the inability to restore virulence upon complementation of the *rbt1*Δ/Δ$^{968\text{-}2166}$ strain (Figure 2.4), it is likely that there is one or more mutations in key virulence genes that are present in both independent isolates of *rbt1*Δ/Δ$^{968\text{-}2166}$ in the Noble

library. Therefore, we performed whole genome sequencing on the mutants to try to determine if there is any other mutation that is the cause of the avirulence phenotype. Initial analysis of sequences using the Yeast Mapping Analysis Pipeline (YMAP) (258,259) revealed significant loss of heterozygosity on the right arm of chromosome 4 (*RBT1* is on chromosome 4 with coordinates 747,331 to 745,166) of *rbt1*Δ/Δ$^{968\text{-}2166}$ and the complemented strain that was not present in other mutants (Figure 3.7A). In addition, the complemented strain showed increased copy number towards the middle to right arm of chromosome 4. While the SN250 background *rbt1*Δ/Δ mutant also showed loss of heterozygosity this was on the left arm of chromosome 4 and that was also present in the complemented strain. Conversely, the *RBT1* mutants in the SC5314 background did not show significant loss of heterozygosity or copy number variation compared to the parent SC5314 strain (Figure 3.7B).

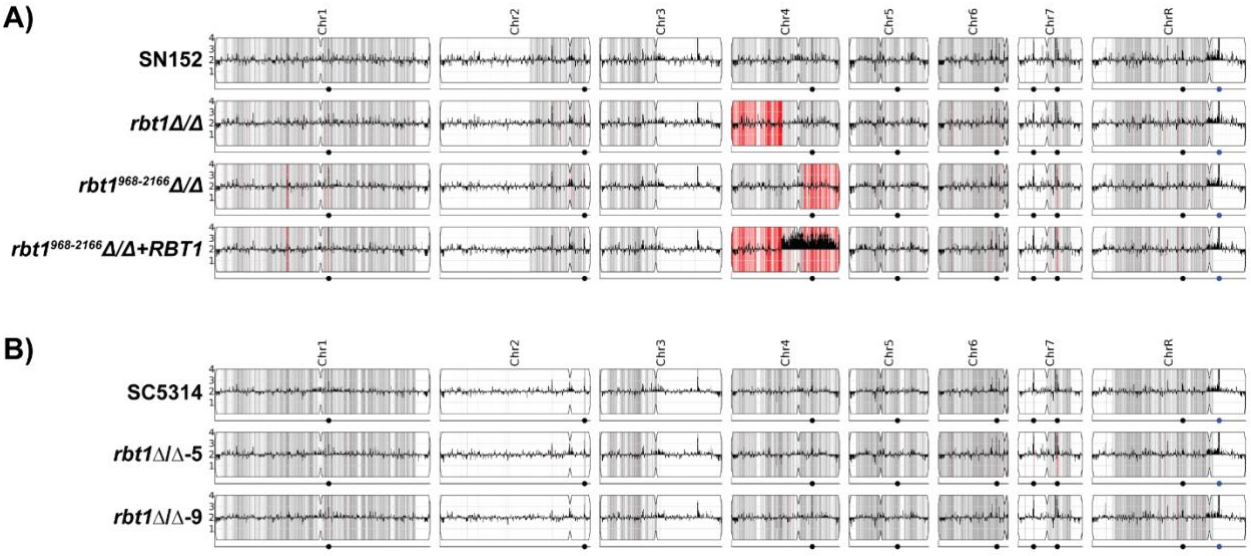

Figure 3.7 YMAP analysis of whole genome sequencing of *RBT1* mutants. *RBT1* is left of the center of chromosome 4 with coordinates 747,331 to 745,166. **A)** YMAP results for Noble background *RBT1* strains. SN152 is the parental strain for this library. Mutant and complemented strains show loss of heterozygosity shown red. The complemented strain *rbt1*Δ/Δ$^{968\text{-}2166}$+*RBT1* shows increased copy number of the middle to right arm of chromosome 4 depicted by the peaks starting near *RBT1*'s allelic location. **B)** YMAP results for SC5314 background *RBT1* mutants.

Figure 3.7 continued

Peaks represent differences in the copy number of a particular location. Mutant strains show mostly consistency with the parental SC5314.

3.4 Discussion

RBT1 is a little studied hyphal cell wall protein that encodes two secreted peptides. Little is known about the role that *RBT1* plays in *C. albicans*. A study by Braun et al (12) suggests that it may play a role in virulence in disseminated infection, but this was complicated by the inability of complementation to restore virulence defects despite multiple independent mutants showing this defect. Similarly, we saw that two independent isolates of the partial deletion mutant *rbt1*Δ/Δ$^{968\text{-}2166}$ were avirulent in the hindbrain infection model, but complementation did not restore virulence. In addition to decreased virulence in systemic infection, previous studies also showed these strains had reduced virulence in rabbit and corneal mouse corneal infection. However, use of *RBT1* mutants with different backgrounds in the mouse corneal infection showed no difference compared to WT (12,260). Similarly, when using CRISPR to create our own full deletion mutants we saw little to no virulence defect compared to WT controls. Sequencing of *RBT1* mutant and wild type strains from the Noble background revealed significant loss of heterozygosity on the right arm of chromosome 4. This suggests that the avirulence observed for *rbt1*Δ/Δ$^{968\text{-}2166}$ is due to off-target genetic differences, and not the partial loss of *RBT1*. Further analysis of the whole genome sequencing data is needed to identify possible differences that may account for this.

The partial deletion mutant *rbt1*Δ/Δ$^{968\text{-}2166}$ still has the first 967 bp intact in which the two secreted peptides are coded for (261). It is unknown whether these peptides are still made and secreted in the partial deletion mutant. While not significant, there was a trend for increased survival when these peptides were injected into SC5314- or *rbt1*Δ/Δ-infected fish shortly

after infection. While there was not a statistically significant difference in survival with the peptides, fish only received one dose shortly after infection; perhaps further treatment with the peptides would have a greater impact. Overall, this data suggests that these peptides may actually play a protective role for the host against *C. albicans* infection, however more work is needed to confirm this.

Because *RBT1* codes for two secreted peptides and is a hyphal cell wall protein, we hypothesized that it is likely that it is interacting with host cells. Therefore, it is interesting to consider the effect it may have on host immune cells such as phagocytes. We observed a trend for increased neutrophil recruitment to *rbt1*Δ/Δ$^{968\text{-}2166}$ as well as *rbt1*Δ/Δ + peptides (compared to *rbt1*Δ/Δ alone) at 6 hours post infection. In addition, there was a trend for increased macrophage recruitment to *rbt1*Δ/Δ infections compared to WT at 6 hours post infection. These trends for increased immune recruitment are encouraging that *RBT1* may indeed be affecting the host immune response. However, further experiments are needed to confirm this and to tease out the role of the cell wall portion of *RBT1* vs. the peptides. By 24 hpi however, there was no difference in immune recruitment; perhaps continued *RBT1* treatment is needed to maintain an effect on immune cells. Since *RBT1* is both found on the surface of hyphae and contains secreted peptides, it is possible that these are playing different roles during infection. Further work to determine the roles of cell wall bound Rbt1 versus the peptides may be interesting.

CHAPTER 4

THE CONTRIBUTION OF LIPASES TO *C. ALBICANS* VIRULENCE

4.1 Introduction

Lipases catalyze the hydrolysis of triglycerides to fatty acids and glycerol. Many microbes secrete lipases. This can serve many purposes for the microbe. The most obvious purpose is for nutrient acquisition, but lipases may also promote virulence by promoting adhesion to host tissue or altering the host immune response through synthesis of bioactive lipids.

4.1.1 Bacterial lipases

Lipases have been shown to contribute to virulence of various bacteria such as *Pseudomonas aeruginosa* and *Staphylococcus aureus* (262). Evidence suggests that the *P. aeruginosa* lipase can limit the monocyte response as preincubation of monocytes with *P. aeruginosa* lipase was shown to limit their migration to zymosan activated serum as well as ROS production. This inhibition was concentration dependent and was abolished when the lipase was heated (262). However, *P. aeruginosa* lipase was seen to have very little effect on neutrophil chemotaxis and ROS production in the same assays (262). Similarly, incubation of rat pulmonary alveolar macrophages with *Pseudomonas cepacia* lipase reduced bacterial uptake in a dose-dependent manner (263). Lipase from *S. aureus* has also been seen to have immunomodulatory effects against innate immune cells. While the effects on chemotaxis were not entirely clear, *S aureus* lipase was shown to decrease killing by granulocytes (264). Both *P. cepacia* and *S. aureus* lipases have shown to impact immune cell morphology. While untreated immune cells tend to spread across a

surface and produce pseudopodia and projections, lipase treatment seems to limit this. Macrophages treated with *P. cepacia* lipase remained rounded (263) and granulocytes treated with *S. aureus* lipase have flat denuded surfaces (264). In addition to bacterial lipases having direct effects on host cells, they have also been seen to act synergistically with other enzymes. König et al (1996) observed that *P. aeruginosa* lipase enhanced phospholipase C (PLC) induced LTB_4 release from human polymorphonuclear leukocytes (PMNs) and 12-hydroxyeicosatetraenoic acid (12-HETE) from human platelets. In contrast, *P aeruginosa* lipase decreased PLC induced ROS production from human PMNs (265). While lipases may be limiting the host immune response through direct interactions with these host cells, lipase activity may indirectly limit the host response. Research by Chena and Alonzo (266) suggests the ester hydrolase activity of *Staphylococcus aureus* lipase Geh acts on the lipoproteins of *S. aureus* to limit their recognition by TLR2 and cytokine production. Immune evasion is just one way in which these lipases can contribute to virulence. In addition to lipase activity, *Staphylococcus epidemidis* lipase GehD has also been shown to promote the ability of the bacteria to bind collagen (267).

4.1.2 *Candida* lipases

Lipases have been found to contribute to virulence in another *Candida* species, *Candida parapsilosis*. *C. parapsilosis* contains two lipases, *LIP1* and *LIP2*. In *C. parapsilosis*, lipases have been seen to contribute to biofilm formation as a lipase deficient strain was not able to form as thick or as complex biofilms on abiotic surfaces as WT *C. parapsilosis* (268). In addition, lipase deficient *C. parapsilosis* was shown to cause significantly less damage to reconstituted human epithelial cells. When

incubated with macrophage-like cells or human dendritic cells, lipase deficient *C. parapsilosis* was taken up and killed more efficiently (268,269). Immature dendritic cells incubated with lipase deficient *C. parapsilosis* showed increased production of IL-1α, IL-6, TNFα, and CXCL8 after 1 hour of infection, and TNFα and CXCL8 remained increased compared to WT at 24 hpi (269). Interestingly, however, dendritic cells co-incubated with lipase deficient *C. parapsilosis* showed more death than those co-incubated with WT *C. parapsilosis*, and these cells had fewer mature lysosomes (269). During mouse intraperitoneal (i.p.) infection, lipase deficient *C. parapsilosis* showed reduced CFU's as early as 2 days post infection in the livers, spleens, and kidneys. By 4 days post infection it was no longer detected, whereas it took mice 7 days to clear WT infection. While there was a big difference in i.p. infection, there was no difference in CFU's or survival in mice infected intravenously suggesting the importance of *C. parapsilosis* lipase for penetrating tissue to cause infection (268).

4.1.2.1 *C. albicans* lipases

C. albicans possess a family of 10 lipase genes (71). Lipases in *C. albicans* have not been studied as extensively as other hydrolytic enzymes such as the secreted aspartyl proteinases, leaving their role in virulence largely unknown. *C. albicans* lipases have been shown to be differentially expressed at different time points or infection conditions with *LIP 5, 6, & 8* being expressed in almost all conditions tested (71–73). Lipases are even seen to be expressed in the absences of lipids (71) suggesting that they may have roles other than for nutrient acquisition. Schofield et al. (73) observed that in immunodeficient mice (defective NK and T cells) inoculated orally with *C. albicans*, mRNA of *LIP1, LIP2, LIP 3, & LIP10* was detectable in

gastric tissues, but not oral tissues. While *LIP2* was mainly found in colonizing samples, *LIP1* and *LIP3* had much higher expression in infected tissue than colonized tissues. This is consistent with the results of Stehr et al (72) with patients suffering from oral candidiasis, where only one patient sample (none for *LIP10*) showed expression of these lipases (*LIP1*, *LIP2*, *LIP3*), while many showed expression of *LIP4, LIP5,* and *LIP8*. Paraje et al., (270) isolated a lipase from the *C. albicans* clinical strain 387 with 66% similarity to the Lipase 9 precursor. This strain has previously been seen to cause a lipid imbalance and fat deposition in the liver during infection. This lipase was seen to cause damage to macrophages and hepatocytes in vitro and promote the accumulation of fatty vacuoles in these cells (270). In addition, this lipase promoted the increase in ROS production from macrophages (271). These data suggest that *C. albicans* lipases are playing important roles during infection.

While it may be hard to tease out the roles of individual lipases to *C. albicans* virulence, *LIP8* has been shown to be important. Deletion of *LIP8* results in reduced virulence in a mouse model of systemic candidiasis, with decreased fungal burden in the liver in kidneys. In fact, no *Candida* was detected in these organs at three days post infection and mice did not die when followed out to 45 days post infection. In addition, mice infected with the strain overexpressing *LIP8* had the lowest survival rate (between Hets, WT, and KO). While this suggests *LIP8* plays a role in virulence, when the infecting dose was increased from $1x10^5$ CFU to $2x10^5$ CFU, *lip8*Δ/Δ did show some virulence, as mice began to die at 11 dpi, where WT infected mice began to die between 5-10 dpi at $1x\ 10^5$ CFU (74).

Recently, *LIP2* has been implicated in virulence (75). Mice with a *lip2*Δ/Δ bloodstream infection had increased survival compared to WT infected mice. Evidence suggests that *LIP2* is not necessary for *C. albicans* to gain entry into mouse liver and kidneys, but is required to maintain infection in these organs, as mice had similar fungal burdens in these organs 1 hpi, but by 24 hpi and on *lip2*Δ/Δ had significantly reduced CFU's. Further investigation suggested that the decreased virulence of *lip2*Δ/Δ was due to increased production of IL-23 from dendritic cells stimulating an enhanced IL-17 response from γδ T cells leading to fungal clearance. Analysis of the lipase activity suggests that *LIP2* is capable freeing palmitic acid, which was able to suppress TLR2/TLR4 mediated IL-23 production from bone marrow derived dendritic cells (75).

While all the evidence suggests that lipases are important virulence factors for many microbes including *C. albicans*, very little is known about how each of the different *C. albicans* lipases contributes to virulence. Much remains to be elucidated about the mechanisms by which these enzymes may contribute to pathogenesis during *C. albicans* infection.

4.2 Materials and methods

4.2.1 *C. albicans* strains and growth conditions

Strains were grown as described in section 2.2.1.

Table 4.1: *C. albicans* Strains

Strain	Genotype	Source
SC5314 (Parental)	WT	
*lip1-10*Δ/Δ	*lip1*Δ/Δ, *lip2*Δ/Δ, *lip3*Δ/Δ, *lip4::FRT*/*lip4::FRT*, *lip5*Δ/Δ, *lip6::FRT*/*lip6::FRT*, *lip7*Δ/Δ, *lip8*Δ/Δ, *lip9*Δ/Δ, *lip10*Δ/Δ	All strains in this table were kindly provided by the Hube lab

Table 4.1 continued

*lip1-10*Δ/Δ-GFP	*lip1*Δ/Δ, *lip2*Δ/Δ, *lip3*Δ/Δ, *lip4::FRT*/*lip4::FRT*, *lip5*Δ/Δ, *lip6::FRT*/*lip6::FRT*, *lip7*Δ/Δ, *lip8*Δ/Δ, *lip9*Δ/Δ, *lip10*Δ/Δ	All strains in this table were kindly provided by the Hube lab
*lip1-10*Δ/Δ-RFP	*lip1*Δ/Δ, *lip2*Δ/Δ, *lip3*Δ/Δ, *lip4::FRT*/*lip4::FRT*, *lip5*Δ/Δ, *lip6::FRT*/*lip6::FRT*, *lip7*Δ/Δ, *lip8*Δ/Δ, *lip9*Δ/Δ, *lip10*Δ/Δ	All strains in this table were kindly provided by the Hube lab
*lip8*Δ/Δ	*lip8*Δ/Δ	All strains in this table were kindly provided by the Hube lab
*lip8,5*Δ/Δ	*lip5*Δ/Δ, *lip8*Δ/Δ	All strains in this table were kindly provided by the Hube lab
*lip1-10*Δ/Δ*:lip8o.e.*	*lip1*Δ/Δ, *lip2*Δ/Δ, *lip3*Δ/Δ, *lip4::FRT*/*lip4::FRT*, *lip5*Δ/Δ, *lip6::FRT*/*lip6::FRT*, *lip7*Δ/Δ, *lip8*Δ/Δ, *lip9*Δ/Δ, *lip10*Δ/Δ, *adh1::(P_OP4-P_TET-LIP8 SAT1 P_OP4-cartTA-T_ACT1)*	All strains in this table were kindly provided by the Hube lab
*lip1-10*Δ/Δ*:lip5o.e.*	*lip1*Δ/Δ, *lip2*Δ/Δ, *lip3*Δ/Δ, *lip4::FRT*/*lip4::FRT*, *lip5*Δ/Δ, *lip6::FRT*/*lip6::FRT*, *lip7*Δ/Δ, *lip8*Δ/Δ, *lip9*Δ/Δ, *lip10*Δ/Δ, *adh1::(P_OP4-P_TET-LIP5 SAT1 P_OP4-cartTA-T_ACT1*	All strains in this table were kindly provided by the Hube lab
*lip1,2,3,10*Δ/Δ	*lip1*Δ/Δ, *lip2*Δ/Δ, *lip3*Δ/Δ, *lip10*Δ/Δ	All strains in this table were kindly provided by the Hube lab
*lip4,5,8,9*Δ/Δ	*lip4::FRT*/*lip4::FRT*, *lip5*Δ/Δ, *lip6::FRT*/*lip6::FRT*, *lip7*Δ/Δ, *lip8*Δ/Δ, *lip9*Δ/Δ,	All strains in this table were kindly provided by the Hube lab

4.2.2 Zebrafish care and use

Zebrafish were cared for as described in section 2.2.3.

Table 4.2: Zebrafish lines

Zebrafish Line	Allele	Source/Reference
AB (Wild Type)	n/a	Zebrafish International Resource Center
Tg(mpeg1:EGFP)	gl22Tg	(205)
Tg(lysC:dsRed)	nz50Tg	(206)

4.2.3 Hindbrain infections

Hindbrain infections were performed as described in section 2.2.4.

4.2.4 Fluorescence microscopy

Fluorescence microscopy was performed as described in section 2.2.6.

4.2.5 Image analysis

Images were analyzed as described in section 2.2.7.

4.2.6 Statistical analysis

Statistical analysis was performed as described in section 3.2.11.

4.3 Results

In order to determine the contribution of lipases to the virulence of *C. albicans*, we tested the virulence of a lipase deficient *C. albicans* in the zebrafish hindbrain infection model (Figure 4.1A). Deletion of lipases 1-10 significantly reduced the virulence in this model (Figure 4.1B). To determine if this reduction in virulence was due to an alteration in the early immune response, we used a *lip1-10*Δ/Δ expressing red or green fluorescent proteins. These strains were injected into the hindbrain ventricle of transgenic zebrafish with the complementary green-fluorescent macrophages or red-fluorescent neutrophils. Fish were imaged at 4 hours post-infection to assess early immune recruitment and containment. Figure 4.1A shows images of *Tg(mpeg:GFP)* zebrafish larvae at 4 hours post-infection infected with *lip1-10*Δ/Δ. We did not observe a significant difference in the recruitment of macrophages (Figure 4.1C) or neutrophils (Figure 4.1D) to a *lip1-10*Δ/Δ infection compared to SC5314 (WT) infection. However, we did see a significant increase in the percent of intracellular *Candida* cells for *lip1-10*Δ/Δ compared to *SC5314* (Figure 4.1E).

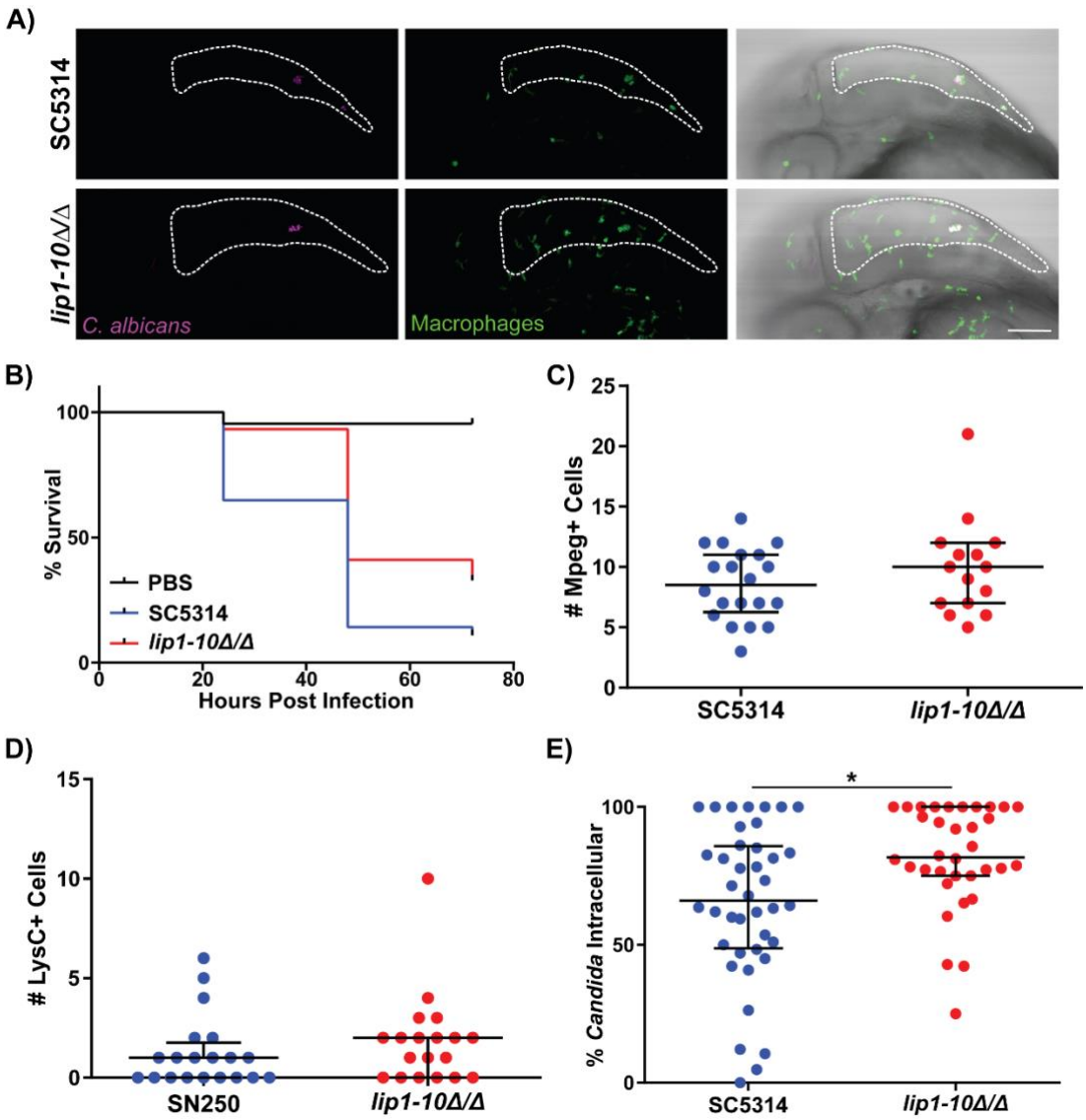

Figure 4.1 Lipase deficient *C. albicans* has reduced virulence. A) *Tg(Mpeg1:GFP)* or *Tg(LysC:dsRed)* (Not pictured) larval zebrafish were imaged by confocal microscopy at 4 hours post infection with WT or lipase deficient *C. albicans*. Images were scored for macrophage *Tg(Mpeg:GFP)* or neutrophil Tg*(LysC:dsRed)* recruitment to the hindbrain and internalization of *C. albicans*. Scalebar is 100um. Hindbrain ventricle is outlined in white. **B)** Kaplan-Meier survival curves fish infected with SC5314 or lipase deficient, *lip1-10*Δ/Δ *C. albicans* show a significant increase in survival of fish infected with lipase deficient *C. albicans* (PBS n=65, SC5314 n=91, *lip1-10*Δ/Δ n=73, p<0.0001). Survival was monitored out to 72 hours post infection. **C)** Number of macrophages recruited to the hindbrain ventricle in SC5314 (n=20) and *lip1-10*Δ/Δ (n=15) infected fish. **D)** Number of neutrophils recruited to the hindbrain ventricle in SC5314 (n=20) and *lip1-10*Δ/Δ (n=19) infected fish. **E)** Fish infected with *lip1-10*Δ/Δ (n=34) had significantly higher percentage containment compared to those infected with SC5314 (n=40, p=0.0095).

Because *LIP5* and *LIP8* are two of the most widely expressed lipases (71–73) and *LIP8* has previously been implicated in virulence (74) we wanted to determine their contribution to virulence in the larval zebrafish model. We observed that *lip8,5*Δ/Δ and *lip8*Δ/Δ had reduced virulence in the zebrafish, but this reduction was not to the same extent as *lip1-10*Δ/Δ (Figure 2A). Because *lip8,5*Δ/Δ and *lip8*Δ/Δ showed reduced virulence, we next wanted to determine if overexpression of *LIP8* or *LIP5* could rescue the virulence defect of *lip1-10*Δ/Δ. However, *lip1-10*Δ/Δ*:lip8o.e.* and *lip1-10*Δ/Δ*:lip5o.e.* still had significantly reduced virulence and did not show rescued virulence as compared to *lip1-10*Δ/Δ (Figure 4.2B). Next, we wanted to determine if lipases for breaking down medium (Lip 1, 2, 3 & 10) or longer chain (Lip 4, 5, 8, & 9) fatty acids were important for virulence. Surprisingly, quadruple lipase mutants, *lip1,2,3,10*Δ/Δ and *lip4,5,8,9*Δ/Δ, showed no difference in virulence compared to SC5314 (Figure 4.2C).

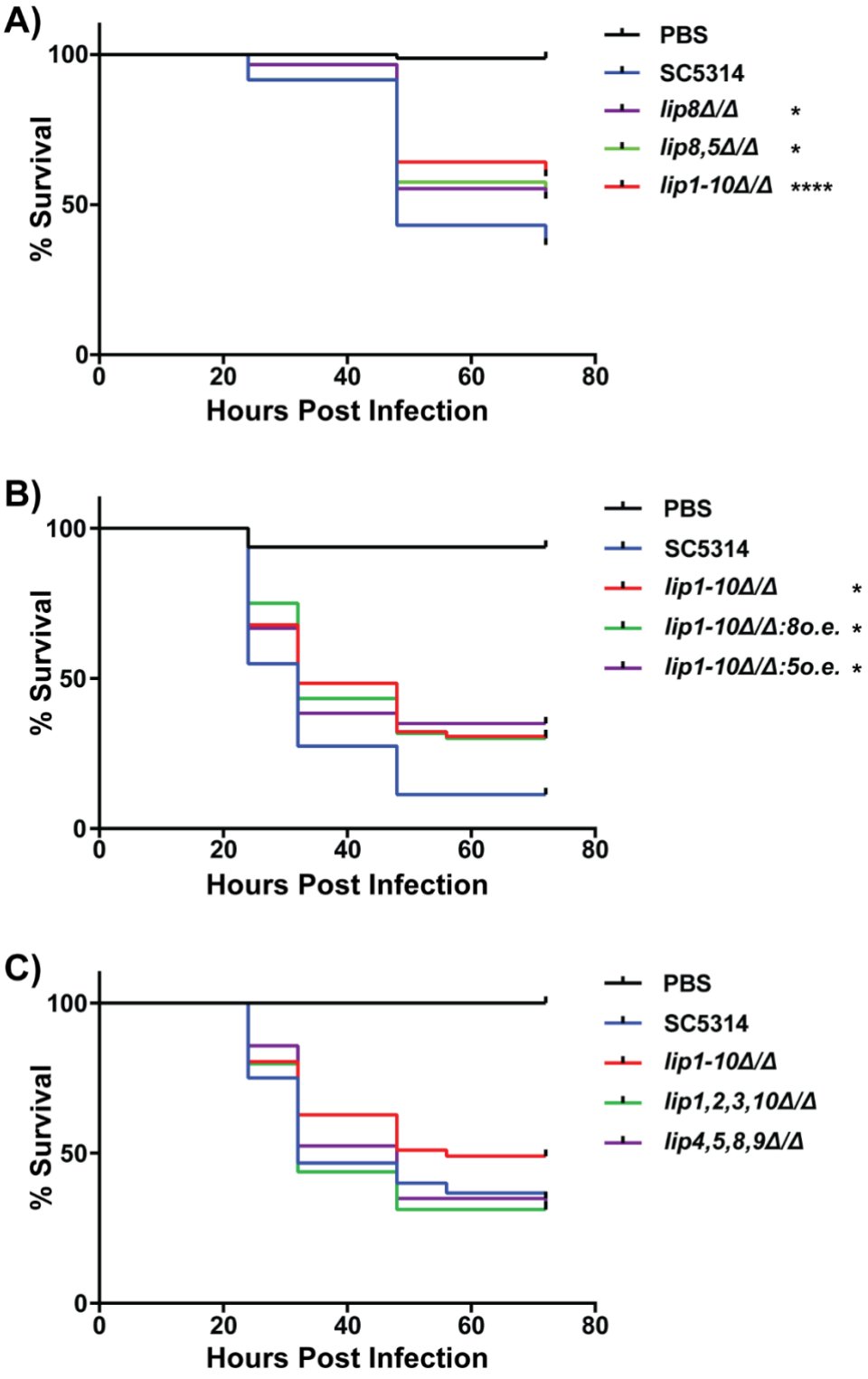

Figure 4.2 Virulence of lipase mutants in the larval zebrafish hindbrain infection model. A) Kaplan-Meier survival curves show an intermediate virulence defect of *lip8*Δ/Δ and *lip8,5*Δ/Δ (PBS n=82, SC5314 n =153, *lip8*Δ/Δ n=150, *lip8,5*Δ/Δ n=167, *lip1-10*Δ/Δ n=148). **B)** Kaplan-

Figure 4.2 continued
Meier survival curves show that overexpression of *LIP8* or *LIP5* in the *lip1-10*Δ/Δ background does not rescue the virulence defect (PBS n=32, SC5314 n=62, *lip1-10*Δ/Δ n=62, *lip1-10*Δ/Δ*:8o.e.* n=60, *lip1-10*Δ/Δ*:5o.e.* n=60). **C)** Kaplan-Meier survival curves do not show a difference in survival of fish infected with *lip1,2,310*Δ/Δ or *lip4,5,8,9* compared to SC5314 (PBS n=35, SC5314 n=60, *lip1-10*Δ/Δ n=51, *lip1,2,3,10*Δ/Δ n=64, *lip4,5,8,9* n=63). Significance: * $p<0.05$, **** $p<0.0001$.

4.4 Discussion

Lipases have been implicated in the virulence of multiple bacteria as well as *C. parapsilosis* and *C. albicans*. Bacterially-produced lipases have been observed to have impacts on host immune cell functions such as chemotaxis, phagocytosis, and killing. *C. albicans* has a family of 10 lipase genes that are differentially expressed during infection and colonization. Very little is known about how these lipases may contribute to the virulence of *C. albicans* either individually or as a group. While *LIP8* and more recently *LIP2* were found to be important for virulence, *LIP2* is the only *C. albicans* lipase that we have insight into the mechanism in which they may contribute to virulence. Evidence suggests that *LIP2* can impact the host immune response by modulating the production of IL-23 from dendritic cells. This leaves us to question whether other *C. albicans* lipases can impact the host immune response as well, and if these lipases can affect other immune cells.

We found that the production of lipases contributes to *C. albicans* virulence, as a lipase-deficient strain showed reduced virulence in our larval zebrafish hindbrain infection model (Figure 4.1B). Even though we did not see an increase in macrophage or neutrophil recruitment to this infection, we observed that *lip1-10*Δ/Δ cells are contained better than WT *C. albicans* (Figure 4.1E). This suggests that *C. albicans* lipases may play a role in limiting phagocytosis by host immune cells.

We saw that both *lip8,5*Δ/Δ and *lip8*Δ/Δ strains showed reduced virulence in hindbrain infection (Figure 4.2A). However, survival of fish infected with *lip8,5*Δ/Δ and *lip8*Δ/Δ was nearly identical suggesting that *LIP8* is the more important lipase for virulence. It remains to be tested if a complemented *lip8*Δ/Δ strain restores the virulence defect. These results support previous data that *LIP8* is important for the virulence of *C. albicans* in a mouse systemic infection model (74). While *LIP8* appears to be an important lipase contributing to *C. albicans* virulence, the overexpression of *LIP8* was not enough to overcome the loss of the other lipases in the *lip1-10*Δ/Δ deletion strain. This may suggest that multiple lipases, including *LIP8*, work together to contribute to *C. albicans* virulence and perhaps modulation of the host immune response.

CHAPTER 5

FUTURE DIRECTIONS

5.1 *C. albicans* phagocyte evasion

We screened 131 mutants in single infections in the zebrafish hindbrain infection model. Of these we identified seven mutants with reproducible hypovirulence, with three of these mutants showing an altered immune response at 4-6 hpi. Fish infected with the *brg1*Δ/Δ mutant showed a reduction in the number of macrophages recruited to the hindbrain infection site compared to SN250 (WT) infected fish. Similarly, *pep8*Δ/Δ infected fish showed a reduction in the number of neutrophils recruited. While these mutants recruited fewer phagocytes, they were still contained just as well as WT. However, both of these mutants showed about a 20% reduction in elongated cells in the hindbrain compared to WT. On the other hand, *nmd5*Δ/Δ was contained better than WT *C. albicans* with the same number of phagocytes recruited. While we saw recruitment of phagocytes at 4-6 hpi there was very little to no induction of an inflammatory cytokine/chemokine response at this time. By 24 hpi however, these mutants showed reduced inflammatory cytokine/chemokine response.

Our screen identified several hypovirulent mutants in the larval zebrafish hindbrain infection model, 3 of which (*brg1*Δ/Δ, *pep8*Δ/Δ, and *nmd5*Δ/Δ) had an altered immune response at 4-6 hpi. We expected an enhanced early immune response to be cause of hypovirulence for some of our mutant strains, with these strains recruiting more macrophages or neutrophils, or having increased phagocytosis. Surprisingly, however, *brg1*Δ/Δ showed reduced macrophage recruitment and *pep8*Δ/Δ showed reduced neutrophil recruitment. We hypothesize that the reduced recruitment may be due to increased containment prior to 4 hours post infection. In order to test this hypothesis, imaging of these infections at earlier

time points would be necessary. In addition, it would be useful to perform time-lapse imaging of these infections earlier on to determine if there are any other altered macrophage and neutrophil dynamics prior to 4 hpi. However, to look at neutrophil dynamics prior to 4 hpi, we would need to use a different reporter for marking neutrophils (ex. *Tg(mpx:GFP)*), as the *lysC* marker that we used here is not turned on much earlier than the 4 hour time point assessed. Similarly, we do not know if these differences in early immune response to *brg1*Δ/Δ, *pep8*Δ/Δ, and *nmd5*Δ/Δ are maintained over the course of infection. To determine if these differences are short lived or maintained throughout infection, imaging of later timepoints such as 12 hpi, 24 hpi, and 48 hpi would be useful. However, at these later timepoints it may be difficult to differentiate between retention of phagocytes at the infection site, versus influx of new phagocytes. To address this we could utilize the *Tg(mpeg1:GAL4/UAS:Kaede)* zebrafish which have photoswitchable macrophages or *Tg(mpx:Dendra2)* which have photoswitchable neutrophils.

β-glucan is a known PAMP of *C. albicans*. Increased exposure of cell wall PAMPs could lead to increased immune recruitment and/or containment. Therefore, it would be interesting to see if *brg1*Δ/Δ, *pep8*Δ/Δ, or *nmd5*Δ/Δ have increased levels of exposed β-glucan or chitin that may be responsible for the altered dynamics that we observed.

Many of the hypovirulent mutants in our screen did not show a difference in the immune response at 4-6 hpi. The hypovirulence with these strains could be associated with a number of things, including reduced ability to form filamentous growth in the hindbrain, reduced ability to cause damage, or increased susceptibility to killing by phagocytes. We can quantify the number of yeast versus elongated cells at 4-6 hpi to determine if there is reduced filamentation early on during infection, as we did for *brg1*Δ/Δ and *pep8*Δ/Δ. We could also

determine if these mutants have increased susceptibility to host macrophages or neutrophils by culturing with murine macrophages, human neutrophils in poly-l-lysine/ZETAG microarrays (118), or imaging Calcofluor white stained iRFP expressing *C. albicans* at later timepoints during hindbrain infection. The latter would allow for differentiating those cells from the inoculum that are dead or alive at a given time post-infection, as dead cells would be Calcofluor white stained but lack cytosolic iRFP.

We observed reduced proinflammatory cytokine production in response to *brg1*Δ/Δ, *pep8*Δ/Δ, and *nmd5*Δ/Δ infections at 24 hpi, as assessed by qPCR of *cxcl8b*, *tnfa*, and *il1b*. This may be due to reduced fungal burden and damage in these hypovirulent strains. Therefore, it would be interesting to determine the fungal burden for the same pools of fish we are using for qPCR to see if there is a correlation between fungal burden and cytokine expression. Recent work with wildtype SC5314 infections suggests that there is not a pronounced association between burden and cytokine expression, however, suggesting that the low response could be due to a decreased ability to elicit cytokine expression (Dhillon et al., unpublished). While we only presented qPCR results for a few cytokines and chemokines at 24 hpi, initial experiments with more cytokines and chemokines did not show consistent results for the others tested. In addition, looking at cytokine and chemokine production at 4 hours post infection did not show very much, if any, induction at this time point, and it was difficult to get enough fish alive to assess at later timepoints. Future experiments could look at pro-inflammatory cytokine and chemokine production between 4 and 24 hours, to see when we see induction of this response, and if the timing and levels are different between hypovirulent mutants and WT infections.

Interestingly, we observed phagocyte recruitment at 4-6 hpi despite the fact that there was little proinflammatory cytokine production. This calls into question what signals are recruiting immune cells at this stage of infection. Studies suggest that ROS is important for recruitment of phagocytes at this early stage of infection (106,107). Therefore, it would be interesting to see if there are differences in the amount of ROS produced in response to infection with these hypovirulent mutants. To analyze this, we could assess the amount of ROS produced in infected fish using the caged H_2-DCF-DA molecule that becomes fluorescent when oxidized (272). Alternatively, for a more localized look, mutant strains could be transformed with the *CTA1*-GFP oxidative stress to image oxidative stress imposed on the *Candida* during hindbrain infection reporter (107,273).

Differences in immune recruitment between WT and yeast-locked *C. albicans* have been observed in ROS deficient fish, but not WT fish (106). Therefore, assessing immune recruitment and containment of the hypovirulent *C. albicans* in ROS deficient zebrafish (DPI treatment, morpholino knockdown, or $p22^{phox-/-\ (sa11798)}$) may elucidate differences in the immune response that we could not observe in WT fish (106,274).

We observed increased containment of *nmd5*Δ/Δ at 4-6 hpi. *NMD5* codes for a karyopherin and is required for nuclear import of Crz1p and Hog1p in *S. cerevisiae*. It is unknown what Nmd5 regulates in *C. albicans*. Therefore, it would be interesting to do RNA-seq experiments with WT and *nmd5*Δ/Δ during infection or incubation with murine macrophages, to see what Nmd5 may be regulating during infection. Genes that are downregulated in *nmd5*Δ/Δ compared to WT could then be tested during hindbrain infection to determine if they also show increased containment during infection.

5.2 *RBT1*

We found the *rbt1*Δ/Δ$^{968\text{-}2166}$ strain to be avirulent in the hindbrain infection model with reduced virulence in yolk infection as well. Sequencing of this mutant revealed that this was only a partial deletion of the *RBT1* gene, leaving intact the first half which codes for two secreted peptides. Creation of our own full deletion mutants, however, showed little to no virulence defect in two different strain backgrounds. Whole genome sequencing of WT, mutant, and complemented strains revealed that the *rbt1*Δ/Δ$^{968\text{-}2166}$ strain had significant loss of heterozygosity on the right arm of chromosome 4, where the *RBT1* gene is located. Surprisingly, infected fish that also received a dose of *RBT1*-encoded peptides showed a trend towards increased survival, with increased neutrophils and a trend for increased macrophages at 6 hpi. By 24 hpi, there was a trend for a reduced *Candida* burden and a reduced # for fish with invasive hyphal growth in those receiving the peptides.

Initial experiments with the partial deletion mutant *rbt1*Δ/Δ$^{968\text{-}2166}$ were promising, as this strain was aviruent in zebrafish hindbrain infection. However, sequencing revealed that this was only a partial deletion mutant, and the portion still present in this mutant codes for two secreted peptides. It is unknown whether or not the peptides are still expressed in this mutant, but this could be analyzed by qPCR or LC-MS. We wanted to determine if the avirulence phenotype would be recapitulated with a full deletion mutant so we used CRISPR to create full deletion mutants. Deletion of *RBT1* from SC5314 and SN250 was difficult and yielded very few colonies. Surprisingly, these full-deletion mutants showed very little if any virulence defect. It would be interesting to create a partial *RBT1* mutant with the same deletion as *rbt1*Δ/Δ$^{968\text{-}2166}$ in the SC5314 background to see if it is avirulent like the Noble mutant, or if it behaves more like our full deletion mutants. In addition, complementation of

*rbt1*Δ/Δ$^{968\text{-}2166}$ did not restore virulence and we were not able to complement the CRISPR mutants. The difficulties in deleting and complementing these strains makes us question the essentiality of *RBT1* in *C. albicans*. Therefore, using a Tet-regulated *RBT1* strain may better help us to elucidate the role of *RBT1* during infection. Thus, it is very likely that the avirulence phenotype associated with *rbt1*Δ/Δ$^{968\text{-}2166}$ mutant is due to off target changes, such as the loss of heterozygosity, and not the partial loss of *RBT1*.

Differences have been seen in the transcriptional networks and roles of genes between different WT strains. In addition, it was recently seen that the common WT lab strain SC5314 does not have functional RNAi pathway (275). Therefore, it would be useful to create *RBT1* mutants in different clinical isolates to assess the role of *RBT1*.

Initial experiments with *RBT1*-encoded peptides suggest that they may be protective to the host. Further experiments are needed to determine this. In these experiments both peptides were only injected shortly after infection. Further treatments with the peptides may further reduce virulence of *C. albicans*. In addition, treatments with one peptide or the other may be useful to determine if one peptide or the other show a protective effect, or the only the combination of both. In addition to the use of peptides in experiments, Tet-regulated strains expressing just the peptides or the cell wall portion of Rbt1 would be useful to determine which portions of Rbt1 may be important, or if they have different roles during infection.

5.3 Lipases

We found that lipase deficient *C. albicans lip1-10*Δ/Δ mutant had reduced virulence in the zebrafish hindbrain infection model. These mutant infections had unchanged macrophage and neutrophil recruitment, but increased fungal containment within phagocytes as compared

to WT (SC5314). We also found that *lip8*Δ/Δ and *lip8,5*Δ/Δ had reduced virulence, but overexpression of *LIP8* or *LIP5* did not rescue the virulence defect of *lip1-10*Δ/Δ. In addition, quadruple lipase mutants *lip1,2,3,10*Δ/Δ and *lip4,5,8,9*Δ/Δ did not show reduced virulence.

We observed that lipases contribute to virulence during hindbrain infection, as the lipase deficient mutant showed reduced virulence. While we saw that *LIP8* in particular appears to contribute to virulence, overexpression of this lipase was not sufficient to restore WT virulence of *lip1-10*Δ/Δ. However, we need to test the virulence of a *lip8*Δ/Δ complemented strain to ensure that this restores virulence. This suggests that more than one lipase may be required for virulence. Surprisingly, quadruple lipase mutant also did not show an attenuation of virulence. This could be because certain combinations of lipases can contribute to virulence and/or there is upregulation of other lipases to compensate for the loss. Therefore, it would be interesting to do qPCR of the lipase genes during infection in infections with the quadruple mutants to see which, if any, of the lipases may be upregulated to compensate for this loss. This may provide important information about which lipases are important for full virulence during infection. In addition, we could test overexpression of certain combinations of lipases in the lipase deficient mutant to see if particular combinations are able to restore WT virulence. It would also be interesting to use fluorescent reporter strains for the individual lipases such as *LIP8* during infection in our zebrafish model to see when these genes are expressed during infection, and if expression is associated with interactions with certain host cells such as macrophages or neutrophils.

5.4 Summary

Our screen identified 7 genes that play a role in virulence in the hindbrain infection model. Of these, *nmd5*Δ/Δ showed increased containment by host cells, while *brg1*Δ/Δ had decreased macrophage recruitment and *pep8*Δ/Δ had decreased neutrophil recruitment at 4-6 hpi. However, more work needs to be done to understand how these genes alter the host immune response. In addition, this work showed a role for lipases and a potential role for *RBT1* in *C. albicans* virulence. Further work needs to be done to determine which of the lipases are important for *C. albicans* virulence. Additionally, due to inconsistent results among *RBT1* mutants much more work needs to be done to determine if *RBT1* is a virulence factor.

REFERENCES

1. Magill SS, O'Leary E, Janelle SJ, Thompson DL, Dumyati G, Nadle J, et al. Changes in Prevalence of Health Care-Associated Infections in U.S. Hospitals. N Engl J Med [Internet]. 2018 Nov [cited 2024 May 10];379(18):1732–44. Available from: https://pubmed.ncbi.nlm.nih.gov/30380384/

2. Statistics | Invasive Candidiasis | Candidiasis | Types of Diseases | Fungal Diseases | CDC [Internet]. [cited 2024 May 10]. Available from: https://www.cdc.gov/fungal/diseases/candidiasis/invasive/statistics.html#two

3. Tsay S, Williams S, Mu Y, Epson E, Johnston H, Farley MM, et al. 363. National Burden of Candidemia, United States, 2017. Open Forum Infect Dis [Internet]. 2018 Nov 26 [cited 2024 May 10];5(Suppl 1):S142. Available from: /pmc/articles/PMC6255127/

4. Morgan J, Meltzer MI, Plikaytis BD, Sofair AN, Huie-White S, Wilcox S, et al. Excess mortality, hospital stay, and cost due to candidemia: a case-control study using data from population-based candidemia surveillance. Infect Control Hosp Epidemiol [Internet]. 2005 Jun [cited 2024 May 10];26(6):540–7. Available from: https://pubmed.ncbi.nlm.nih.gov/16018429/

5. Candida infections of the mouth, throat, and esophagus | Fungal Diseases | CDC [Internet]. [cited 2024 May 10]. Available from: https://www.cdc.gov/fungal/diseases/candidiasis/thrush/index.html#one

6. Blostein F, Levin-Sparenberg E, Wagner J, Foxman B. Recurrent vulvovaginal candidiasis. Ann Epidemiol. 2017 Sep 1;27(9):575-582.e3.

7. Vaginal Candidiasis | Fungal Diseases | CDC [Internet]. [cited 2024 May 10]. Available from: https://www.cdc.gov/fungal/diseases/candidiasis/genital/index.html

8. Ardizzoni A, Wheeler RT, Pericolini E. It Takes Two to Tango: How a Dysregulation of the Innate Immunity, Coupled With Candida Virulence, Triggers VVC Onset. Vol. 12, Frontiers in Microbiology. 2021.

9. Burgess TB, Condliffe AM, Elks PM. A Fun-Guide to Innate Immune Responses to Fungal Infections. Journal of Fungi 2022, Vol 8, Page 805 [Internet]. 2022 Jul 29 [cited 2024 May 10];8(8):805. Available from: https://www.mdpi.com/2309-608X/8/8/805/htm

10. Seman BG, Moore JL, Scherer AK, Blair BA, Manandhar S, Jones JM, et al. Yeast and filaments have specialized, independent activities in a zebrafish model of Candida albicans infection. Infect Immun. 2018;86(10).

11. Lo HJ, Köhler JR, Didomenico B, Loebenberg D, Cacciapuoti A, Fink GR. Nonfilamentous C. albicans mutants are avirulent. Cell [Internet]. 1997 Sep 5 [cited 2024 May 21];90(5):939–49. Available from: http://www.cell.com/article/S009286740080358X/fulltext

12. Braun BR, Steven Head W, Wang MX, Johnson AD, Head WS, Wang MX, et al. Identification and Characterization of TUP1-Regulated Genes in Candida albicans. Genetics [Internet]. 2000 [cited 2019 Aug 10];156(1):31–44. Available from: https://www.ncbi.nlm.nih.gov/pmc/articles/PMC1461230/pdf/10978273.pdf

13. Sudbery PE. Growth of Candida albicans hyphae. Nature Reviews Microbiology 2011 9:10 [Internet]. 2011 Aug 16 [cited 2024 May 13];9(10):737–48. Available from: https://www.nature.com/articles/nrmicro2636

14. Chen H, Zhou X, Ren B, Cheng L. The regulation of hyphae growth in Candida albicans. Virulence [Internet]. 2020 [cited 2024 Apr 24];11. Available from: https://doi.org/10.1080/21505594.2020.1748930

15. Taschdjian CL, Burchall JJ, Kozinn PJ. Rapid Identification of Candida Albicans by Filamentation on Serum and Serum Substitutes. AMA J Dis Child [Internet]. 1960 Feb 1 [cited 2024 May 21];99(2):212–5. Available from: https://jamanetwork.com/journals/jamapediatrics/fullarticle/499410

16. Mühlschlegel FA, Fonzi WA. PHR2 of Candida Albicans Encodes a Functional Homolog of the pH-regulated Gene PHR1 with an Inverted Pattern of pH-Dependent Expression. Mol Cell Biol [Internet]. 1997 Oct 1 [cited 2024 May 21];17(10):5960–7. Available from: https://www.tandfonline.com/doi/abs/10.1128/MCB.17.10.5960

17. Castilla R, Passeron S, Cantore ML. N-Acetyl-d-Glucosamine Induces Germination in Candida albicans through a Mechanism Sensitive to Inhibitors of cAMP-Dependent Protein Kinase. Cell Signal. 1998 Nov 1;10(10):713–9.

18. Cassone A, Sullivan PA, Shepherd MG. N-acetyl-D-glucosamine-induced morphogenesis in Candida albicans. Microbiologica [Internet]. 1985 Jan 1 [cited 2024 May 21];8(1):85–99. Available from: https://europepmc.org/article/med/3883103

19. Witchley JN, Penumetcha P, Abon N V., Woolford CA, Mitchell AP, Noble SM. Candida albicans Morphogenesis Programs Control the Balance between Gut Commensalism and Invasive Infection. Cell Host Microbe [Internet]. 2019 Mar 13 [cited 2024 May 19];25(3):432-443.e6. Available from: http://www.cell.com/article/S1931312819301040/fulltext

20. Lane S, Birse C, Zhou S, Matson R, Liu H. DNA Array Studies Demonstrate Convergent Regulation of Virulence Factors by Cph1, Cph2, and Efg1 in Candida albicans. Journal of Biological Chemistry [Internet]. 2001 Dec 28 [cited 2024 May 21];276(52):48988–96. Available from: http://www.jbc.org/article/S0021925820881368/fulltext

21. Leberer E, Harcus D, Broadbent ID, Clark KL, Dignard D, Ziegelbauer K, et al. Signal transduction through homologs of the Ste20p and Ste7p protein kinases can trigger hyphal formation in the pathogenic fungus Candida albicans. Proceedings of the National Academy of Sciences [Internet]. 1996 Nov 12 [cited 2024 May 21];93(23):13217–22. Available from: https://www.pnas.org/doi/abs/10.1073/pnas.93.23.13217

22. Stoldt VR, Sonneborn A, Leuker CE, Ernst JF. Efg1p, an essential regulator of morphogenesis of the human pathogen Candida albicans, is a member of a conserved class of bHLH proteins regulating morphogenetic processes in fungi. EMBO J [Internet]. 1997 Apr 15 [cited 2024 May 21];16(8):1982–91. Available from: https://pubmed.ncbi.nlm.nih.gov/9155024/

23. Leberer E, Harcus D, Dignard D, Johnson L, Ushinsky S, Thomas DY, et al. Ras links cellular morphogenesis to virulence by regulation of the MAP kinase and cAMP signalling pathways in the pathogenic fungus Candida albicans. Mol Microbiol [Internet]. 2001 Nov 1 [cited 2024 May 21];42(3):673–87. Available from: https://onlinelibrary.wiley.com/doi/full/10.1046/j.1365-2958.2001.02672.x

24. Feng Q, Summers E, Guo B, Fink G. Ras signaling is required for serum-induced hyphal differentiation in Candida albicans. J Bacteriol [Internet]. 1999 Oct 15 [cited 2024 May 21];181(20):6339–46. Available from: https://journals.asm.org/doi/10.1128/jb.181.20.6339-6346.1999

25. Davis D, Wilson RB, Mitchell AP. RIM101-Dependent and -Independent Pathways Govern pH Responses in Candida albicans. Mol Cell Biol [Internet]. 2000 Feb 1 [cited 2024 May 21];20(3):971–8. Available from: https://www.tandfonline.com/doi/abs/10.1128/MCB.20.3.971-978.2000

26. Braun BR, Johnson AD. Control of filament formation in Candida albicans by the transcriptional repressor TUP1. Science [Internet]. 1997 Jul 4 [cited 2024 May 21];277(5322):105–9. Available from: https://pubmed.ncbi.nlm.nih.gov/9204892/

27. Braun BR, Kadosh D, Johnson AD. NRG1, a repressor of filamentous growth in C.albicans, is down-regulated during filament induction. EMBO Journal. 2001 Sep 3;20(17):4753–61.

28. Murad AMA, Leng P, Straffon M, Wishart J, Macaskill S, MacCallum D, et al. NRG1 represses yeast–hypha morphogenesis and hypha-specific gene expression in Candida albicans. EMBO J [Internet]. 2001 Sep 3 [cited 2024 May 21];20(17):4742–52. Available from: https://www.embopress.org/doi/10.1093/emboj/20.17.4742

29. Kadosh D, Johnson AD. Induction of the Candida albicans filamentous growth program by relief of transcriptional repression: A genome-wide analysis. Mol Biol Cell [Internet]. 2005 Apr 6 [cited 2024 May 21];16(6):2903–12. Available from: https://www.molbiolcell.org/doi/10.1091/mbc.e05-01-0073

30. Kadosh D, Johnson AD. Rfg1, a Protein Related to the Saccharomyces cerevisiae Hypoxic Regulator Rox1, Controls Filamentous Growth and Virulence in Candida albicans. Mol Cell Biol [Internet]. 2001 Apr 1 [cited 2024 May 21];21(7):2496–505. Available from: https://www.tandfonline.com/doi/abs/10.1128/MCB.21.7.2496-2505.2001

31. Banerjee M, Thompson DS, Lazzell A, Carlisle PL, Pierce C, Monteagudo C, et al. UME6, a novel filament-specific regulator of Candida albicans hyphal extension and virulence. Mol Biol Cell [Internet]. 2008 Apr 23 [cited 2024 May 21];19(4):1354–65. Available from: https://www.molbiolcell.org/doi/10.1091/mbc.e07-11-1110

32. Martin R, Moran GP, Jacobsen ID, Heyken A, Domey J, Sullivan DJ, et al. The Candida albicans-Specific Gene EED1 Encodes a Key Regulator of Hyphal Extension. PLoS One [Internet]. 2011 [cited 2024 May 21];6(4):e18394. Available from: https://journals.plos.org/plosone/article?id=10.1371/journal.pone.0018394

33. Gow NAR, Hube B. Importance of the Candida albicans cell wall during commensalism and infection. Curr Opin Microbiol. 2012 Aug 1;15(4):406–12.

34. Gantner BN, Simmons RM, Underhill DM. Dectin-1 mediates macrophage recognition of Candida albicans yeast but not filaments. EMBO Journal [Internet]. 2005 Mar 23 [cited 2024 May 21];24(6):1277–86. Available from: https://www.embopress.org/doi/10.1038/sj.emboj.7600594

35. Braun BR, Johnson AD. TUP1, CPH1 and EFG1 Make Independent Contributions to Filamentation in Candida albicans. Genetics [Internet]. 2000 [cited 2019 Aug 10];155:57–67. Available from: https://www.ncbi.nlm.nih.gov/pmc/articles/PMC1461068/pdf/10790384.pdf

36. Gow NAR, van de Veerdonk FL, Brown AJP, Netea MG. Candida albicans morphogenesis and host defence: discriminating invasion from colonization. Nat Rev Microbiol [Internet]. 2012 Feb 12 [cited 2019 Sep 16];10(2):112–22. Available from: http://www.nature.com/articles/nrmicro2711

37. Grubb SEW, Murdoch C, Sudbery PE, Saville SP, Lopez-Ribot JL, Thornhill MH. Adhesion of Candida albicans to endothelial cells under physiological conditions of flow. Infect Immun [Internet]. 2009 Sep [cited 2024 May 15];77(9):3872–8. Available from: https://journals.asm.org/doi/10.1128/iai.00518-09

38. Dalle F, Wächtler B, L'Ollivier C, Holland G, Bannert N, Wilson D, et al. Cellular interactions of Candida albicans with human oral epithelial cells and enterocytes. Cell Microbiol. 2010;12(2):248–71.

39. Zhao X, Pujol C, Soll DR, Hoyer LL. Allelic variation in the contiguous loci encoding Candida albicans ALS5, ALS1 and ALS9. [cited 2024 May 15]; Available from: http://www-sequence.stanford.edu/group/candida

40. Höfs S, Mogavero S, Hube B. Interaction of Candida albicans with host cells: virulence factors, host defense, escape strategies, and the microbiota. Journal of Microbiology 2016 54:3 [Internet]. 2016 Feb 27 [cited 2024 May 12];54(3):149–69. Available from: https://link.springer.com/article/10.1007/s12275-016-5514-0

41. Sheppard DC, Yeaman MR, Welch WH, Phan QT, Fu Y, Ibrahim AS, et al. Functional and structural diversity in the Als protein family of Candida albicans. Journal of Biological Chemistry [Internet]. 2004 Jul 16 [cited 2024 May 15];279(29):30480–9. Available from: http://www.jbc.org/article/S0021925819710679/fulltext

42. Phan QT, Myers CL, Fu Y, Sheppard DC, Yeaman MR, Welch WH, et al. Als3 Is a Candida albicans Invasin That Binds to Cadherins and Induces Endocytosis by Host Cells. PLoS Biol [Internet]. 2007 Mar [cited 2024 May 15];5(3):e64. Available from: https://journals.plos.org/plosbiology/article?id=10.1371/journal.pbio.0050064

43. Staab JF, Bradway SD, Fidel PL, Sundstrom P. Adhesive and Mammalian Transglutaminase Substrate Properties of Candida albicans Hwp1. Science (1979) [Internet]. 1999 Mar 5 [cited 2024 May 15];283(5407):1535–8. Available from: https://www.science.org/doi/10.1126/science.283.5407.1535

44. Poltermann S, Kunert A, Von Der Heide M, Eck R, Hartmann A, Zipfel PF. Gpm1p is a factor H-, FHL-1-, and plasminogen-binding surface protein of Candida albicans. Journal of Biological Chemistry [Internet]. 2007 Dec 28 [cited 2024 May 13];282(52):37537–44. Available from: http://www.jbc.org/article/S0021925820777082/fulltext

45. Luo S, Poltermann S, Kunert A, Rupp S, Zipfel PF. Immune evasion of the human pathogenic yeast Candida albicans: Pra1 is a Factor H, FHL-1 and plasminogen binding surface protein. Mol Immunol. 2009 Dec 1;47(2–3):541–50.

46. Casanova M, Lopez-Ribot JL, Monteagudo C, Llombart-Bosch A, Sentandreu R, Martinez JP. Identification of a 58-kilodalton cell surface fibrinogen-binding mannoprotein from Candida albicans. Infect Immun [Internet]. 1992 [cited 2024 May 13];60(10):4221–9. Available from: https://journals.asm.org/journal/iai

47. Gulati M, Nobile CJ. Candida albicans biofilms: development, regulation, and molecular mechanisms. 2016 [cited 2024 May 13]; Available from: http://dx.doi.org/10.1016/j.micinf.2016.01.002

48. Fox E, Hartooni N, Nobile CJ. Biofilms and Antifungal Resistance. 2014 [cited 2024 May 21]; Available from: https://www.researchgate.net/publication/269106002

49. Andes DR, Group for the MS, Safdar N, Group for the MS, Baddley JW, Group for the MS, et al. Impact of Treatment Strategy on Outcomes in Patients with Candidemia and Other Forms of Invasive Candidiasis: A Patient-Level Quantitative Review of Randomized Trials. Clinical Infectious Diseases [Internet]. 2012 Apr 15 [cited 2024 May 21];54(8):1110–22. Available from: https://dx.doi.org/10.1093/cid/cis021

50. LaFleur MD, Kumamoto CA, Lewis K. Candida albicans biofilms produce antifungal-tolerant persister cells. Antimicrob Agents Chemother [Internet]. 2006 Nov [cited 2024 May 21];50(11):3839–46. Available from: https://journals.asm.org/doi/10.1128/aac.00684-06

51. Mathé L, Van Dijck P. Recent insights into Candida albicans biofilm resistance mechanisms. Curr Genet [Internet]. 2013 Nov 25 [cited 2024 May 21];59(4):251–64. Available from: https://link.springer.com/article/10.1007/s00294-013-0400-3

52. Nett J, Lincoln L, Marchillo K, Massey R, Holoyda K, Hoff B, et al. Putative role of β-1,3 glucans in Candida albicans biofilm resistance. Antimicrob Agents Chemother [Internet]. 2007 Feb [cited 2024 May 21];51(2):510–20. Available from: https://journals.asm.org/doi/10.1128/aac.01056-06

53. Ramage G, Bachmann S, Patterson TF, Wickes BL, López-Ribot JL. Investigation of multidrug efflux pumps in relation to fluconazole resistance in Candida albicans biofilms. Journal of Antimicrobial Chemotherapy [Internet]. 2002 Jun 1 [cited 2024 May 21];49(6):973–80. Available from: https://dx.doi.org/10.1093/jac/dkf049

54. Mukherjee PK, Chandra J, Kuhn DM, Ghannoum MA. Mechanism of fluconazole resistance in Candida albicans biofilms: Phase-specific role of efflux pumps and membrane sterols. Infect Immun [Internet]. 2003 Aug 1 [cited 2024 May 21];71(8):4333–40. Available from: https://journals.asm.org/doi/10.1128/iai.71.8.4333-4340.2003

55. Douglas LJ. Candida biofilms and their role in infection. Trends Microbiol [Internet]. 2003 Jan 1 [cited 2024 May 21];11(1):30–6. Available from: http://www.cell.com/article/S0966842X02000021/fulltext

56. Chandra J, Kuhn DM, Mukherjee PK, Hoyer LL, McCormick T, Ghannoum MA. Biofilm formation by the fungal pathogen Candida albicans: Development, architecture, and drug resistance. J Bacteriol [Internet]. 2001 [cited 2024 May 21];183(18):5385–94. Available from: https://journals.asm.org/doi/10.1128/jb.183.18.5385-5394.2001

57. Nett JE, Zarnowski R, Cabezas-Olcoz J, Brooks EG, Bernhardt J, Marchillo K, et al. Host contributions to construction of three device-associated Candida albicans biofilms. Infect Immun [Internet]. 2015 [cited 2024 May 21];83(12):4630–8. Available from: https://journals.asm.org/doi/10.1128/iai.00931-15

58. Zarnowski R, Westler WM, Lacmbouh GA, Marita JM, Bothe JR, Bernhardt J, et al. Novel entries in a fungal biofilm matrix encyclopedia. mBio [Internet]. 2014 [cited 2024 May 21];5(4):1–13. Available from: https://journals.asm.org/doi/10.1128/mbio.01333-14

59. Nobile CJ, Fox EP, Nett JE, Sorrells TR, Mitrovich QM, Hernday AD, et al. A recently evolved transcriptional network controls biofilm development in Candida albicans. Cell [Internet]. 2012 Jan 20 [cited 2024 May 19];148(1–2):126–38. Available from: http://www.cell.com/article/S0092867411013614/fulltext

60. Fox EP, Nobile CJ. A sticky situation. Transcription [Internet]. 2012 Nov 18 [cited 2024 May 21];3(6):315–22. Available from: https://www.tandfonline.com/doi/abs/10.4161/trns.22281

61. Bonhomme J, d'Enfert C. Candida albicans biofilms: building a heterogeneous, drug-tolerant environment. Curr Opin Microbiol. 2013 Aug 1;16(4):398–403.

62. Nobile CJ, Andes DR, Nett JE, Smith FJ, Yue F, Phan QT, et al. Critical Role of Bcr1-Dependent Adhesins in C. albicans Biofilm Formation In Vitro and In Vivo. PLoS Pathog [Internet]. 2006 [cited 2024 May 21];2(7):e63. Available from: https://journals.plos.org/plospathogens/article?id=10.1371/journal.ppat.0020063

63. Nobile CJ, Schneider HA, Nett JE, Sheppard DC, Filler SG, Andes DR, et al. Article Complementary Adhesin Function in C. albicans Biofilm Formation. Current Biology. 18:1017–24.

64. Nobile CJ, Nett JE, Andes DR, Mitchell AP. Function of Candida albicans adhesin hwp1 in biofilm formation. Eukaryot Cell [Internet]. 2006 Oct [cited 2024 May 21];5(10):1604–10. Available from: https://journals.asm.org/doi/10.1128/ec.00194-06

65. Nobile CJ, Mitchell AP. Regulation of Cell-Surface Genes and Biofilm Formation by the C. albicans Transcription Factor Bcr1p. Current Biology. 2005;15:1150–5.

66. Ramage G, Vandewalle K, Lo ¤ Pez-Ribot J¤ L, Wickes BL. The filamentation pathway controlled by the Efg1 regulator protein is required for normal biofilm formation and development in Candida albicans. FEMS Microbiol Lett [Internet]. 2002 Aug 1 [cited 2024 May 21];214(1):95–100. Available from: https://dx.doi.org/10.1111/j.1574-6968.2002.tb11330.x

67. Nett JE, Sanchez H, Cain MT, Ross KM, Andes DR. Interface of Candida albicans biofilm matrix-associated drug resistance and cell wall integrity regulation. Eukaryot Cell [Internet]. 2011 Dec [cited 2024 May 21];10(12):1660–9. Available from: https://journals.asm.org/doi/10.1128/ec.05126-11

68. Nobile CJ, Nett JE, Hernday AD, Homann OR, Deneault JS, Nantel A, et al. Biofilm Matrix Regulation by Candida albicans Zap1. PLoS Biol [Internet]. 2009 Jun [cited 2024 May 21];7(6):e1000133. Available from: https://journals.plos.org/plosbiology/article?id=10.1371/journal.pbio.1000133

69. Uppuluri P, Pierce CG, Thomas DP, Bubeck SS, Saville SP, Lopez-Ribot JL. The transcriptional regulator Nrg1p controls Candida albicans biofilm formation and dispersion. Eukaryot Cell [Internet]. 2010 Oct [cited 2024 May 21];9(10):1531–7. Available from: https://journals.asm.org/journal/ec

70. Uppuluri P, Chaturvedi AK, Srinivasan A, Banerjee M, Ramasubramaniam AK, Köhler JR, et al. Dispersion as an Important Step in the Candida albicans Biofilm Developmental Cycle. PLoS

Pathog [Internet]. 2010 Mar [cited 2024 May 21];6(3):e1000828. Available from: https://journals.plos.org/plospathogens/article?id=10.1371/journal.ppat.1000828

71. Hube B, Stehr F, Bossenz M, Mazur A, Kretschmar M, Schäfer W. Secreted lipases of Candida albicans: cloning, characterisation and expression analysis of a new gene family with at least ten members. Arch Microbiol [Internet]. 2000 [cited 2022 Mar 6];174(5):362–74. Available from: https://pubmed.ncbi.nlm.nih.gov/11131027/

72. Stehr F, Felk A, Gácser A, Kretschmar M, Mähnß B, Neuber K, et al. Expression analysis of the Candida albicans lipase gene family during experimental infections and in patient samples. FEMS Yeast Res [Internet]. 2004 Jan 1 [cited 2024 May 4];4(4–5):401–8. Available from: https://dx.doi.org/10.1016/S1567-1356(03)00205-8

73. Schofield DA, Westwater C, Warner T, Balish E. Differential Candida albicans lipase gene expression during alimentary tract colonization and infection. FEMS Microbiol Lett [Internet]. 2005 Mar 15 [cited 2022 Mar 6];244(2):359–65. Available from: https://pubmed.ncbi.nlm.nih.gov/15766791/

74. Gácser A, Stehr F, Kröger C, Kredics L, Schäfer W, Nosanchuk JD. Lipase 8 affects the pathogenesis of Candida albicans. Infect Immun [Internet]. 2007 Oct [cited 2024 May 4];75(10):4710–8. Available from: https://journals.asm.org/doi/10.1128/iai.00372-07

75. Basso P, Dang E V., Urisman A, Cowen LE, Madhani HD, Noble SM. Deep tissue infection by an invasive human fungal pathogen requires lipid-based suppression of the IL-17 response. Cell Host Microbe [Internet]. 2022 Nov 9 [cited 2024 May 4];30(11):1589-1601.e5. Available from: http://www.cell.com/article/S1931312822005170/fulltext

76. Hube B, Naglik J. Candida albicans proteinases: Resolving the mystery of a gene family. Microbiology (N Y) [Internet]. 2001 Aug 1 [cited 2024 May 18];147(8):1997–2005. Available from: https://www.microbiologyresearch.org/content/journal/micro/10.1099/00221287-147-8-1997

77. Naglik JR, Moyes D, Makwana J, Kanzaria P, Tsichlaki E, Weindl G, et al. Quantitative expression of the Candida albicans secreted aspartyl proteinase gene family in human oral and vaginal candidiasis. Microbiology (N Y) [Internet]. 2008 Nov 1 [cited 2024 May

18];154(11):3266–80. Available from: https://www.microbiologyresearch.org/content/journal/micro/10.1099/mic.0.2008/022293-0

78. Correia A, Lermann U, Teixeira L, Cerca F, Botelho S, Gil Da Costa RM, et al. Limited role of secreted aspartyl proteinases Sap1 to Sap6 in Candida albicans virulence and host immune response in murine hematogenously disseminated candidiasis. Infect Immun [Internet]. 2010 Nov [cited 2024 May 19];78(11):4839–49. Available from: https://journals.asm.org/doi/10.1128/iai.00248-10

79. Gropp K, Schild L, Schindler S, Hube B, Zipfel PF, Skerka C. The yeast Candida albicans evades human complement attack by secretion of aspartic proteases. Mol Immunol. 2009 Dec 1;47(2–3):465–75.

80. Pietrella D, Pandey N, Gabrielli E, Pericolini E, Perito S, Kasper L, et al. Secreted aspartic proteases of Candida albicans activate the NLRP3 inflammasome. Eur J Immunol [Internet]. 2013 Mar 1 [cited 2024 Apr 8];43(3):679–92. Available from: https://onlinelibrary.wiley.com/doi/full/10.1002/eji.201242691

81. Gabrielli E, Sabbatini S, Roselletti E, Kasper L, Perito S, Hube B, et al. In vivo induction of neutrophil chemotaxis by secretory aspartyl proteinases of Candida albicans. Virulence [Internet]. 2016 Oct 2 [cited 2024 Apr 8];7(7):819–25. Available from: https://www.tandfonline.com/doi/abs/10.1080/21505594.2016.1184385

82. Villar CC, Kashleva H, Nobile CJ, Mitchell AP, Dongari-Bagtzoglou A. Mucosal tissue invasion by Candida albicans is associated with E-cadherin degradation, mediated by transcription factor Rim101p and protease Sap5p. Infect Immun [Internet]. 2007 May [cited 2024 May 18];75(5):2126–35. Available from: https://journals.asm.org/journal/iai

83. Kumar R, Saraswat D, Tati S, Edgerton M. Novel aggregation properties of Candida albicans secreted aspartyl proteinase sap6 mediate virulence in oral Candidiasis. Infect Immun [Internet]. 2015 [cited 2024 Apr 8];83(7):2614–26. Available from: https://journals.asm.org/doi/10.1128/iai.00282-15

84. Meiller TF, Hube B, Schild L, Shirtliff ME, Scheper MA, Winkler R, et al. A Novel Immune Evasion Strategy of Candida albicans: Proteolytic Cleavage of a Salivary Antimicrobial Peptide.

PLoS One [Internet]. 2009 Apr 7 [cited 2024 May 17];4(4):e5039. Available from: https://journals.plos.org/plosone/article?id=10.1371/journal.pone.0005039

85. Albrecht A, Felk A, Pichova I, Naglik JR, Schaller M, de Groot P, et al. Glycosylphosphatidylinositol-anchored Proteases of Candida albicans Target Proteins Necessary for Both Cellular Processes and Host-Pathogen Interactions *. 2006;

86. Moyes DL, Wilson D, Richardson JP, Mogavero S, Tang SX, Wernecke J, et al. Candidalysin is a fungal peptide toxin critical for mucosal infection HHS Public Access. Nature [Internet]. 2016 [cited 2024 Feb 16];532(7597):64–8. Available from: http://www.nature.com/authors/editorial_policies/license.html#termsReprints

87. Russell CM, Schaefer KG, Dixson A, Gray ALH, Pyron RJ, Alves DS, et al. The Candida albicans virulence factor candidalysin polymerizes in solution to form membrane pores and damage epithelial cells. Elife. 2022 Sep 1;11.

88. Russell CM, Rybak JA, Miao J, Peters BM, Barrera FN. Candidalysin: Connecting the pore forming mechanism of this virulence factor to its immunostimulatory properties. 2022 [cited 2024 Feb 16]; Available from: https://doi.org/10.1016/j.jbc.2022.102829

89. Ho J, Yang X, Nikou SA, Kichik N, Donkin A, Ponde NO, et al. Candidalysin activates innate epithelial immune responses via epidermal growth factor receptor. [cited 2024 Feb 16]; Available from: https://doi.org/10.1038/s41467-019-09915-2

90. König A, Hube B, Kasper L. toxins The Dual Function of the Fungal Toxin Candidalysin during Candida albicans-Macrophage Interaction and Virulence. [cited 2024 May 8]; Available from: www.mdpi.com/journal/toxins

91. Kasper L, König A, Koenig PA, Gresnigt MS, Westman J, Drummond RA, et al. The fungal peptide toxin Candidalysin activates the NLRP3 inflammasome and causes cytolysis in mononuclear phagocytes. [cited 2024 May 8]; Available from: www.nature.com/naturecommunications

92. Roselletti E, Perito S, Gabrielli E, Mencacci A, Pericolini E, Sabbatini S, et al. NLRP3 inflammasome is a key player in human vulvovaginal disease caused by Candida albicans. Scientific Reports 2017 7:1 [Internet]. 2017 Dec 19 [cited 2024 May 8];7(1):1–10. Available from: https://www.nature.com/articles/s41598-017-17649-8

93. Richardson JP, Willems HME, Moyes DL, Shoaie S, Barker KS, Tan SL, et al. Candidalysin Drives Epithelial Signaling, Neutrophil Recruitment, and Immunopathology at the Vaginal Mucosa. 2018 [cited 2024 May 8]; Available from: https://doi.org/10.1128/IAI

94. Swidergall M, Khalaji M, Solis N V, Moyes DL, Drummond RA, Hube B, et al. The Journal of Infectious Diseases Candidalysin Is Required for Neutrophil Recruitment and Virulence During Systemic Candida albicans Infection. The Journal of Infectious Diseases ®. 2019;220:1477–88.

95. Unger L, Skoluda S, Backman E, Amulic B, Ponce-Garcia FM, Etiaba CN, et al. Candida albicans induces neutrophil extracellular traps and leucotoxic hypercitrullination via candidalysin . EMBO Rep [Internet]. 2023 Nov 6 [cited 2024 May 8];24(11). Available from: https://www.embopress.org/doi/10.15252/embr.202357571

96. Drummond RA, Saijo S, Iwakura Y, Brown GD. The role of Syk/CARD9 coupled C-type lectins in antifungal immunity. Eur J Immunol [Internet]. 2011 Jan 11 [cited 2024 May 21];41(2):276–81. Available from: https://www.ncbi.nlm.nih.gov/pmc/articles/pmid/21267996/?tool=EBI

97. Naglik JR, Moyes D. Epithelial Cell Innate Response to Candida albicans. https://doi.org/101177/0022034511399285 [Internet]. 2011 Mar 25 [cited 2024 May 21];23(1):50–5. Available from: https://journals.sagepub.com/doi/10.1177/0022034511399285

98. Bäckhed F, Hornef M. Toll-like receptor 4-mediated signaling by epithelial surfaces: necessity or threat? Microbes Infect. 2003 Sep 1;5(11):951–9.

99. Weindl G, Naglik JR, Kaesler S, Biedermann T, Hube B, Korting HC, et al. Human epithelial cells establish direct antifungal defense through TLR4-mediated signaling. J Clin Invest [Internet]. 2007 Dec 3 [cited 2024 May 21];117(12):3664–72. Available from: http://www.jci.org

100. Vautier S, MacCallum DM, Brown GD. C-type lectin receptors and cytokines in fungal immunity. Cytokine. 2012 Apr 1;58(1):89–99.

101. Taylor PR, Tsoni SV, Willment JA, Dennehy KM, Rosas M, Findon H, et al. Dectin-1 is required for β-glucan recognition and control of fungal infection. Nature Immunology 2006 8:1 [Internet]. 2006 Dec 10 [cited 2024 May 21];8(1):31–8. Available from: https://www.nature.com/articles/ni1408

102. McGreal EP, Rosas M, Brown GD, Zamze S, Wong SYC, Gordon S, et al. The carbohydrate-recognition domain of Dectin-2 is a C-type lectin with specificity for high mannose. Glycobiology [Internet]. 2006 May 1 [cited 2024 May 21];16(5):422–30. Available from: https://dx.doi.org/10.1093/glycob/cwj077

103. Saijo S, Ikeda S, Yamabe K, Kakuta S, Ishigame H, Akitsu A, et al. Dectin-2 Recognition of α-Mannans and Induction of Th17 Cell Differentiation Is Essential for Host Defense against Candida albicans. Immunity. 2010 May 28;32(5):681–91.

104. Moyes DL, Runglall M, Murciano C, Shen C, Nayar D, Thavaraj S, et al. A biphasic innate immune MAPK response discriminates between the yeast and hyphal forms of candida albicans in epithelial cells. Cell Host Microbe [Internet]. 2010 Sep 16 [cited 2024 May 21];8(3):225–35. Available from: http://www.cell.com/article/S1931312810002520/fulltext

105. Dühring S, Germerodt S, Skerka C, Zipfel PF, Dandekar T, Schuster S. Host-pathogen interactions between the human innate immune system and Candida albicans—understanding and modeling defense and evasion strategies. Front Microbiol [Internet]. 2015 Jun 30 [cited 2019 Sep 16];6:625. Available from: http://journal.frontiersin.org/Article/10.3389/fmicb.2015.00625/abstract

106. Brothers KM, Gratacap RL, Barker SE, Newman ZR, Norum A, Wheeler RT. NADPH Oxidase-Driven Phagocyte Recruitment Controls Candida albicans Filamentous Growth and Prevents Mortality. PLoS Pathog. 2013;9(10).

107. Brothers KM, Newman ZR, Wheeler RT. Live Imaging of Disseminated Candidiasis in Zebrafish Reveals Role of Phagocyte Oxidase in Limiting Filamentous Growth. Eukaryot Cell. 2011;10(7):932–44.

108. Steele C, Fidel PL. Cytokine and chemokine production by human oral and vaginal epithelial cells in response to Candida albicans. Infect Immun [Internet]. 2002 [cited 2024 May 21];70(2):577–83. Available from: https://journals.asm.org/doi/10.1128/iai.70.2.577-583.2002

109. Gilbert AS, Wheeler RT, May RC. Fungal Pathogens: Survival and Replication within Macrophages. Cold Spring Harb Perspect Med [Internet]. 2015 Jul 1 [cited 2024 May 21];5(7). Available from: /pmc/articles/PMC4484954/

110. Kinchen JM, Ravichandran KS. Phagosome maturation: going through the acid test. Nat Rev Mol Cell Biol [Internet]. 2008 Oct [cited 2024 May 21];9(10):781. Available from: /pmc/articles/PMC2908392/

111. Takemura R, Stenberg PE, Bainton DF, Werb Z. Rapid Redistribution of Clathrin onto Macrophage Plasma Membranes in Response to Fc Receptor-Ligand Interaction During Frustrated Phagocytosis. [cited 2024 May 21]; Available from: http://rupress.org/jcb/article-pdf/102/1/55/1458797/55.pdf

112. Bain JM, Alonso MF, Childers DS, Walls CA, Mackenzie K, Pradhan A, et al. Immune cells fold and damage fungal hyphae. Proc Natl Acad Sci U S A [Internet]. 2021 Apr 13 [cited 2024 May 18];118(15). Available from: https://www.pnas.org

113. Cheng SC, Joosten LAB, Kullberg BJ, Netea MG. Interplay between Candida albicans and the mammalian innate host defense. Infect Immun [Internet]. 2012 Apr [cited 2024 May 12];80(4):1304–13. Available from: https://journals.asm.org/journal/iai

114. Lacy P. Mechanisms of Degranulation in Neutrophils. Allergy, Asthma & Clinical Immunology [Internet]. 2006 Sep 15 [cited 2024 May 21];2(3):1–11. Available from: https://aacijournal.biomedcentral.com/articles/10.1186/1710-1492-2-3-98

115. Swamydas M, Gao JL, Break TJ, Johnson MD, Jaeger M, Rodriguez CA, et al. CXCR1-mediated Neutrophil Degranulation and Fungal Killing Promotes Candida Clearance and Host Survival. Sci Transl Med [Internet]. 2016 Jan 1 [cited 2024 May 21];8(322):322ra10. Available from: /pmc/articles/PMC4938152/

116. Urban CF, Ermert D, Schmid M, Abu-Abed U, Goosmann C, Nacken W, et al. Neutrophil Extracellular Traps Contain Calprotectin, a Cytosolic Protein Complex Involved in Host Defense against Candida albicans. PLoS Pathog [Internet]. 2009 Oct [cited 2024 May 21];5(10):e1000639. Available from: https://journals.plos.org/plospathogens/article?id=10.1371/journal.ppat.1000639

117. Isles HM, Loynes CA, Alasmari S, Kon FC, Henry KM, Kadochnikova A, et al. Pioneer neutrophils release chromatin within in vivo swarms. Elife. 2021 Jul 1;10.

118. Hopke A, Scherer A, Kreuzburg S, Abers MS, Zerbe CS, Dinauer MC, et al. Neutrophil swarming delays the growth of clusters of pathogenic fungi. [cited 2024 May 18]; Available from: https://doi.org/10.1038/s41467-020-15834-4

119. Hopke A, Irimia D. Ex Vivo Human Neutrophil Swarming Against Live Microbial Targets. Methods in Molecular Biology [Internet]. 2020 [cited 2024 May 18];2087:107–16. Available from: https://link.springer.com/protocol/10.1007/978-1-0716-0154-9_8

120. Alex H, Scherer A, Kreuzburg S, Abers MS, Zerbe CS, Dinauer MC, et al. Neutrophil swarming delays the growth of clusters of pathogenic fungi. Nature Communications 2020 11:1 [Internet]. 2020 Apr 27 [cited 2024 May 20];11(1):1–15. Available from: https://www.nature.com/articles/s41467-020-15834-4

121. Böttger EC, Metzger S, Bitter-Suermann D, Stevenson G, Kleindienst S, Burger R. Impaired humoral immune response in complement C3-deficient guinea pigs: absence of secondary antibody response. Eur J Immunol [Internet]. 1986 Jan 1 [cited 2024 May 21];16(10):1231–5. Available from: https://onlinelibrary.wiley.com/doi/full/10.1002/eji.1830161008

122. Tsoni SV, Kerrigan AM, Marakalala MJ, Srinivasan N, Duffield M, Taylor PR, et al. Complement C3 plays an essential role in the control of opportunistic fungal infections. Infect Immun [Internet]. 2009 Sep [cited 2024 May 21];77(9):3679–85. Available from: https://journals.asm.org/doi/10.1128/iai.00233-09

123. Rambach G, Speth C. Complement in Candida albicans infections. Front Biosci (Elite Ed) [Internet]. 2009 Jun 1 [cited 2024 May 21];1(1):1–12. Available from: https://europepmc.org/article/med/19482619

124. Zipfel PF, Skerka C. Complement, Candida, and cytokines: The role of C5a in host response to fungi. Eur J Immunol [Internet]. 2012 Apr 1 [cited 2024 May 21];42(4):822–5. Available from: https://onlinelibrary.wiley.com/doi/full/10.1002/eji.201242466

125. Robert R, Mahaza C, Miegeville M, Ponton J, Agne` A, Marot-Leblond A, et al. Binding of Resting Platelets to Candida albicans Germ Tubes. Infect Immun [Internet]. 1996 [cited 2024 May 21];64(9):3752–7. Available from: https://journals.asm.org/journal/iai

126. Robert R, Nail S, Marot-Leblond A, Cottin J, Miegeville M, Quenouillere S, et al. Adherence of platelets to Candida species in vivo. Infect Immun [Internet]. 2000 Feb [cited 2024 May 21];68(2):570–6. Available from: https://journals.asm.org/doi/10.1128/iai.68.2.570-576.2000

127. Tang YQ, Yeaman MR, Selsted ME. Antimicrobial Peptides from Human Platelets †. Infect Immun [Internet]. 2002 [cited 2019 Apr 16];70(12):6524–33. Available from: http://iai.asm.org/

128. Schultz CM, Goel A, Dunn A, Knauss H, Huss C, Launder D, et al. Stepping Up to the Plate(let) against Candida albicans. 2020 [cited 2024 May 18]; Available from: https://doi.org/10.1128/IAI

129. Zuchtriegel G, Uhl B, Puhr-Westerheide D, Pörnbacher M, Lauber K, Krombach F, et al. Platelets Guide Leukocytes to Their Sites of Extravasation. PLoS Biol [Internet]. 2016 [cited 2019 Mar 1];14(5):e1002459. Available from: www.lmu.de

130. Page C, Pitchford S. Neutrophil and platelet complexes and their relevance to neutrophil recruitment and activation. Int Immunopharmacol [Internet]. 2013 [cited 2019 May 1];17:1176–84. Available from: http://dx.doi.org/10.1016/j.intimp.2013.06.004

131. Lisman T. Platelet-neutrophil interactions as drivers of inflammatory and thrombotic disease. Cell Tissue Res [Internet]. 2018 [cited 2019 Apr 16];371:567–76. Available from: https://doi.org/10.1007/s00441-017-2727-4

132. Launder D, Dillon JT, Wuescher LM, Glanz T, Abdul-Aziz N, Mein-Chiain Yi E, et al. Immunity to pathogenic mucosal C. albicans infections mediated by oral megakaryocytes activated by IL-17 and candidalysin. 2024 [cited 2024 May 18]; Available from: https://doi.org/10.1016/j.mucimm.2024.01.003

133. Richardson JP, Moyes DL. Adaptive immune responses to Candida albicans infection. Virulence [Internet]. 2015 Jan 1 [cited 2024 May 21];6(4):327. Available from: /pmc/articles/PMC4601188/

134. Gross O, Poeck H, Bscheider M, Dostert C, Hannesschläger N, Endres S, et al. Syk kinase signalling couples to the Nlrp3 inflammasome for anti-fungal host defence. Nature 2009 459:7245 [Internet]. 2009 Apr 1 [cited 2024 May 21];459(7245):433–6. Available from: https://www.nature.com/articles/nature07965

135. Hise AG, Tomalka J, Ganesan S, Patel K, Hall BA, Brown GD, et al. An Essential Role for the NLRP3 Inflammasome in Host Defense against the Human Fungal Pathogen Candida albicans. Cell Host Microbe [Internet]. 2009 May 8 [cited 2024 May 21];5(5):487–97. Available from: http://www.cell.com/article/S1931312809001437/fulltext

136. O'meara TR, Duah K, Guo CX, Maxson ME, Gaudet RG, Koselny K, et al. High-throughput screening identifies genes required for Candida albicans induction of macrophage pyroptosis. mBio [Internet]. 2018 [cited 2019 Aug 27];9(4):1–20. Available from: https://doi.org/10.1128/mBio

137. O'meara TR, Cowen LE. Insights into the host-pathogen interaction: C. albicans manipulation of macrophage pyroptosis. 2018 [cited 2024 May 18];5(12). Available from: www.microbialcell.com

138. Yang D, Chertov O, Bykovskaia SN, Chen Q, Buffo MJ, Shogan J, et al. β-Defensins: Linking innate and adaptive immunity through dendritic and T cell CCR6. Science (1979) [Internet]. 1999 Oct 15 [cited 2024 May 21];286(5439):525–8. Available from: https://www.science.org/doi/10.1126/science.286.5439.525

139. Thorley AJ, Goldstraw P, Young A, Tetley TD. Primary Human Alveolar Type II Epithelial Cell CCL20 (Macrophage Inflammatory Protein-3α)–Induced Dendritic Cell Migration.

https://doi.org/101165/rcmb2004-0196OC [Internet]. 2012 Dec 20 [cited 2024 May 21];32(4):262–7. Available from: www.atsjournals.org

140. Beno DW, Stöver AG, Mathews HL. Growth inhibition of Candida albicans hyphae by CD8+ lymphocytes. The Journal of Immunology [Internet]. 1995 May 15 [cited 2024 May 21];154(10):5273–81. Available from: https://dx.doi.org/10.4049/jimmunol.154.10.5273

141. Bacci A, Montagnoli C, Perruccio K, Bozza S, Gaziano R, Pitzurra L, et al. Dendritic cells pulsed with fungal RNA induce protective immunity to Candida albicans in hematopoietic transplantation. J Immunol [Internet]. 2002 Mar 15 [cited 2024 May 21];168(6):2904–13. Available from: https://pubmed.ncbi.nlm.nih.gov/11884461/

142. D'Ostiani CF, Del Sero G Del, Bacci A, Montagnoli C, Spreca A, Mencacci A, et al. Dendritic cells discriminate between yeasts and hyphae of the fungus Candida albicans. Implications for initiation of T helper cell immunity in vitro and in vivo. J Exp Med [Internet]. 2000 May 15 [cited 2024 May 21];191(10):1661–73. Available from: https://pubmed.ncbi.nlm.nih.gov/10811860/

143. Smeltz RB, Chen J, Ehrhardt R, Shevach EM. Role of IFN-γ in Th1 Differentiation: IFN-γ Regulates IL-18Rα Expression by Preventing the Negative Effects of IL-4 and by Inducing/Maintaining IL-12 Receptor β2 Expression. The Journal of Immunology [Internet]. 2002 Jun 15 [cited 2024 May 21];168(12):6165–72. Available from: https://dx.doi.org/10.4049/jimmunol.168.12.6165

144. Chung Y, Chang SH, Martinez GJ, Yang XO, Nurieva R, Kang HS, et al. Critical Regulation of Early Th17 Cell Differentiation by Interleukin-1 Signaling. Immunity [Internet]. 2009 Apr 17 [cited 2024 May 21];30(4):576–87. Available from: http://www.cell.com/article/S1074761309001423/fulltext

145. McGeachy MJ, Chen Y, Tato CM, Laurence A, Joyce-Shaikh B, Blumenschein WM, et al. The interleukin 23 receptor is essential for the terminal differentiation of interleukin 17–producing effector T helper cells in vivo. Nature Immunology 2009 10:3 [Internet]. 2009 Feb 1 [cited 2024 May 21];10(3):314–24. Available from: https://www.nature.com/articles/ni.1698

146. Huang W, Na L, Fidel PL, Schwarzenberger P. Requirement of interleukin-17A for systemic anti-Candida albicans host defense in mice. J Infect Dis [Internet]. 2004 Aug 1 [cited 2024 May 21];190(3):624–31. Available from: https://pubmed.ncbi.nlm.nih.gov/15243941/

147. De Luca A, Zelante T, D'Angelo C, Zagarella S, Fallarino F, Spreca A, et al. IL-22 defines a novel immune pathway of antifungal resistance. Mucosal Immunol [Internet]. 2010 [cited 2024 May 21];3(4):361–73. Available from: https://pubmed.ncbi.nlm.nih.gov/20445503/

148. Carrow EW, Hector RF, Domer JE. Immunodeficient CBA/N mice respond effectively to Candida albicans. Clin Immunol Immunopathol. 1984 Dec 1;33(3):371–80.

149. Matthews RC, Burnie JP, Howat D, Rowland T, Walton F. Autoantibody to heat-shock protein 90 can mediate protection against systemic candidosis. Immunology [Internet]. 1991 Sep [cited 2024 May 21];74(1):20. Available from: /pmc/articles/PMC1384665/?report=abstract

150. Brena S, Cabezas-Olcoz J, Moragues MD, Fernández De Larrinoa I, Domínguez A, Quindós G, et al. Fungicidal monoclonal antibody C7 interferes with iron acquisition in Candida albicans. Antimicrob Agents Chemother [Internet]. 2011 Jul [cited 2024 May 21];55(7):3156–63. Available from: https://pubmed.ncbi.nlm.nih.gov/21518848/

151. De Bernardis F, Boccanera M, Adriani D, Spreghini E, Santoni G, Cassone A. Protective role of antimannan and anti-aspartyl proteinase antibodies in an experimental model of Candida albicans vaginitis in rats. Infect Immun [Internet]. 1997 [cited 2024 May 21];65(8):3399–405. Available from: https://pubmed.ncbi.nlm.nih.gov/9234804/

152. Brena S, Omaetxebarría MJ, Elguezabal N, Cabezas J, Moragues MD, Pontón J. Fungicidal monoclonal antibody C7 binds to Candida albicans Als3. Infect Immun [Internet]. 2007 Jul [cited 2024 May 21];75(7):3680–2. Available from: https://pubmed.ncbi.nlm.nih.gov/17452471/

153. Hopke A, Brown AJP, Hall RA, Wheeler RT. Dynamic Fungal Cell Wall Architecture in Stress Adaptation and Immune Evasion. Trends Microbiol [Internet]. 2018 Apr 1 [cited 2024 May 19];26(4):284–95. Available from: http://www.cell.com/article/S0966842X18300192/fulltext

154. Fernández-Arenas E, Bleck CKE, Nombela C, Gil C, Griffiths G, Diez-Orejas R. Candida albicans actively modulates intracellular membrane trafficking in mouse macrophage phagosomes. Cell Microbiol [Internet]. 2009 Apr 1 [cited 2024 May 21];11(4):560–89. Available from: https://onlinelibrary.wiley.com/doi/full/10.1111/j.1462-5822.2008.01274.x

155. Frohner IE, Bourgeois C, Yatsyk K, Majer O, Kuchler K. Candida albicans cell surface superoxide dismutases degrade host-derived reactive oxygen species to escape innate immune surveillance. Mol Microbiol [Internet]. 2009 Jan 1 [cited 2024 May 21];71(1):240–52. Available from: https://onlinelibrary.wiley.com/doi/full/10.1111/j.1365-2958.2008.06528.x

156. Polke M, Hube B, Jacobsen ID. Candida Survival Strategies. 2015 [cited 2020 Apr 19]; Available from: http://dx.doi.org/10.1016/bs.aambs.2014.12.002

157. Hromatka BS, Noble SM, Johnson AD. Transcriptional response of Candida albicans to nitric oxide and the role of the YHB1 gene in nitrosative stress and virulence. Mol Biol Cell [Internet]. 2005 Oct 19 [cited 2024 May 21];16(10):4814–26. Available from: https://www.molbiolcell.org/doi/10.1091/mbc.e05-05-0435

158. Vylkova S, Lorenz MC. Modulation of Phagosomal pH by Candida albicans Promotes Hyphal Morphogenesis and Requires Stp2p, a Regulator of Amino Acid Transport. PLoS Pathog [Internet]. 2014 [cited 2024 May 21];10(3):e1003995. Available from: https://journals.plos.org/plospathogens/article?id=10.1371/journal.ppat.1003995

159. Szafranski-Schneider E, Swidergall M, Cottier F, Tielker D, Román E, Pla J, et al. Msb2 Shedding Protects Candida albicans against Antimicrobial Peptides. PLoS Pathog [Internet]. 2012 Feb [cited 2024 May 14];8(2):e1002501. Available from: https://journals.plos.org/plospathogens/article?id=10.1371/journal.ppat.1002501

160. Swidergall M, Ernst AM, Ernst JF. Candida albicans mucin Msb2 is a broad-range protectant against antimicrobial peptides. Antimicrob Agents Chemother [Internet]. 2013 Aug [cited 2024 May 14];57(8):3917–22. Available from: https://journals.asm.org/doi/10.1128/aac.00862-13

161. Uwamahoro N, Verma-Gaur J, Shen HH, Qu Y, Lewis R, Lu J, et al. The Pathogen Candida albicans Hijacks Pyroptosis for Escape from Macrophages. mBio [Internet]. 2014 May 1 [cited 2019 Oct 10];5(2):e00003-14. Available from: http://www.ncbi.nlm.nih.gov/pubmed/24667705

162. Olivier FAB, Hilsenstein V, Weerasinghe H, Weir A, Hughes S, Crawford S, et al. The escape of Candida albicans from macrophages is enabled by the fungal toxin candidalysin and two host cell death pathways. Cell Rep. 2022 Sep 20;40(12):111374.

163. Bain JM, Lewis LE, Okai B, Quinn J, Gow NAR, Erwig LP. Non-lytic expulsion/exocytosis of Candida albicans from macrophages. Fungal Genetics and Biology. 2012;49:677–8.

164. Scherer Id AK, Id BAB, Id JP, Seman BG, 1¤b ID, Kelleyid JB, et al. Redundant Trojan horse and endothelial-circulatory mechanisms for host-mediated spread of Candida albicans yeast. 2020 [cited 2024 May 7]; Available from: https://doi.org/10.1371/journal.ppat.1008414

165. Luo S, Hartmann A, Dahse HM, Skerka C, Zipfel PF. Secreted pH-Regulated Antigen 1 of Candida albicans Blocks Activation and Conversion of Complement C3. The Journal of Immunology [Internet]. 2010 Aug 15 [cited 2024 May 13];185(4):2164–73. Available from: https://dx.doi.org/10.4049/jimmunol.1001011

166. Luo S, Blom AM, Rupp S, Hipler UC, Hube B, Skerka C, et al. The pH-regulated Antigen 1 of Candida albicans Binds the Human Complement Inhibitor C4b-binding Protein and Mediates Fungal Complement Evasion * □ S. 2011 [cited 2024 May 13]; Available from: http://www.jbc.org

167. Rosowski EE, Knox BP, Archambault LS, Huttenlocher A, Keller NP, Wheeler RT, et al. The Zebrafish as a Model Host for Invasive Fungal Infections. Journal of Fungi [Internet]. 2018 Dec 13 [cited 2019 Apr 24];4(4):136. Available from: http://www.mdpi.com/2309-608X/4/4/136

168. Masud S, Torraca V, Meijer AH. Modeling Infectious Diseases in the Context of a Developing Immune System. Curr Top Dev Biol. 2017 Jan 1;124:277–329.

169. Walters KB, Green JM, Surfus JC, Yoo SK, Huttenlocher A. Live imaging of neutrophil motility in a zebrafish model of WHIM syndrome. Blood [Internet]. 2010 Oct 14 [cited 2024 May 7];116(15):2803–11. Available from: https://dx.doi.org/10.1182/blood-2010-03-276972

170. Deng Q, Yoo SK, Cavnar PJ, Green JM, Huttenlocher A. Dual Roles for Rac2 in Neutrophil Motility and Active Retention in Zebrafish Hematopoietic Tissue. Dev Cell [Internet]. 2011 [cited 2019 Apr 21];21:735–45. Available from: https://www.cell.com/action/showPdf?pii=S1534-5807%2811%2900305-4

171. Bernut A, Nguyen-Chi M, Halloum I, Herrmann JL, Lutfalla G, Kremer L. Mycobacterium abscessus-Induced Granuloma Formation Is Strictly Dependent on TNF Signaling and Neutrophil Trafficking. Behr MA, editor. PLoS Pathog [Internet]. 2016 Nov 2 [cited 2019 Aug 28];12(11):e1005986. Available from: https://dx.plos.org/10.1371/journal.ppat.1005986

172. Gratacap RL, Scherer AK, Seman BG, Wheeler RT. Control of Mucosal Candidiasis in the Zebrafish Swim Bladder Depends on Neutrophils That Block Filament Invasion and Drive Extracellular-Trap Production. Infect Immun [Internet]. 2017 [cited 2019 Apr 13];85(9). Available from: https://doi.org/10.1128/IAI.00276-17.

173. Voelz K, Gratacap RL, Wheeler RT. A zebrafish larval model reveals early tissue-specific innate immune responses to Mucor circinelloides. Dis Model Mech [Internet]. 2015 [cited 2019 Apr 17];8:1375–88. Available from: http://dmm.biologists.org/content/dmm/8/11/1375.full.pdf?with-ds=yes

174. Bergeron AC, Seman BG, Hammond JH, Archambault LS, Hogan DA, Wheeler RT. Candida albicans and Pseudomonas aeruginosa Interact To Enhance Virulence of Mucosal Infection in Transparent Zebrafish. Infect Immun [Internet]. 2017 Nov 1 [cited 2019 Jun 20];85(11):e00475-17. Available from: http://www.ncbi.nlm.nih.gov/pubmed/28847848

175. Archambault LS, Trzilova D, Gonia S, Gale C, Wheeler RT. Intravital imaging reveals divergent cytokine and cellular immune responses to candida albicans and candida parapsilosis. mBio [Internet]. 2019 May 1 [cited 2024 May 7];10(3). Available from: https://journals.asm.org/doi/10.1128/mbio.00266-19

176. Benedict K, Jackson BR, Chiller T, Beer KD. Estimation of Direct Healthcare Costs of Fungal Diseases in the United States. Clinical Infectious Diseases [Internet]. 2019 May 17 [cited 2024 May 19];68(11):1791–7. Available from: https://dx.doi.org/10.1093/cid/ciy776

177. Brown GD, Denning DW, Gow NAR, Levitz SM, Netea MG, White TC. Hidden killers: Human fungal infections. Sci Transl Med [Internet]. 2012 Dec 19 [cited 2024 May 19];4(165). Available from: https://www.science.org/doi/10.1126/scitranslmed.3004404

178. Smith DJ, Gold JAW, Benedict K, Wu K, Lyman M, Jordan A, et al. Public Health Research Priorities for Fungal Diseases: A Multidisciplinary Approach to Save Lives. Journal of Fungi 2023, Vol 9, Page 820 [Internet]. 2023 Aug 3 [cited 2024 May 19];9(8):820. Available from: https://www.mdpi.com/2309-608X/9/8/820/htm

179. Brown R, Priest E, Naglik JR, Richardson JP. Fungal Toxins and Host Immune Responses. Front Microbiol [Internet]. 2021 Apr 13 [cited 2024 May 19];12:643639. Available from: www.frontiersin.org

180. Goyal S, Castrillón-Betancur JC, Klaile E, Slevogt H. The interaction of human pathogenic fungi with C-type lectin receptors. Front Immunol [Internet]. 2018 Jun 4 [cited 2024 May 19];9(JUN):331844. Available from: www.frontiersin.org

181. Hernández-Chávez M, Pérez-García L, Niño-Vega G, Mora-Montes H. Fungal Strategies to Evade the Host Immune Recognition. Journal of Fungi [Internet]. 2017 Sep 23 [cited 2019 Sep 16];3(4):51. Available from: http://www.mdpi.com/2309-608X/3/4/51

182. Kadosh D. Regulatory mechanisms controlling morphology and pathogenesis in Candida albicans. Curr Opin Microbiol. 2019 Dec 1;52:27–34.

183. Oliver JC, Ferreira CBRJ, Silva NC, Dias ALT. Candida spp. and phagocytosis: multiple evasion mechanisms. Antonie van Leeuwenhoek 2019 112:10 [Internet]. 2019 May 11 [cited 2024 May 19];112(10):1409–23. Available from: https://link.springer.com/article/10.1007/s10482-019-01271-x

184. Ost KS, O'Meara TR, Stephens WZ, Chiaro T, Zhou H, Penman J, et al. Adaptive immunity induces mutualism between commensal eukaryotes. Nature [Internet]. 2021 Jul 14 [cited 2024 May 19];596(7870):114–8. Available from: https://www.ncbi.nlm.nih.gov/pmc/articles/PMC8904204

185. Seider K, Heyken A, Lüttich A, Miramón P, Hube B. Interaction of pathogenic yeasts with phagocytes: survival, persistence and escape. Curr Opin Microbiol. 2010 Aug 1;13(4):392–400.

186. Singh DK, Tóth R, Gácser A. Mechanisms of Pathogenic Candida Species to Evade the Host Complement Attack. Front Cell Infect Microbiol. 2020 Mar 12;10:514598.

187. Brown GD. Innate antifungal immunity: The key role of phagocytes. Annu Rev Immunol [Internet]. 2011 Apr 23 [cited 2024 May 19];29(Volume 29, 2011):1–21. Available from: https://www.annualreviews.org/content/journals/10.1146/annurev-immunol-030409-101229

188. Dambuza IM, Levitz SM, Netea MG, Brown GD. Fungal Recognition and Host Defense Mechanisms. Microbiol Spectr [Internet]. 2017 Aug 25 [cited 2024 May 19];5(4). Available from: https://journals.asm.org/doi/10.1128/microbiolspec.funk-0050-2016

189. Jawale C V., Biswas PS. Local antifungal immunity in the kidney in disseminated candidiasis. Curr Opin Microbiol. 2021 Aug 1;62:1–7.

190. Lionakis MS, Iliev ID, Hohl TM. Immunity against fungi. JCI Insight [Internet]. 2017 Jun 2 [cited 2024 May 19];2(11). Available from: https://doi.org/10.1172/jci.insight.93156:e93156.https://doi.org/10.1172/jci.insight.93156.

191. Netea MG, Joosten LAB, Van Der Meer JWM, Kullberg BJ, Van De Veerdonk FL. Immune defence against Candida fungal infections. Nature Reviews Immunology 2015 15:10 [Internet]. 2015 Sep 21 [cited 2024 May 19];15(10):630–42. Available from: https://www.nature.com/articles/nri3897

192. Drummond RA, Collar AL, Swamydas M, Rodriguez CA, Lim JK, Mendez LM, et al. CARD9-Dependent Neutrophil Recruitment Protects against Fungal Invasion of the Central Nervous System. PLoS Pathog [Internet]. 2015 [cited 2024 May 19];11(12):e1005293. Available from: https://mdanderson.elsevierpure.com/en/publications/card9-dependent-neutrophil-recruitment-protects-against-fungal-in

193. Drummond RA. What fungal CNS infections can teach us about neuroimmunology and CNS-specific immunity. Semin Immunol. 2023 May 1;67:101751.

194. Urban CF, Nett JE. Neutrophil extracellular traps in fungal infection. Semin Cell Dev Biol. 2019 May 1;89:47–57.

195. Da A, Dantas S, Lee KK, Raziunaite I, Schaefer K, Wagener J, et al. Cell biology of Candida albicans-host interactions. [cited 2024 May 19]; Available from: http://dx.doi.org/10.1016/j.mib.2016.08.006

196. Jiménez-López C, Lorenz MC. Fungal Immune Evasion in a Model Host–Pathogen Interaction: Candida albicans Versus Macrophages. PLoS Pathog [Internet]. 2013 Nov [cited 2024 May 19];9(11):e1003741. Available from: https://journals.plos.org/plospathogens/article?id=10.1371/journal.ppat.1003741

197. Williams TJ, Gonzales-Huerta LE, Armstrong-James D. Fungal-Induced Programmed Cell Death. Journal of Fungi 2021, Vol 7, Page 231 [Internet]. 2021 Mar 20 [cited 2024 May 19];7(3):231. Available from: https://www.mdpi.com/2309-608X/7/3/231/htm

198. Tobin DM, May RC, Wheeler RT. Zebrafish: A See-Through Host and a Fluorescent Toolbox to Probe Host–Pathogen Interaction. PLoS Pathog [Internet]. 2012 Jan [cited 2024 May 19];8(1):e1002349. Available from: https://journals.plos.org/plospathogens/article?id=10.1371/journal.ppat.1002349

199. Bergeron AC, Barker SE, Brothers KM, Prasad BC, Wheeler RT. Polyclonal anti-Candida antibody improves phagocytosis and overall outcome in zebrafish model of disseminated candidiasis. Dev Comp Immunol. 2017 Mar 1;68:69–78.

200. Noble SM, French S, Kohn LA, Chen V, Johnson AD. Systematic screens of a Candida albicans homozygous deletion library decouple morphogenetic switching and pathogenicity. Nature Genetics 2010 42:7 [Internet]. 2010 Jun 13 [cited 2024 May 19];42(7):590–8. Available from: https://www.nature.com/articles/ng.605

201. Reuß O, Vik Å, Kolter R, Morschhäuser J. The SAT1 flipper, an optimized tool for gene disruption in Candida albicans. Gene. 2004 Oct 27;341(1–2):119–27.

202. Wu Y, Du S, Johnson JL, Tung HY, Landers CT, Liu Y, et al. Microglia and amyloid precursor protein coordinate control of transient Candida cerebritis with memory deficits. Nature Communications 2019 10:1 [Internet]. 2019 Jan 4 [cited 2024 May 19];10(1):1–15. Available from: https://www.nature.com/articles/s41467-018-07991-4

203. Moyes DL, Wilson D, Richardson JP, Mogavero S, Tang SX, Wernecke J, et al. Candidalysin is a fungal peptide toxin critical for mucosal infection. Nature 2016 532:7597 [Internet]. 2016 Mar 30 [cited 2024 May 19];532(7597):64–8. Available from: https://www.nature.com/articles/nature17625

204. Peters BM, Palmer GE, Nash AK, Lilly EA, Fidel PL, Noverra MC. Fungal morphogenetic pathways are required for the hallmark inflammatory response during Candida albicans vaginitis. Infect Immun [Internet]. 2014 Feb 11 [cited 2024 May 19];82(2):532–43. Available from: https://journals.asm.org/doi/10.1128/iai.01417-13

205. Animals NRC (US) C for the U of the G for the C and U of L. Guide for the Care and Use of Laboratory Animals. Guide for the Care and Use of Laboratory Animals [Internet]. 2011 Dec 27 [cited 2024 May 19]; Available from: https://www.ncbi.nlm.nih.gov/books/NBK54050/

206. Ellett F, Pase L, Hayman JW, Andrianopoulos A, Lieschke GJ. mpeg1 promoter transgenes direct macrophage-lineage expression in zebrafish. 2011 [cited 2024 May 8]; Available from: www.gene-tools.com

207. Hall C, Flores M, Storm T, Crosier K, Crosier P. The zebrafish lysozyme C promoter drives myeloid-specific expression in transgenic fish. BMC Dev Biol [Internet]. 2007 May 4 [cited 2024 May 8];7(1):1–17. Available from: https://bmcdevbiol.biomedcentral.com/articles/10.1186/1471-213X-7-42

208. Brothers KM, Wheeler RT. Non-invasive Imaging of Disseminated Candidiasis in Zebrafish Larvae. JoVE (Journal of Visualized Experiments) [Internet]. 2012 Jul 30 [cited 2024 May 20];(65):e4051. Available from: https://www.jove.com/v/4051/non-invasive-imaging-disseminated-candidiasis-zebrafish-larvae-video

209. de Oliveira S, Lopez-Muñoz A, Martínez-Navarro FJ, Galindo-Villegas J, Mulero V, Calado Â. Cxcl8-l1 and Cxcl8-l2 are required in the zebrafish defense against Salmonella Typhimurium. Dev Comp Immunol. 2015 Mar 1;49(1):44–8.

210. Nguyen-Chi M, Laplace-Builhe B, Travnickova J, Luz-Crawford P, Tejedor G, Phan QT, et al. Identification of polarized macrophage subsets in zebrafish. Elife. 2015 Jul 8;4(JULY 2015).

211. Gratacap RL, Rawls JF, Wheeler RT. Mucosal candidiasis elicits NF-κB activation, proinflammatory gene expression and localized neutrophilia in zebrafish. DMM Disease Models and Mechanisms [Internet]. 2013 Sep 1 [cited 2024 May 8];6(5):1260–70. Available from: https://dx.doi.org/10.1242/dmm.012039

212. Mattingly CJ, Hampton TH, Brothers KM, Griffin NE, Planchart A. Perturbation of defense pathways by low-dose Arsenic exposure in zebrafish embryos. Environ Health Perspect [Internet]. 2009 [cited 2024 May 8];117(6):981–7. Available from: https://ehp.niehs.nih.gov/doi/10.1289/ehp.0900555

213. Lewis LE, Bain JM, Lowes C, Gillespie C, Rudkin FM, Gow NAR, et al. Stage Specific Assessment of Candida albicans Phagocytosis by Macrophages Identifies Cell Wall Composition and Morphogenesis as Key Determinants. PLoS Pathog [Internet]. 2012 Mar [cited 2024 May 19];8(3):e1002578. Available from: https://journals.plos.org/plospathogens/article?id=10.1371/journal.ppat.1002578

214. Mallick EM, Bergeron AC, Jones SK, Newman ZR, Brothers KM, Creton R, et al. Phenotypic plasticity regulates Candida albicans interactions and virulence in the vertebrate host. Front Microbiol [Internet]. 2016 May 26 [cited 2024 May 19];7(MAY):203534. Available from: www.frontiersin.org

215. Mao Y, Solis N V., Filler SG, Mitchell AP. Functional Dichotomy for a Hyphal Repressor in Candida albicans. mBio [Internet]. 2023 Mar 1 [cited 2024 May 19];14(2). Available from: https://journals.asm.org/doi/10.1128/mbio.00134-23

216. Sharma A, Mitchell AP. Strain variation in gene expression impact of hyphal cyclin Hgc1 in Candida albicans. G3 Genes|Genomes|Genetics [Internet]. 2023 Aug 30 [cited 2024 May 19];13(9). Available from: https://dx.doi.org/10.1093/g3journal/jkad151

217. Solis N V., Wakade RS, Glazier VE, Ollinger TL, Wellington M, Mitchell AP, et al. Systematic Genetic Interaction Analysis Identifies a Transcription Factor Circuit Required for

Oropharyngeal Candidiasis. mBio [Internet]. 2022 Feb 1 [cited 2024 May 19];13(1). Available from: https://journals.asm.org/doi/10.1128/mbio.03447-21

218. Cleary IA, Lazzell AL, Monteagudo C, Thomas DP, Saville SP. BRG1 and NRG1 form a novel feedback circuit regulating Candida albicans hypha formation and virulence. Mol Microbiol [Internet]. 2012 Aug 1 [cited 2024 May 19];85(3):557–73. Available from: https://onlinelibrary.wiley.com/doi/full/10.1111/j.1365-2958.2012.08127.x

219. Du H, Guan G, Xie J, Sun Y, Tong Y, Zhang L, et al. Roles of Candida albicans Gat2, a GATA-Type Zinc Finger Transcription Factor, in Biofilm Formation, Filamentous Growth and Virulence. PLoS One [Internet]. 2012 Jan 19 [cited 2024 May 19];7(1):e29707. Available from: https://journals.plos.org/plosone/article?id=10.1371/journal.pone.0029707

220. Thomas G, Bain JM, Budge S, Brown AJP, Ames RM. Identifying Candida albicans Gene Networks Involved in Pathogenicity. Front Genet [Internet]. 2020 Apr 24 [cited 2024 May 19];11:530601. Available from: www.frontiersin.org

221. Gervais NC, Halder V, Shapiro RS. A data library of Candida albicans functional genomic screens. FEMS Yeast Res [Internet]. 2021 Dec 2 [cited 2024 May 19];21(7):60. Available from: https://dx.doi.org/10.1093/femsyr/foab060

222. Bai C, Ramanan N, Wang YM, Wang Y. Spindle assembly checkpoint component CaMad2p is indispensable for Candida albicans survival and virulence in mice. Mol Microbiol [Internet]. 2002 Jul 1 [cited 2024 May 19];45(1):31–44. Available from: https://onlinelibrary.wiley.com/doi/full/10.1046/j.1365-2958.2002.02995.x

223. Csank C, Schröppel K, Leberer E, Harcus D, Mohamed O, Meloche S, et al. Roles of the Candida aibicans mitogen-activated protein kinase homolog, Cek1p, in hyphal development and systemic candidiasis. Infect Immun [Internet]. 1998 [cited 2024 May 19];66(6):2713–21. Available from: https://journals.asm.org/doi/10.1128/iai.66.6.2713-2721.1998

224. Davis D, Edwards J, Mitchell AP, Ibrahim AS. Candida albicans RIM101 pH response pathway is required for host-pathogen interactions. Infect Immun [Internet]. 2000 [cited 2024 May 19];68(10):5953–9. Available from: https://journals.asm.org/doi/10.1128/iai.68.10.5953-5959.2000

225. Arora A, Singh A. Exploring the role of neutrophils in infectious and noninfectious pulmonary disorders. Int Rev Immunol [Internet]. 2024 [cited 2024 May 19];43(1):41–61. Available from: https://www.tandfonline.com/doi/abs/10.1080/08830185.2023.2222769

226. Geiger J, Wessels D, Lockhart SR, Soll DR. Release of a Potent Polymorphonuclear Leukocyte Chemoattractant Is Regulated by White-Opaque Switching in Candida albicans. Infect Immun [Internet]. 2004 Feb [cited 2024 May 19];72(2):667–77. Available from: https://journals.asm.org/doi/10.1128/iai.72.2.667-677.2004

227. Parker D, Prince A. Innate Immunity in the Respiratory Epithelium. https://doi.org/101165/rcmb2011-0011RT [Internet]. 2012 Dec 20 [cited 2024 May 19];45(2):189–201. Available from: www.atsjournals.org

228. Selvatici R, Falzarano S, Mollica A, Spisani S. Signal transduction pathways triggered by selective formylpeptide analogues in human neutrophils. Eur J Pharmacol. 2006 Mar 18;534(1–3):1–11.

229. Ferrigno P, Posas F, Koepp D, Saito H, Silver PA. Regulated nucleo/cytoplasmic exchange of HOG1 MAPK requires the importin β homologs NMD5 and XPO1. EMBO J [Internet]. 1998 Oct 1 [cited 2024 May 19];17(19):5606–14. Available from: https://www.embopress.org/doi/10.1093/emboj/17.19.5606

230. Polizotto RS, Cyert MS. Calcineurin-dependent nuclear import of the transcription factor Crz1p requires Nmd5p. Journal of Cell Biology [Internet]. 2001 Sep 3 [cited 2024 May 19];154(5):951–60. Available from: http://www.jcb.org/cgi/doi/10.1083/jcb.200104078

231. Brenes LR, Lohse MB, Hartooni N, Johnson AD. A Set of Diverse Genes Influence the Frequency of White-Opaque Switching in Candida albicans. G3 Genes|Genomes|Genetics [Internet]. 2020 Aug 1 [cited 2024 May 19];10(8):2593–600. Available from: https://dx.doi.org/10.1534/g3.120.401249

232. Enjalbert B, Smith DA, Cornell MJ, Alam I, Nicholls S, Brown AJP, et al. Role of the Hog1 stress-activated protein kinase in the global transcriptional response to stress in the fungal

pathogen Candida albicans. Mol Biol Cell [Internet]. 2006 Feb 7 [cited 2024 May 19];17(2):1018–32. Available from: https://www.molbiolcell.org/doi/10.1091/mbc.e05-06-0501

233. O'Meara TR, O'Meara MJ. DeORFanizing Candida albicans Genes using Coexpression. mSphere [Internet]. 2021 Feb 24 [cited 2024 May 20];6(1). Available from: https://journals.asm.org/doi/10.1128/msphere.01245-20

234. Williams RB, Lorenz MC. Multiple alternative carbon pathways combine to promote candida albicans stress resistance, immune interactions, and virulence. mBio [Internet]. 2020 Jan 1 [cited 2024 May 19];11(1). Available from: https://journals.asm.org/doi/10.1128/mbio.03070-19

235. Deng Q, Harvie EA, Huttenlocher A. Distinct signalling mechanisms mediate neutrophil attraction to bacterial infection and tissue injury. Cell Microbiol [Internet]. 2012 Apr 1 [cited 2024 May 19];14(4):517–28. Available from: https://onlinelibrary.wiley.com/doi/full/10.1111/j.1462-5822.2011.01738.x

236. LeBert DC, Huttenlocher A. Inflammation and wound repair. Semin Immunol. 2014 Aug 1;26(4):315–20.

237. Sadik CD, Luster AD. Lipid-cytokine-chemokine cascades orchestrate leukocyte recruitment in inflammation. J Leukoc Biol [Internet]. 2012 Feb 1 [cited 2024 May 19];91(2):207–15. Available from: https://dx.doi.org/10.1189/jlb.0811402

238. delFresno C, Soulat D, Roth S, Blazek K, Udalova I, Sancho D, et al. Interferon-β Production via Dectin-1-Syk-IRF5 Signaling in Dendritic Cells Is Crucial for Immunity to C.albicans. Immunity [Internet]. 2013 Jun 27 [cited 2024 May 19];38(6):1176–86. Available from: http://www.cell.com/article/S1074761313002355/fulltext

239. Majer O, Bourgeois C, Zwolanek F, Lassnig C, Kerjaschki D, Mack M, et al. Type I Interferons Promote Fatal Immunopathology by Regulating Inflammatory Monocytes and Neutrophils during Candida Infections. PLoS Pathog [Internet]. 2012 Jul [cited 2024 May 19];8(7):e1002811. Available from: https://journals.plos.org/plospathogens/article?id=10.1371/journal.ppat.1002811

240. Jaeger M, van der Lee R, Cheng SC, Johnson MD, Kumar V, Ng A, et al. The RIG-I-like helicase receptor MDA5 (IFIH1) is involved in the host defense against Candida infections. European Journal of Clinical Microbiology and Infectious Diseases [Internet]. 2015 May 1 [cited 2024 May 19];34(5):963–74. Available from: https://link.springer.com/article/10.1007/s10096-014-2309-2

241. Patin EC, Thompson A, Orr SJ. Pattern recognition receptors in fungal immunity. Semin Cell Dev Biol. 2019 May 1;89:24–33.

242. Monniot C, Boisramé A, Da Costa G, Chauvel M, Sautour M, Bougnoux ME, et al. Rbt1 Protein Domains Analysis in Candida albicans Brings Insights into Hyphal Surface Modifications and Rbt1 Potential Role during Adhesion and Biofilm Formation. Arkowitz RA, editor. PLoS One. 2013 Dec 5;8(12):e82395.

243. Braun BR, Steven Head W, Wang MX, Johnson AD, Head WS, Wang MX, et al. Identification and Characterization of TUP1-Regulated Genes in Candida albicans. Genetics. 2000;156(1):31–44.

244. Staab JF, Bradway SD, Fidel PL, Sundstrom P. Adhesive and Mammalian Transglutaminase Substrate Properties of Candida albicans Hwp1 . Science (1979). 1999 Mar 5;283(5407):1535–8.

245. Nantel A, Dignard D, Bachewich C, Harcus D, Marcil A, Bouin AP, et al. Transcription Profiling of Candida albicans Cells Undergoing the Yeast-to-Hyphal Transition □ D. Mol Biol Cell. 2002;13:3452–65.

246. Braun BR, Johnson AD. TUP1, CPH1 and EFG1 Make Independent Contributions to Filamentation in Candida albicans. Genetics. 2000;155:57–67.

247. Lane S, Birse C, Zhou S, Matson R, Liu H. DNA Array Studies Demonstrate Convergent Regulation of Virulence Factors by Cph1, Cph2, and Efg1 in Candida albicans*. J Biol Chem. 2001;276(52):48988–96.

248. Martin R, Albrecht-Eckardt D, Brunke S, Hube B, Hü Nniger K. A Core Filamentation Response Network in Candida albicans Is Restricted to Eight Genes. PLoS One. 2013;8(3):58613.

249. Bensen ES, Martin SJ, Li M, Berman J, Davis DA. Transcriptional profiling in Candida albicans reveals new adaptive responses to extracellular pH and functions for Rim101p. Mol Microbiol. 2004 Dec;54(5):1335–51.

250. Lotz H, Sohn K, Brunner H, Mühlschlegel FA, Rupp S. RBR1, a novel pH-regulated cell wall gene of Candida albicans, is repressed by RIM101 and activated by NRG1. Eukaryot Cell. 2004 Jun;3(3):776–84.

251. Braun BR, Kadosh D, Johnson AD. NRG1, a repressor of filamentous growth in C.albicans, is down-regulated during filament induction. EMBO Journal. 2001 Sep 3;20(17):4753–61.

252. Rossignol T, Ding C, Guida A, D'Enfert C, Higgins DG, Butler G. Correlation between biofilm formation and the hypoxic response in Candida parapsilosis. Eukaryot Cell. 2009 Apr;8(4):550–9.

253. Ene I V., Bennett RJ. Hwp1 and related adhesins contribute to both mating and biofilm formation in Candida albicans. Eukaryot Cell. 2009;8(12):1909–13.

254. Jackson BE, Mitchell BM, Wilhelmus KR. Corneal Virulence of Candida albicans Strains Deficient in Tup1-Regulated Genes. Investigative Opthalmology & Visual Science. 2007 Jun 1;48(6):2535–9.

255. Hoffman CS. Preparation of Yeast DNA. Curr Protoc Mol Biol [Internet]. 1997 Jul 1 [cited 2024 Aug 6];39(1):13.11.1-13.11.4. Available from: https://onlinelibrary.wiley.com/doi/full/10.1002/0471142727.mb1311s39

256. Noble SM, French S, Kohn LA, Chen V, Johnson AD. Systematic screens of a Candida albicans homozygous deletion library decouple morphogenetic switching and pathogenicity. Nat Genet. 2010 Jul 13;42(7):590–8.

257. Mishchenko Y. A fast algorithm for computation of discrete Euclidean distance transform in three or more dimensions on vector processing architectures. Signal Image Video Process [Internet].

2015 Jan 19 [cited 2024 May 20];9(1):19–27. Available from: https://link.springer.com/article/10.1007/s11760-012-0419-9

258. Abbey D, Hickman M, Gresham D, Berman J. High-resolution SNP/CGH microarrays reveal the accumulation of loss of heterozygosity in commonly used Candida albicans strains. G3: Genes, Genomes, Genetics [Internet]. 2011 Dec [cited 2024 May 5];1(7):523–30. Available from: https://pubmed.ncbi.nlm.nih.gov/22384363/

259. Abbey DA, Funt J, Lurie-Weinberger MN, Thompson DA, Regev A, Myers CL, et al. YMAP: a pipeline for visualization of copy number variation and loss of heterozygosity in eukaryotic pathogens. Genome Med [Internet]. 2014 Nov 20 [cited 2024 May 5];6(11):1–15. Available from: https://pubmed.ncbi.nlm.nih.gov/25505934/

260. Jackson BE, Mitchell BM, Wilhelmus KR. Corneal Virulence of Candida albicans Strains Deficient in Tup1-Regulated Genes. Investigative Opthalmology & Visual Science [Internet]. 2007 Jun 1 [cited 2019 Sep 16];48(6):2535–9. Available from: http://iovs.arvojournals.org/article.aspx?doi=10.1167/iovs.06-0909

261. Monniot C, Boisramé A, Da Costa G, Chauvel M, Sautour M, Bougnoux ME, et al. Rbt1 Protein Domains Analysis in Candida albicans Brings Insights into Hyphal Surface Modifications and Rbt1 Potential Role during Adhesion and Biofilm Formation. Arkowitz RA, editor. PLoS One [Internet]. 2013 Dec 5 [cited 2019 Aug 17];8(12):e82395. Available from: https://dx.plos.org/10.1371/journal.pone.0082395

262. Jaeger KE, Kharazmi A, Høiby N. Extracellular lipase of Pseudomonas aeruginosa: biochemical characterization and effect on human neutrophil and monocyte function in vitro. Microb Pathog. 1991;10(3):173–82.

263. Straus DC, Lonon MK, Hutson JC. Inhibition of rat alveolar macrophage phagocytic function by a Pseudornonas cepacia lipase. J Med Microbiol. 1992;37:335–40.

264. Rollof J, Braconier JH, Söderström C, Nilsson-Ehle P. Interference ofStaphylococcus aureus lipase with human granulocyte function. European Journal of Clinical Microbiology & Infectious Diseases. 1988 Aug;7(4):505–10.

265. König B, Jaeger KE, Sage AE, Vasil ML, König W. Role of Pseudomonas aeruginosa lipase in inflammatory mediator release from human inflammatory effector cells (platelets, granulocytes, and monocytes). Infect Immun [Internet]. 1996 [cited 2022 May 30];64(8):3252–8. Available from: https://journals.asm.org/journal/iai

266. Chen X, Alonzo F. Bacterial lipolysis of immune-activating ligands promotes evasion of innate defenses. Proc Natl Acad Sci U S A. 2019 Feb 26;116(9):3764–73.

267. Bowden MG, Visai L, Longshaw CM, Holland KT, Speziale P, Hö M. Is the GehD Lipase from Staphylococcus epidermidis a Collagen Binding Adhesin?*. 2002 [cited 2022 May 30]; Available from: http://www.jbc.org

268. Gácser A, Schäfer W, Nosanchuk JD, Trofa D. Targeted gene deletion in Candida parapsilosis demonstrates the role of secreted lipase in virulence. J Clin Invest [Internet]. [cited 2022 Jul 20]; Available from: https://jci.me/32294/pdfhttp://www.jci.orgVolume

269. Nagy I, Filkor K, Németh T, Hamari Z, Vágvölgyi C, Gácser A. In vitro interactions of Candida parapsilosis wild type and lipase deficient mutants with human monocyte derived dendritic cells. BMC Microbiol [Internet]. 2011 May 29 [cited 2024 May 4];11(1):1–9. Available from: https://bmcmicrobiol.biomedcentral.com/articles/10.1186/1471-2180-11-122

270. Paraje MG, Correa SG, Renna MS, Theumer M, Sotomayor CE. Candida albicans-secreted lipase induces injury and steatosis in immune and parenchymal cells. https://doi.org/101139/W08-048 [Internet]. 2009 [cited 2024 May 4];54(8):647–59. Available from: https://cdnsciencepub.com/doi/10.1139/W08-048

271. Paraje MG, Correa SG, Albesa I, Sotomayor CE. Lipase of Candida albicans induces activation of NADPH oxidase and l-arginine pathways on resting and activated macrophages. Biochem Biophys Res Commun. 2009 Dec 11;390(2):263–8.

272. Goody MF, Peterman E, Sullivan C, Kim CH. Quantification of the Respiratory Burst Response as an Indicator of Innate Immune Health in Zebrafish. J Vis Exp [Internet]. 2013 [cited 2024 May 20];(79):50667. Available from: /pmc/articles/PMC3871927/

273. Enjalbert B, MacCallum DM, Odds FC, Brown AJP. Niche-specific activation of the oxidative stress response by the pathogenic fungus Candida albicans. Infect Immun [Internet]. 2007 May [cited 2024 May 20];75(5):2143–51. Available from: https://journals.asm.org/doi/10.1128/iai.01680-06

274. Schoen TJ, Rosowski EE, Knox BP, Bennin D, Keller NP, Huttenlocher A. Neutrophil phagocyte oxidase activity controls invasive fungal growth and inflammation in zebrafish. 2019;

275. Iracane E, Arias-Sardá C, Maufrais C, Ene I V., d'Enfert C, Buscaino A. Identification of an active RNAi pathway in Candida albicans. Proceedings of the National Academy of Sciences [Internet]. 2024 Apr 23 [cited 2024 May 21];121(17):e2315926121. Available from: https://www.pnas.org/doi/abs/10.1073/pnas.2315926121

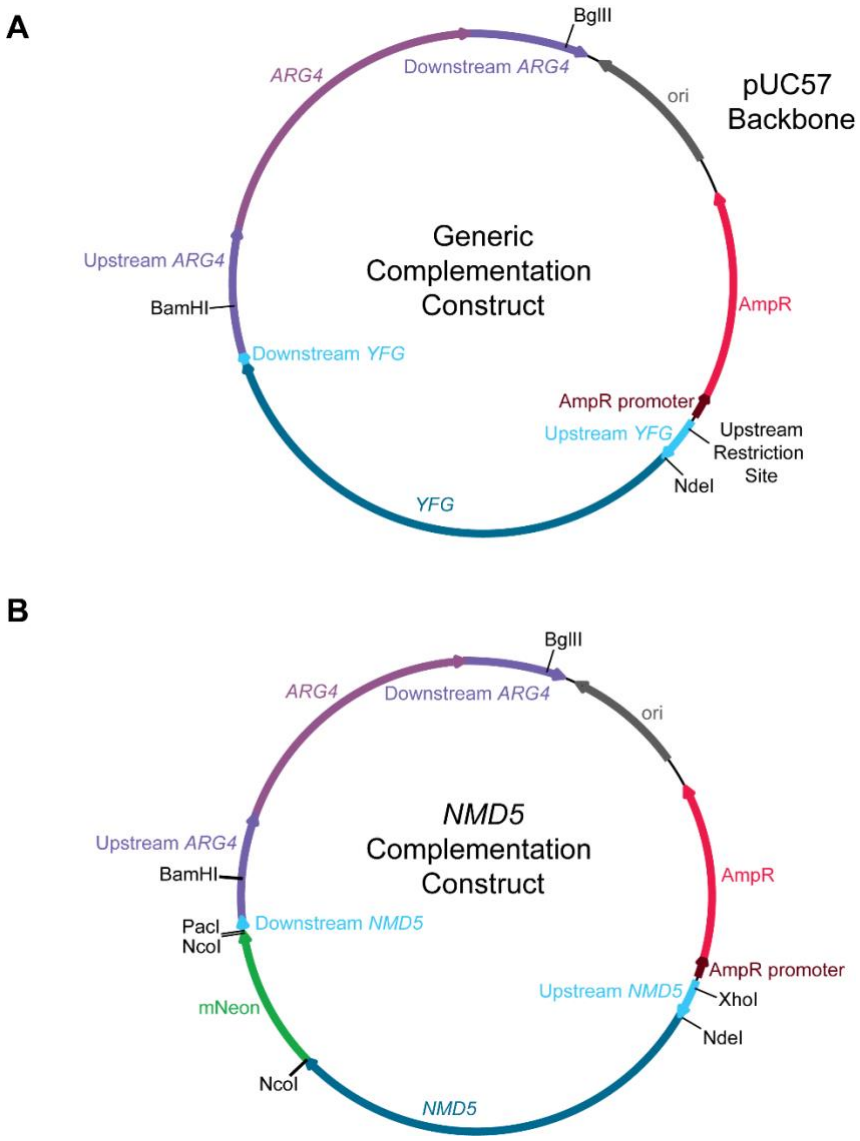

Figure A.1 Complementation constructs A) Plasmid showing the design of the construct for complementation of mutant strains. All plasmids contained a BglII cut site downstream of *ARG4*, a BamHI cutsite upstream of *ARG4*, an NdeI cutsite at the ORF start site, and another restriction cut site in the complementary upstream region of the gene of interest. The upstream restriction site and the BglII restriction site were used to excise the fragment for complementation. **B)** Plasmid showing the design of the construct for complementation of *NMD5*. The *NMD5* complementation construct contains mNeon to enable screening of transformants for fluorescence to assess functional complementation. The XhoI and BglII restriction sites were used to excise the fragment for complementation. Sequences of ORFs with upstream and downstream regions used in complementation constructs is provided in Table A.3.

Figure A.2 Sequence of *RBT1* long allele

ATGAGATTTGCAACTGCCCAACTCGCTGCCCTCGCTTACTACATTTTATCCACTGAGGC
TACTTTCCCATTATTGGGTGACATCTTTAATTGTATTCCACACAACACTCCTCCTGTCTG
TACTGACTTGGGTCTTTACCACGATAGCTCCATTTCCCTTAGTGGTTCCAAGAACAAG
AGAGAAGCTGAAATTGTCAATGAAGATGGTACAATTGAAAAGAGAACTTTTGGAAGC
GCTGGTGTAAATGCCGGTTTCAATGCCGCATTTGTCGTGTCTAATGCCAAAAAATTATC
TGACGGTTCTTATGGTATTGATTGTAACTTCAAGAGTGATTCTTCTGTCCAATTGAACC
TGGCCTTTGGTAAAAAAGTTAAACAATTGAGTATCACCGGTACTGGTTATTCTGATATT
TCATTATTAGGAAATGTTGCTAATCCATTTGAATGGTCAGCTTCCTTGAAAGTCAAAGC
AGAAATTGTTAAAGGAAAATGTTGTCTTCCATCAGGTTTCAGAATCGTTACAGATTTC
GAAAGCAACTGTCCTGAATTTGATGCCATCAAACAATTTTTTGGCAGTTCTCAAATAA
TTTACAAAGTCAATGCCGTTTCTAACGCAATTGGTACTTTTGATGCTTCTGCATTATTC
AATGCTCAAGTCAAAGCCTTCCCTGCCAAGAGAGAATTAGATGAATTTGAAGAATTA
AGTAACGATGGTGTTACTCACAGCAAGAGAACTTTGGGTTTGCTTTTGGGTTTGCTTA
AGAAAGTTACTGGTGGATGTGATACTTTACAACAATTCTGTTGGGACTGTCAATGTGA
CACCCCATCTCCATCAACTACCACCGTAAGTACTTCATCTGCTCCATCTACTTCCCCAG
AATCATCTGCTCCATCTACTACTACAGTTACCACTTCATCTTCTCCAGTTACTTCTCCAG
AATCTAGTGTTCCAGAAACTACTACCGTTACTACTTCATCTGTCCCAGAAACTACTCC
AGAATCATCAGCTCCAGAAACCACCACAGTTACTACTTCATCTGTTCCTTCTACTACC
CCAGAGTCTTCTGCTCCAGAAACCACTCCAGAATCATCAGCTCCAGAATCTAGTGTTC
CAGAATCATCAGCTCCAGAAACCACTCCAGAATCATCAGCTCCAGAATCTAGTGTTCC
AGAATCATCAGCTCCAGAAACTGAAACTGAAACCACTCCAACTGCTCACTTAACTAC
TACTACTGCTCAAACTACTACTGTTATAACTGTTACTTCATGCTCTAACAATGCTTGTA
GCAAAACTGAAGTAACCACAGGTGTTGTTGTTGTCACTTCTGAAGATACTATTTACAC
TACCTTCTGTCCATTAACTGAAACCACCCCAGTTCCTTCAAGTGTTGATTCTACTTCAG
TCACTTCTGCTCCAGAAACCACCCCAGAATCTACTGCCCCAGAATCATCTGCTCCAGA
ATCTAGTGCCCCAGAATCATCTGCACCAGTCACTGAAACACCAACTGGTCCAGTTTCC
ACTGTTACTGAGCAATCAAAGACCATCGTCACCATCACCTCATGCTCCAACAATGCAT
GCAGTGAATCTAAGGTCACCACTGGTGTTGTTGTTGTTACATCTGAAGATACTGTTTA
CACTACATTCTGTCCATTAACTGAAACTACTCCAGCTACTGAATCAGCCCCAGAATCA
TCTGCACCAGCCACTGAATCAGTTCCAGCTACTGAAAGTGCTCCAGTTGCTCCAGAA
TCATCTGCACCAGGTACTGAAACCGCACCAGCTACCGAATCAGCTCCTGCCACTGAA
AGTTCTCCAGTTGCTCCAGGTACTGAATCTTCCCCAGTTGCCCCAGAATCATCAGCAC
CAGCTACTGAATCAGCACCAGCCACCGAATCTTCCCCAGTTGCTCCAGGTACTGAAA
CCACTCCAGCTACTCCAGGTGCTGAATCAACTCCAGTTGCTCCAGTTGCCCCAGAATC
ATCAGCTCCAGCTGTTGAATCTTCTCCAGTTGCTCCAGGTGTCGAAACTACTCCAGTT
GCACCAGTTGCTCCTTCTACCACTGCAAAAACTAGTGCTCTCGTCTCTACGACTGAGG
GTACTATTCCAACTACATTAGAATCTGTTCCTGCCATTCAACCATCTGCTAACTCCTCAT
ACACTATTGCTTCAGTCTCTTCATTCGAAGGTGCTGGTAACAACATGAGATTAACTTAT
GGTGCTGCTATTATTGGTCTTGCTGCATTCTTGATCTAA

Figure A.3 Sequence of *RBT1* short allele

ATGAGATTTGCAACTGCCCAACTCGCTGCCCTCGCTTACTACATTTTATCCACTGAGG
CTACTTTCCCATTATTGGGTGACATCTTTAATTGTATTCCACACAACACTCCTCCTGT
CTGTACTGACTTGGGTCTTTACCACGATAGCTCCATTTCCCTTGGTGGTTCCAAGAAC
AAGAGAGAAGCTGAAATTGCCAATAAAGATGGTACAATTGAAAAGAGAACTTTTGG
AAGCGCTGGTGTAAATGCCGGTTTCAATGCCGCATTTGTCGTGTCTAATGCCAAAAA
ATTATCTGACGGTTCTTATGGTATTGATTGTAACTTCAAGAGTGATTCTTCTGTCCAA
TTGAACCTGGCCTTTGGTAAAAAAGTTAAACAATTGAGTATCACTGGTACTGGTTAT
TCTGATATTTCATTATTAGGAAATGTTGCTAATCCATTTGAATGGTCAGCTTCCTTGA
AAGTCAAAGCAGAAATTGTTAAAGGAAAATGTTGTCTTCCATCAGGTTTCAGAATCG
TTACAGATTTCGAAAGCAACTGTCCTGAATTTGATGCCATCAAACAATTTTTTGGCA
GTTCTCAAATAATTTACAAAGTCAATGCCGTTTCTAACGCAATTGGTACTTTTGATGC
TTCTGCATTATTCAATGCTCAAGTCAAAGCCTTCCCTGCCAAGAGAGAATTAGATGA
ATTTGAAGAATTAAGTAACGATGGTGTTACTCACAGCAAGAGAACTTTGGGTTTGCT
TTTGGGTTTGCTTAAGAAAGTTACTGGTGGATGTGATACTTTACAACAATTCTGTTGG
GACTGTCAATGTGACACCCCATCTCCATCAACTACCACCGTAAGTACTTCATCTGCT
CCATCTACTTCCCCAGAATCATCTGCTCCATCTACTACTACAGTTACCACTTCATCTT
CTCCAGTTACTTCTCCAGAATCTAGTGTTCCAGAAACTACTACCGTTACTACTTCATC
TGTCCCAGAAACTACTCCAGAATCATCAGCTCCAGAAACCACCACAGTTACTACTTC
ATCTGTTCCTTCTACTACCCCAGAGTCTTCTGCTCCAGAAACCACTCCAGAATCATCA
GCTCCAGAATCTAGTGTTCCAGAATCATCTGCTCCAGAATCTAGTGCCCCAGAATCA
TCTGCACCAGCCACTGAAACACCAACTGGTCCAGTTTCCACTGTTACTGAGCAATCA
AAGACCATCGTCACCATCACCTCATGCTCCAACAATGCATGCAGTGAATCTAAGGTC
ACCACTGGTGTTGTTGTTGTTACATCTGAAGATACTGTTTACACTACATTCTGTCCAT
TAACTGAAACTACTCCAGCTACTGAATCAGCCTCAGAATCATCTGCACCAGCCACTG
AATCAGTCCCAGCTACTGAAAGTGCTCCAGTTGCTCCAGAATCATCTGCACCAGGTA
CTGAAACCGCTCCAGCTACCGAATCAGCTCCTGCCACCGAATCTTCCCCAGTTGCTC
CAGGTACTGAAACCACTCCAGCTACTCCAGGTGCTGAATCAACTCCAGTTACTCCAG
TTGCCCCAGAATCATCAGCTCCAGCTGTTGAATCTTCTCCAGTTGCTCCAGGTGTCGA
AACTACTCCAGTTGCACCAGTTGCTCCTTCTACCACTGCAAAAACTAGTGCTCTCGT
CTCTACGACTGAGGGTACTATTCCAACTACATTAGAATCTGTTCCTGCCATTCAACC
ATCTGCTAACTCCTCATACACTATTGCTTCAGTCTCTTCATTCGAAGGTGCTGGTAAC
AACATGAGATTAACTTATGGTGCTGCTATTATTGGTCTTGCTGCATTCTTGATCTAA

Table A.1: Full list of *C. albicans* strains used in this study. All mutants tested in this study and which stages of testing they passed. https://doi.org/10.6084/m9.figshare.25877515.v1

Table A.2: Immune response to mutant *C. albicans* infections. Summary statistics of the immune response to infection for all mutant *C. albicans* infections imaged. https://doi.org/10.6084/m9.figshare.25877539.v1

Table A.3: Complementation construct sequences. Sequences used for complementation for each mutant, as well as *C. dubliensis ARG4* used in each of the complementation constructs. Complementation constructs were constructed by inserting these sequences into the pUC57 background. https://doi.org/10.6084/m9.figshare.25877545.v1

BIOGRAPHY OF THE AUTHOR

Bailey A. Blair was born in Bangor, Maine on December 20, 1993. She was raised in Bucksport, Maine and graduated from Bucksport High School in 2012. She then attended Franklin Pierce University majoring in Biology and Mathematics and graduating in 2016 with a Bachelor of Science. After graduating she then attended the University of Maine for a PhD in Biomedical Science. Bailey is a candidate for the Doctorate of Philosophy in Biomedical Science from the University of Maine in August 2024.